TECHNICAL REPORT STANDARD TITLE PAGE

1. Report No.	2. Government Accession No.	3. Recipient's Catalog No.
TX-95 1369-1F		

4. Title and Subtitle	5. Report Date
Predicting Rheological Parameters of Reclaimed Asphalt Cement with Wave Propagation Techniques	July, 1996
	6. Performing Organization Code

7. Author(s)	8. Performing Organization Report No.
Nazarian, S., Pezo R., Nori, S.R.G. and Picornell M.	Research Report 1369-1F

9. Performing Organization Name and Address	10. Work Unit No.
Center for Geotechnical and Highway Materials Research. The University of Texas at El Paso El Paso, Texas 79968-0516	11. Contract or Grant No. Study No. 0-1369

12. Sponsoring Agency Name and Address	13. Type of Report and Period Covered
Texas Department of Transportation P.O. Box 5080, Austin, Texas 78763	Report (Sept. 1, 1993-Aug 31, 1995)
	14. Sponsoring Agency Code

15. Supplementary Notes

Research Performed in Cooperation with TxDOT and FHWA
Research Study Title: TESTING METHODS FOR RECLAIMED ASPHALT PAVEMENT

16. Abstract

A methodology to predict the theological parameters of asphalt cement from elastic modulus or from the indirect tensile (IDT) strength of the mix is presented. Wave propagation techniques were used to determine the modulus of the mix. Numerous specimens, prepared from four different mixtures with different asphalt contents and voids in the total mixes (VTM's), were-oven aged for different periods. The elastic modulus and IDT strength of each specimen were determined, and its asphalt cement was recovered to evaluate its rheological properties. The effects of different parameters, such as asphalt content and VTM, on relationships between elastic modulus or IDT strength with rheological properties were determined.

Models were developed for determining the penetration and kinematic viscosity of the asphalt using the elastic modulus or IDT strength of the mix. Prediction charts were also generated to estimate the asphalt grade of the material using the elastic modulus of the mix. In general, it was found that wave propagation techniques can be used as an alternative to the Abson recovery to estimate the rheological parameters of the asphalt cement. However, more work in calibrating the molds is needed.

17. Key Words	18. Distribution Statement
Asphalt, Abson Recovery, Modulus, Laboratory Testing, Flexible Pavements, wave propagation, viscosity, penetration	No restrictions. This document is available to the public through the National Technical Information Service, 5285 Port Royal Road, Springfield, Virginia 22161

19. Security Classif. (of this report)	20. Security Classif. (of this page)	21. No. of Pages	22. Price
Unclassified	Unclassified	85	

Form DOT F 1700.7 (8-69)

Predicting Rheological Parameters of Reclaimed Asphalt Cement with Wave Propagation Techniques

by

Soheil Nazarian, Ph.D., P.E.
Rafael Pezo, Ph.D.
Srinivas R.G. Nori, MSCE
and
Miguel Picornell, Ph.D.

Research Project 0-1369

TESTING METHODS FOR RECLAIMED ASPHALT PAVEMENT

Conducted for

Texas Department of Transportation

in cooperation with

Federal Highway Administration

The Center for Geotechnical and Highway Materials Research
The University of Texas at El Paso
El Paso, TX 79968-0516
Research Report 1369-1F
July, 1996

The contents of this report reflect the views of the authors, who are responsible for the facts and the accuracy of the data presented herein. The contents do not necessarily reflect the official views or policies of the Texas Department of Transportation or the Federal Highway Administration. This report does not constitute a standard, specification, or regulation.

NOT INTENDED FOR CONSTRUCTION, BIDDING, OR PERMIT PURPOSES

Soheil Nazarian, Ph.D., P.E. (69263)
Rafael Pezo, Ph.D.
Srinivas R.G. Nori, MSCE
Miguel Picornell, Ph.D.

Acknowledgements

The authors would like to give their sincere appreciation to Dale Rand and Maghsoud Tahmoressi of the TxDOT Materials and Test Division for their ever-present support. Many thanks are also extended to the laboratory personnel of the El Paso District for providing assistance in many aspects of this project.

The research assistants on this project were Nalini Vemuri and Oscar Contreras.

Abstract

Asphalt recycling has become an attractive rehabilitation alternative to pavement engineers. As the rheological parameters of asphalt change with time due to "aging" phenomena, it is essential to properly characterize the reclaimed asphalt pavement (RAP) materials to ensure a high quality pavement and to avoid excessive maintenance costs. Existing methods of determining rheological parameters of RAP material involve many steps and suffer from problems, such as the use of hazardous solvents.

In this study, a methodology is presented to predict the rheological parameters of asphalt cement from elastic modulus or from the indirect tensile strength (IDT strength) of the mix. Wave propagation techniques were used to determine the modulus of the mix. Numerous specimens, prepared from several different mixtures with different asphalt contents and voids in the total mixes (VTM's), were oven-aged for different periods. The elastic modulus and IDT strength of each specimen were determined, and its asphalt cement was recovered to evaluate its rheological properties. The effects of different parameters, such as asphalt content and VTM, on relationships between elastic modulus or IDT strength with rheological properties were determined.

Models were developed for determining the penetration and kinematic viscosity of the asphalt using the elastic modulus or IDT strength of the mix. Prediction charts were also generated to estimate the asphalt grade of the material using the elastic modulus of the mix.

In general, it was found that the wave propagation techniques are feasible as an alternative to the Abson recovery to estimate the rheological parameters of the asphalt cement. However, field verification is necessary before concrete conclusions can be drawn.

Executive Summary

Due to growing environmental and economical concerns, asphalt recycling has become an attractive rehabilitation alternative technique. As the rheological parameters of asphalt change with time due to aging, its constituent properties have to be measured before it can be blended with virgin materials. This would ensure high-quality pavement and avoid excessive maintenance cost. The existing methods using Abson recovery includes many problems like utilization of hazardous solvents. The wave propagation techniques can be used to determine the rheological parameters of asphalt without using the hazardous solvents in extraction and recovery process.

A laboratory study was conducted from several different mix designs with three different asphalt contents and VTM's. Specimens were aged for 0, 1, 2, 7, and 28 days at 85°C in an oven. All specimens were tested for their elastic moduli and IDT strengths. Wave propagation equipment was used to measure the elastic moduli of specimens. The asphalt binder contained in the specimens were extracted and recovered to measure their rheological parameters.

Analyses were conducted to identify mix parameters that best correlate to modulus and IDT strength. Based on the correlation amongst the parameters, models were developed for predicting the penetration and the kinematic viscosity using the elastic modulus or IDT strength.

Using these models along with ASTM specifications for different grades of asphalt, prediction charts were generated to estimate the asphalt grade of RAP materials knowing their moduli or strengths.

Implementation Statement

All the required equipment manufactured at UTEP can be duplicated for use by the TxDOT personnel. The testing methodology was drafted and tested on several materials. In our opinion, the test methodology is easy and the equipment is inexpensive enough to be implemented on trial basis so that the possible logistical and practical problems with the protocol can be addressed.

Table of Contents

List of Tables

List of Figures

Chapter 1

Introduction

Problem Statement

The recycling of asphaltic concrete pavements has become increasingly popular, due to a growing concern over the disposal of asphalt and aggregate. It is anticipated that asphalt recycling will become a key component in the paving process.

In the hot-mix method of recycling, 20 to 70 percent of reclaimed asphalt pavement (RAP) materials are added to virgin materials. To ensure the quality of pavement and to avoid excessive maintenance costs, RAP materials should be properly characterized before they are blended with virgin asphalt and aggregate. Since the asphalt cement hardens with time ("ages"), the rheological properties of aged asphalt cement have to be evaluated. This is typically done by extracting and recovering the asphalt cement from the RAP material. The major problem with this process, besides being labor-intensive, is that the utilization of hazardous solvents, in which the disposal is expensive and difficult. A simple and economical methodology, that uses a nondestructive method, is required to assess the degree of aging characteristics of RAP material.

Objectives and Approach

The main objective of this study is to evaluate the feasibility of developing a prediction model, using wave propagation techniques to determine the rheological properties of hardened asphalt cement in a RAP from its elastic modulus. If the approach is found feasible and encouraging, further investigation can be made prior to the implementation of this methodology in recycling activities.

An extensive literature survey was carried out to identify important parameters that may affect the aging process. Factors, such as type of mix, aging methods for asphaltic concrete mixtures, and

testing methods on asphaltic concrete specimens and on asphalt binder, were evaluated to achieve the objective. A test program was formulated considering all of the above factors. Various research activities in the test program include the following: preparation and aging of asphaltic concrete specimens, testing the specimens before and after aging, for their elastic modulus and IDT strength, and determining such rheological properties as kinematic viscosity and penetration of the recovered asphalt cement. Finally, based on the correlation coefficients among different testing variables, prediction models were obtained to determine the rheological parameters of RAP material.

A Texas gyratory compactor was used to prepare the specimens. Long term oven aging (LTOA) at 85 °C, recommended by Bell (1990), was used to age the asphaltic concrete specimens. For the most part, a V-Meter manufactured by James Instruments, Inc. was used to generate the necessary compressional waves through the asphaltic concrete specimens to find the elastic modulus. The indirect tensile strength (IDT Strength) of each specimen was then determined. The asphalt in each specimen was finally extracted and recovered. The kinematic viscosity at 135°C (275°F) and the penetration at 25°C (77°F) of the recovered asphalt were measured.

The data collected from different tests was analyzed to develop prediction models. These models can be used to estimate the penetration and kinematic viscosity of RAP materia, using either elastic modulus or indirect tensile strength.

Organization

Chapter 2 contains a review of existing literature on the phenomena of aging, on aging methods on mixtures, on test methods for evaluating aging potential, and on existing methodology for reusing RAP materials.

Chapter 3 describes the methodology used to correlate the aging characteristics of a RAP material with its elastic modulus, as well as, the experimental design and testing procedures used in this study.

The presentation and discussion of laboratory results used to evaluate the effects of different testing variables on the elastic modulus and the IDT strength of the mix are presented in Chapter 4.

Chapter 5 contains the statistical analysis of data used to develop the best possible prediction models that relate the rheological parameters of the binder to the stiffness of the mix. Also shown are the prediction charts to estimate the asphalt grade.

A study to optimize the test set up developed under this project is included in Chapter 6. A brief summary and conclusions are given in Chapter 7.

Results from all laboratory tests and other supporting information are presented in Appendices A through G.

Chapter 2

Literature Review

Introduction

This chapter contains a summary of existing literature with regards to the phenomena of aging, artificial aging methods, and testing methods related to the aging of hot-mix asphalt binders and mixtures.

Aging Phenomenon

The hardening or stiffening of asphalt binder with time has been referred to as age hardening, embrittlement, or, more simply, "aging." The hardening in binders occurs in two stages (Bell, 1990). The first stage occurs during the construction phase and is primarily due to the loss of volatile components and oxidation, while the mix is hot. The second stage occurs while the mixture is in service and is primarily due to progressive oxidation over time. The aging of binder results in an increase in both the elastic modulus and brittleness of the mix. The increase in the elastic modulus can improve the load distribution within the pavement structure, but the increase in brittleness may lead to pavement cracking (Kim et al., 1986). The aging of binder depends on various factors, including asphalt characteristics, asphalt film thickness around the aggregate surface, air voids in the asphaltic concrete mixture (Roberts et al., 1991), and the adsorptive nature of aggregate (Verhasselt and Choquet, 1992). The type of aggregate also affects the aging of the mix (Sosnovake et al., 1992). This influence relates to the chemical interaction between aggregate and binder. According to Harvey and Monismith (1992), variations in fine content, even within typical gradation specifications, can affect the aging of the mix. The above factors are considered in the present study to develop the experimental design.

Aging Methods for Mixtures

Various researchers have developed a variety of promising laboratory aging methods to simulate field aging, for short-term and long-term aging of asphaltic concrete mixtures (Bell, 1990). Pressure oxidation treatment (Lee, 1973; Kim et al., 1986; and Bell et al., 1991), extended oven aging (Tia et al., 1988; Von Quintas et al., 1991; and Bell et al., 1991), and infrared/ultraviolet treatment (Vallerga et al., 1957) are promising methods for long-term aging. Laboratory oven-aging at 135°C and 85°C or 100°C, simulates short- or long-term field aging, respectively (Bell et al., 1994). In their study, Bell et al. validated the laboratory oven-aging procedures to simulate the field aging for laboratory specimens prepared to the gradations, asphalt contents, and air void content, similar to those obtained from field cores. Finally, they concluded that oven aging procedures were representative in most cases and they suggested that further study was needed to develop prediction models. In the present study, oven aging at 85°C was used to age the specimens in the laboratory.

Test Methods for Evaluating Aging Potential

Various test methods exist, for evaluating the aging potential of asphalt binders and mixtures. The most common methods are summarized in the next section.

Asphalt Binder

The performance of an asphaltic concrete mixture, in service, is affected by the aging characteristics of the asphalt binder (Huang et al., 1993). The aging of asphalt binder can be determined from changes in its rheological properties, such as viscosity and penetration. The penetration at 25°C (77°F) and viscosity at either 135°C (275°F) or 60°C (140°F) are usually specified. The extent of age hardening can be quantified in terms of retained penetration (R.P.) and aging index (A.I.), which are defined as (Roberts et al., 1991)

$$R.P. = \frac{Penetration of Aged Asphalt}{Penetration of Original Asphalt} * 100 \qquad (2.1)$$

$$A.I. = \frac{Viscosity of Aged Asphalt}{Viscosity of Original Asphalt} \qquad (2.2)$$

In this study, Equations 2.1 and 2.2 are used to investigate the changes in the rheological properties of the recovered asphalt.

A most recent procedure to evaluate the degree of aging involves the separation of asphalt into fractions of various molecular sizes, which is referred to as High Pressured Gel Permeation Chromatography (HP-GPC) (Roberts et al., 1991). In the procedure asphalt molecules can be classified into large, medium and small (LMS, MMS, and SMS). The changes in relative amounts

of different sizes are used to assess the extent of aging of asphalt cement (Neureldin et al., 1989).The aging (simulated in the laboratory) would cause an increase in the LMS, and decrease in the MMS and SMS.

Asphaltic Concrete Mixtures

Resilient Modulus (M_R) test has been used by many researchers to measure the modulus of HMA (Roberts et al., 1991). The M_R test has become more popular, because of its simplicity and applicability to test field cores. Bell et al. (1994) observed an increase in the resilient modulus with the extent of aging of mix.

Tia et al. (1988), and Von Quintus et al. (1991) used the indirect tensile strength (IDT Strength) method to evaluate the extent of aging. The strain, at failure, was found to be a good indicator of the aging effects, rather than the tensile strength. Norman et al. (1990) studied the relationship between penetration at 25°C (77°F) of recovered asphalt and the indirect tensile strength of the mix. Two types of aggregates and fifteen types of asphalt, which have three different asphalt grades were used in their study. They observed a strong correlation between these two parameters. The values of penetration decrease with the increase in the IDT strength of the mix. They also concluded that the asphalt and aggregate types significantly affect the relationship between penetration and IDT strength values. Similarly, they concluded the tensile strength decreases with an increase in VTM and asphalt cement. They felt that asphalt composition is another factor which appeared to play a role in determining the IDT strength of asphalt mixtures.

Neureldin and Wood (1992) characterized the performance of the hot-mix recycled asphalt paving mixtures, in comparison with a virgin mix. In their study, four different mixes were prepared with identical aggregate gradations and asphalt binders satisfying AC-20 specifications. The only difference was that the first mix was a virgin mix (asphalt and aggregate) and the other three were recycled mixtures with three different rejuvenating agents. The asphalt Institute blending chart (MS-20) was considered for developing the mix design for the recycled mixtures. Three different asphalt contents were selected. The mixtures were compacted using a kneading compactor. The Marshall stability tests are utilized to measure stability. Nondestructive tests, using sonic pulse velocity to measure elastic modulus and resilient modulus tests, were conducted on the specimens prepared. They found that the pulse velocity test parameters were neither sensitive to the binder content, nor to the binder type. The author felt the lack of sensitivity in the elastic modulus test was due to similar behavior between all the mixtures in the elastic range. It was suggested that pulse velocity test could be used for determining pavement thickness, on the basis of the layered elastic theory solutions, due to a low statistical variation in pulse velocity and mosulus of elasticity. They recommended the use of resilient modulus test for designing asphaltic concrete mixtures (virgin or recycled), because the test results were sensitive to both binder content and type. The conventional Marshall stability test results were appropriate to identify binders (virgin or recycled) with potential to produce mixtures with higher strength. In the present study, wave propagation techniques using compressional wave velocity, were utilized to identify the extent of aging.

Nazarian et al. (1992) utilized a simple laboratory and two nondestructive field testing techniques to determine the variations in modulus with aging. The high frequency surface-wave and body-wave methods were utilized to determine the shear and compression wave velocities. From these two parameters, the elastic modulus and Poisson's ratio of the material were calculated. The values of elastic modulus and Poisson's ratio are indicative of the stiffness and the brittleness of the material. Through laboratory and field case studies, they concluded that the wave propagation techniques, when used properly, can yield valuable information about the aging properties of asphaltic concrete layers.

The above techniques were successfully used by Li (1994) to determine the degree of aging of asphaltic concrete. In his laboratory study, Li determined the variation of elastic modulus with temperature and aging period. He concluded that the change in modulus was inversely proportional to the voids in total mix (VTM) and to the asphalt content. In addition, three models simulating real pavement conditions were prepared, and placed in different locations to determine the environmental effects. From this study, he concluded that oxidation due to ultraviolet was probably the most critical factor for aging.

Laboratory Compaction Devices

Consuegra et al. (1989) selected five different devices to evaluate the ability to simulate the field compaction. They included the following devices in their evaluation: a) a mobile steel wheel simulator, b) a Texas gyratory compactor, c) a California kneading compactor, d) a Marshall impact hammer, and e) an Arizona vibratory-kneading compactor. Resilient modulus, indirect tensile strength and strain at failure, and tensile creep tests were conducted on specimens prepared in the laboratory and on the field cores. They concluded that the Texas gyratory compactor ranked first in terms of its ability to produce compacted mixtures with engineering properties similar to those produced in the field. They also concluded that the Texas gyratory compactor was the most prudent choice for preparing specimens used in mixture design and analysis. In the present study, the Texas Gyratory compactor was used to compact the asphaltic concrete specimens.

Asphalt Pavement Recycling

The Asphalt Institute (1981) has developed a design methodology for reusing RAP materials. The procedure is briefly explained below.

The asphalt content and absolute viscosity of the RAP material are determined by the extraction and recovery procedures. Using the blend chart shown in Figure 2.1, the absolute viscosity and a selected target viscosity are marked. A line is drawn and extended to the right axis to determine the grade of the new asphalt to be used in the mix. In this procedure, the asphalt has to be recovered using Abson recovery procedure, which involves the use of hazardous chemicals.

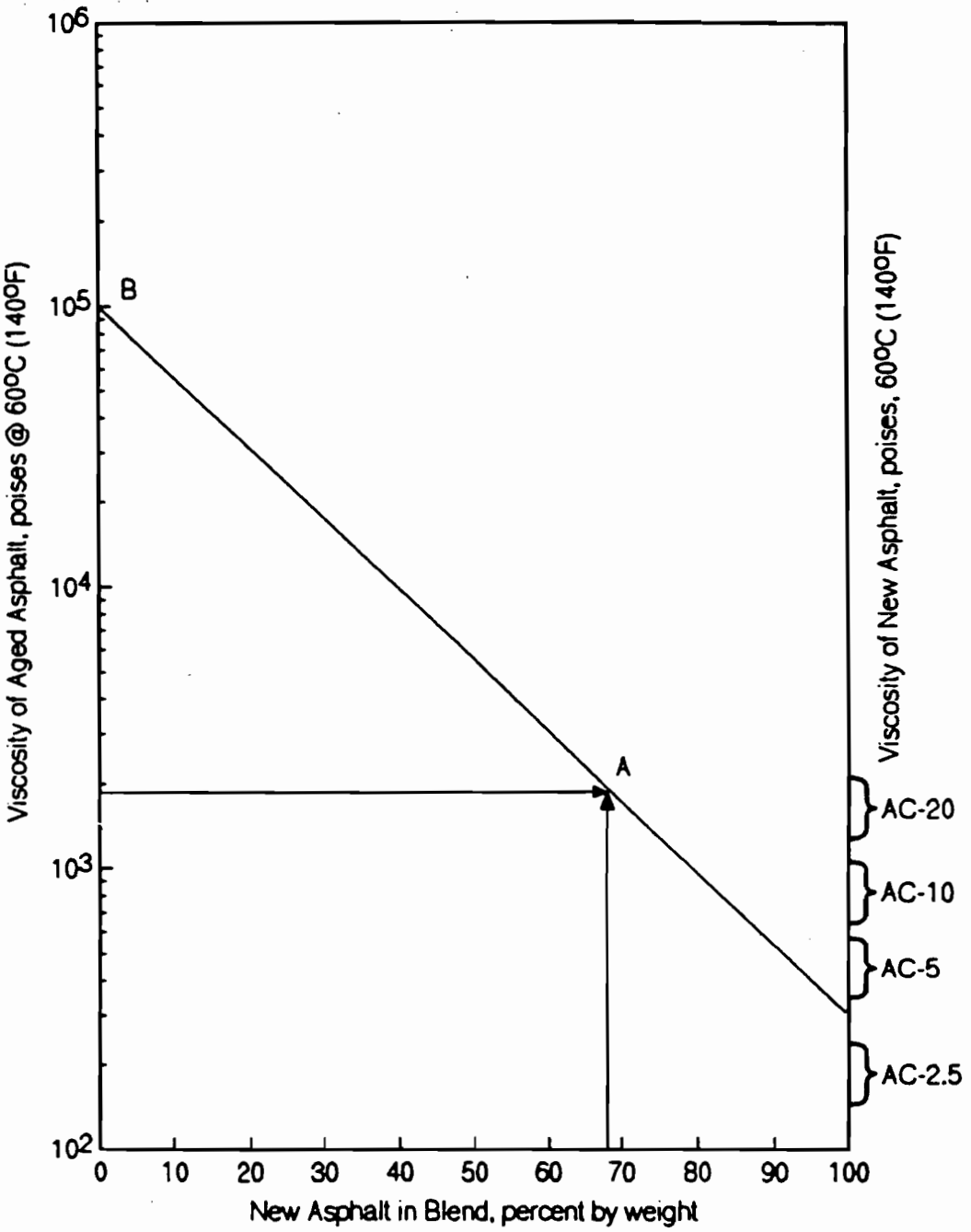

Figure 2.1 - Blending Chart for Reclaimed Asphalt and New Asphalt Cements (From Asphalt Institute, 1981).

Solvent Removal From Recovered Asphalt

Many researchers have had problems caused by residual solvents present in the recovered asphalt from Abson method (Cipione et al., 1991). The residual solvent causes a significant decrease in the viscosity of the recovered asphalt. This effect may mask most of the effects of aging on rheological parameters, such as penetration and viscosity. Burr et al. (1990), in an attempt to evaluate the Abson recovery procedure, recommended to increase the minimum recovery time after the final drop in the secondary distillation from 5 minutes to 20 minutes for asphalt specimens of 100 gm. They also indicated that asphalt subjected to elevated temperature over an extended period of time could become significantly hardened. Similar problems have been encountered in this study. The presence of solvent in AC and of fines in the AC-solvent solution were encountered with the conventional recovery procedure, even after centrifuging at high speeds. The minimum recovery time was increased to fifteen minutes, which was close to the recommendations of above researchers.

Chapter 3

Methodology of Research

Introduction

This chapter presents a methodology to correlate the rheological properties of asphalt binders with the elastic moduli or indirect tensile strengths of mixtures. A test program comprising various activities to be performed was developed. A full factorial experiment comprising all the factors that might affect aging process was constructed. These items, as well as, the data reduction methodologies are described next.

Test Program

Figure 3.1 outlines the skeleton of the research activities. Specimens were prepared as per mix design and compacted using a Texas gyratory compactor. One replicate was made for each specimen and the pair of specimens were age conditioned. Each pair of specimens fall into either of two cases: "virgin" or "aged" specimens. The "virgin" specimens were tested for their elastic moduli and indirect tensile strengths (IDTS) without any age conditioning. The pair of "aged" specimens were first tested to determine their elastic moduli, and then placed in the oven set at 85°C, for aging. After the pair of specimens were aged for a predetermined period, their elastic moduli (final moduli) and their IDTS were measured. In both cases, after the moduli and strengths were determined, the asphalt binder from each specimen was extracted and recovered to find its penetration and kinematic viscosity. To recover sufficient asphalt for conducting penetration and viscosity tests, the two specimens were mixed together for extraction and recovery. Finally, as discussed later, the data were analyzed to obtain a correlation.

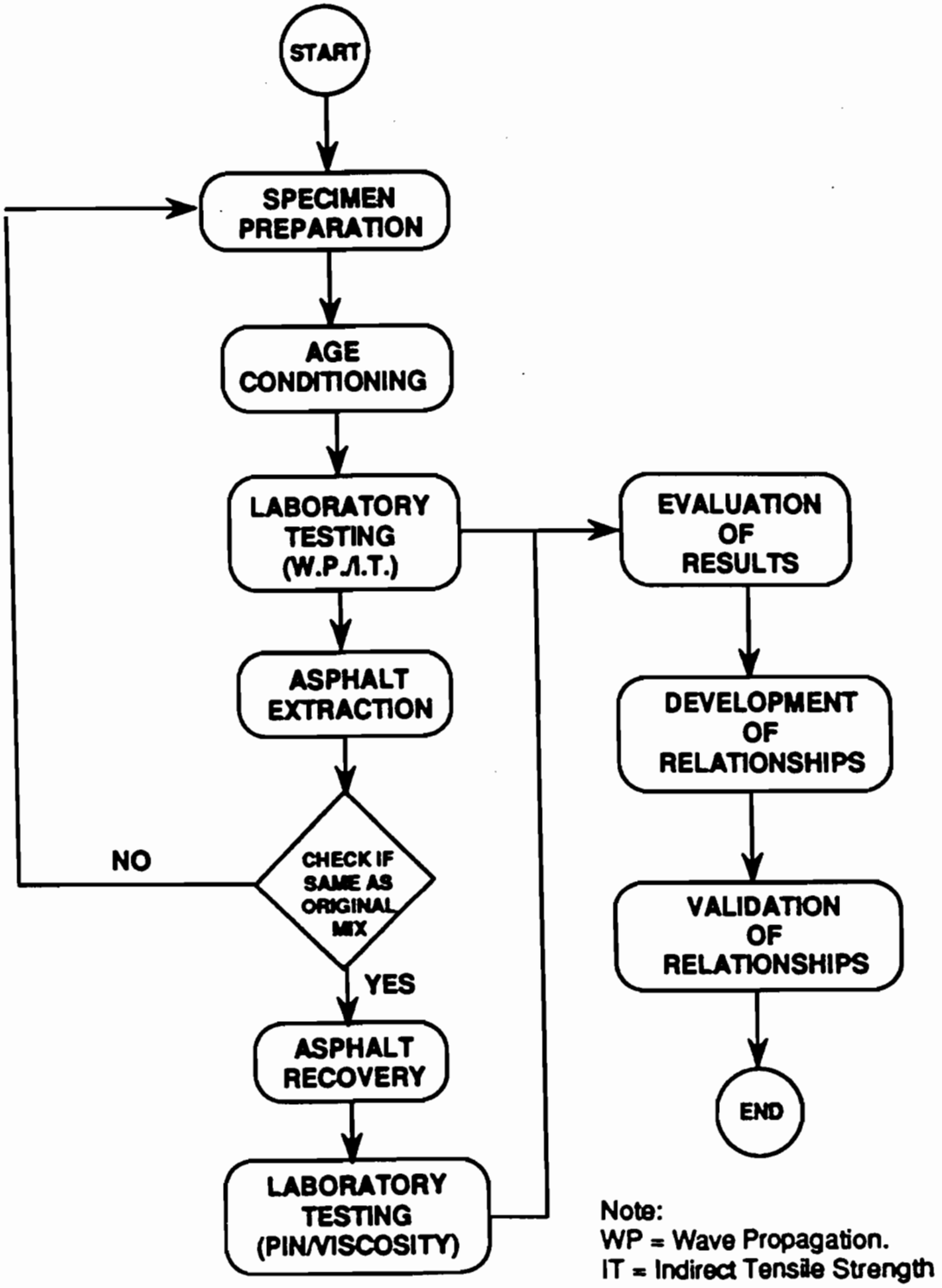

Figure 3.1 - Flow Chart of Research Activities.

Factorial Experiment

A complete factorial experiment was devised considering various factors that affect the aging of AC mixes. The factorial is shown in Table 3.1. Two different mixtures were considered in the experimental program: one from a HMA plant in El Paso, Texas and the other from Austin, Texas. The details of the mix designs are enclosed in Appendix A.

The optimum asphalt content for both mixes was about 5 percent. Three different asphalt contents of 4, 5, and 6 percent were selected for each mix to study the effects of asphalt content. Similarly, specimens were prepared using different compaction efforts to achieve three levels of voids in the total mix (VTM) i.e., 3, 5 and 7 percent (target VTM's). The specimens were aged to different aging periods of either one, two, seven, or twenty eight days. The labelling of the specimens is shown in Table 3.1 and is described below.

Each label has four digits. The first digit indicates the source of the mix, whether it is from El Paso (P) or from Austin (A). The second and third digits of the label indicate the nominal asphalt content and VTM. The fourth digit indicates the aging period and can vary from 0 to 9. One replicate was prepared for each specimen; therefore, if the fourth digit is 0 or 1, it will represent a virgin specimen (no aging). Similarly, 2 or 3 represents one day of aging, 4 or 5 two days of aging, 6 or 7 seven days of aging, and finally, 8 or 9 twenty eight days of aging. The experiment required the preparation of one hundred and eighty specimens.

Properties of Materials Tested

As mentioned in the previous section, two mix designs were considered in this study. The properties of the virgin asphalt cement used in both mix designs, i.e., penetration at 25°C (77°F) and kinematic viscosity at 135°C (275°F) were determined in the laboratory. The test results are shown in Table 3.2.

The Austin's mix design, identified as "1D". The aggregates contained rock (limestone) and sand obtained from Hunter Pit of Colorado Materials quarry. The asphalt, obtained from the Texas Fuel and Asphalt Co., Corpus Christi, Texas, was AC-20.

The El Paso's mix design was identified as a type "D" mix design. The aggregates contained rock (Dolomite) and sand obtained from Mc-Kelligan Canyon and American Basin of El Paso, respectively. The asphalt, obtained from Chevron USA Inc., was again an AC-20.

Specimen Preparation

The asphalt, sufficient to prepare two specimens at a time, was transferred into small cans. This was done to prevent aging of asphalt cement. The asphalt can was placed in an oven maintained at 150±1°C (300±2°F) one hour before mixing. The aggregates required for preparing the specimens were weighed as per mix design and placed in the same oven one day in advance. The mixing bowl

Table 3.1 - Design of Complete Factorial Experiment.

ASPHALT MIX	EL PASO									AUSTIN								
ASPHALT CONTENT, %	4			5			6			4			5			6		
AIR VOIDS, %	3	5	7	3	5	7	3	5	7	3	5	7	3	5	7	3	5	7
AGING PERIOD, DAYS																		
0	P430 P431	P450 P451	P470 P471	P530 P531	P550 P551	P570 P571	P630 P631	P650 P651	P670 P671	A430 A431	A450 A451	A470 A471	A530 A531	A550 A531	A570 A571	A630 A631	A650 A651	A670 A671
1	P432 P433	P452 P453	P472 P473	P532 P533	P552 P553	P572 P573	P632 P633	P652 P653	P672 P673	A432 A433	A452 A453	A472 A473	A532 A533	A552 A553	A572 A573	A632 A633	A652 A653	A672 A673
2	P434 P435	P454 P455	P474 P475	P534 P535	P554 P555	P574 P575	P634 P635	P654 P655	P674 P675	A434 A435	A454 A455	A474 A475	A534 A535	A554 A555	A574 A575	A634 A635	A654 A655	A674 A675
7	P436 P437	P456 P457	P476 P477	P536 P537	P556 P557	P576 P577	P636 P637	P656 P657	P676 P677	A436 A437	A456 A457	A476 A477	A536 A537	A556 A557	A576 A577	A636 A637	A656 A657	A676 A677
28	P438 P439	P458 P459	P478 P479	P538 P539	P558 P559	P578 P579	P638 P639	P658 P659	P678 P679	A438 A439	A458 A459	A478 A479	A538 A539	A558 A559	A578 A579	A638 A639	A658 A659	A678 A679

and the whip of the asphalt concrete mixer were also placed in the oven fifteen minutes, before the mixing process. Test Method TEX-204-F was utilized to mix the asphalt and the aggregates. The mixture, along with the mold and base plate of the gyratory compactor, were preheated for fifteen minutes to maintain a temperature of 120±2°C (250±5°F), while compacting the mixture. Test Meghod TEX-206-F was used to compact the specimens. The specimens were mormally 102 mm in diameter and 50 mm in height.

Table 3.2 - Rheological Properties of Virgin Asphalt Cements.

Property of Asphalt Cement	El Paso Mix	Austin Mix
Penetration at 25°C, 1/10 mm	59	59
Kinematic Viscosity at 135°C, Cst	360	341

Using test method TEX-207-F, the VTM of each specimen was calculated. If the variation of the VTM from the target VTM was less than 0.25 percent, the specimen was considered for testing, otherwise it was discarded. The data sheets used to record the results are enclosed in Appendix B.

Laboratory Testing of Specimens

Tests were conducted on each specimen to determine its elastic modulus and its indirect tensile strength. Since the modulus tests were nondestructive, it was possible to use the same specimen to measure the strength. The experimental setup and the test procedure for each experiment are presented below.

Elastic Modulus Test

A schematic of the laboratory test setup is shown in Figure 3.2 and a picture is shown in Figure 3.3. The elastic modulus of the specimen was measured using a V-meter manufactured by James Instruments, Inc. The instrument contains a pulse generator and a timing circuit, coupled with piezoelectric transmitting and receiving transducers. In this study, a pulse with a dominant frequency of 54 KHz was used to generate the necessary waves. The timing circuit digitally displays the travel time of the wave through the specimen. To ensure full contact between the transducers and the specimen, special removable epoxy couplant caps were used on both transducers. To secure the specimen in between the transducers, a loading plate was placed on the top of the specimen and a spring supporting system was placed under the bottom of the transmitting transducer.

The specimen was placed in a container filled with distilled water. The container was in turn placed in a temperature-controlled chamber. The water was maintained at 25 ± 0.1°C (77° ± 0.2°F) for about fifteen minutes to ensure a constant temperature.

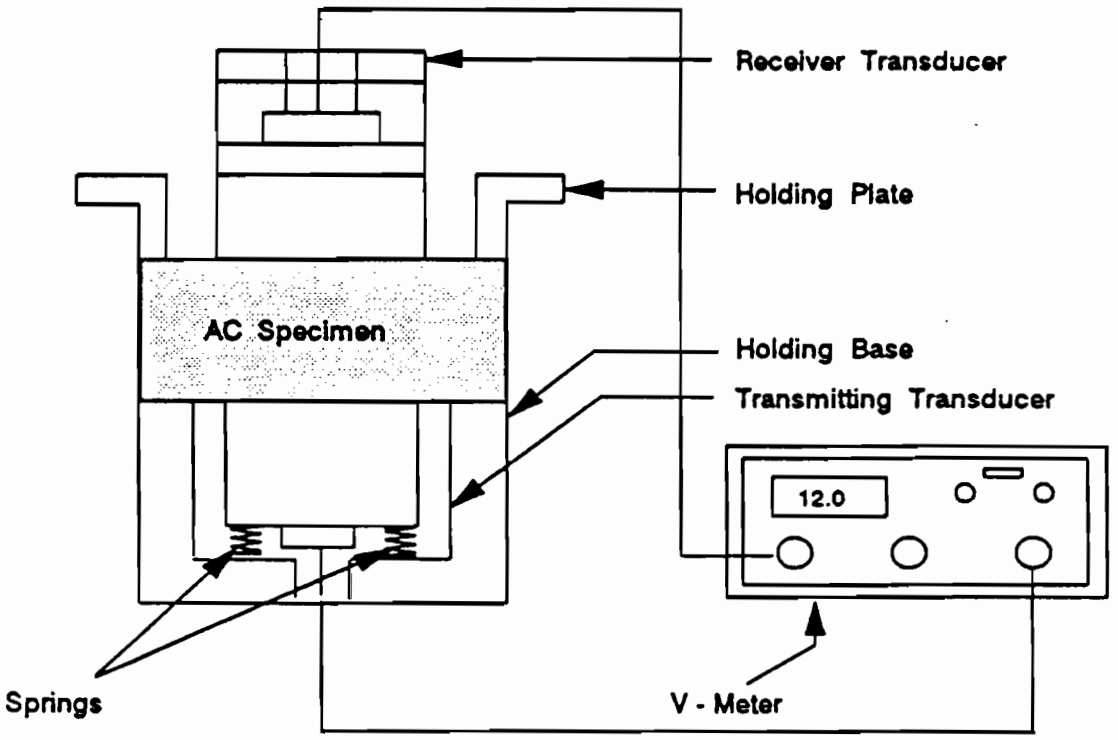

Figure 3.2 - Schematic of Laboratory Testing Setup for Elastic Modulus Test.

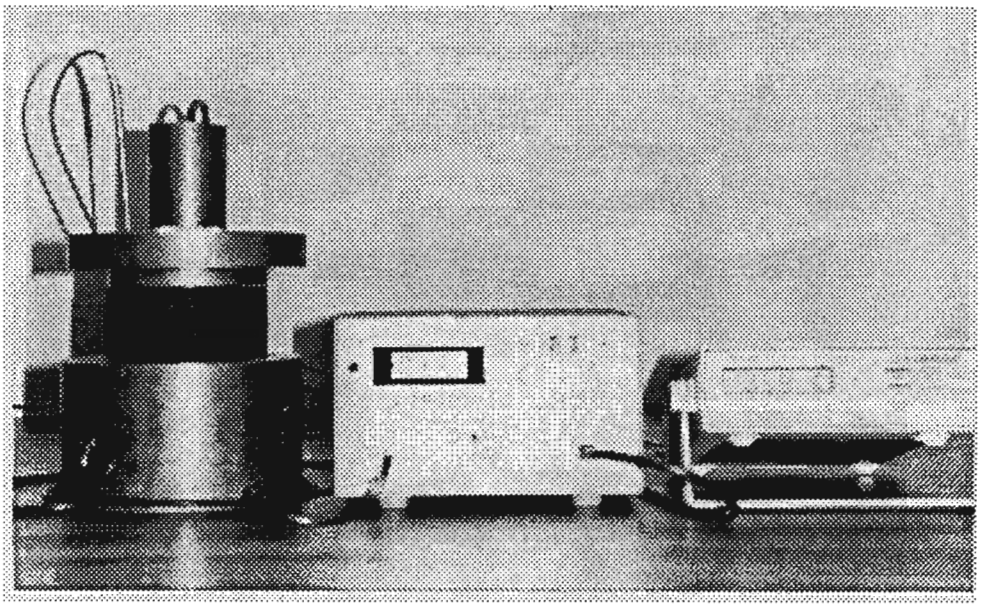

Figure 3.3 - Picture of Laboratory Setup.

The specimen was removed, saturate-surface dried using a wet cloth, and securely placed in between the transducers. It was observed that the travel time was gradually decreasing in the first few seconds. This effect was studied by recording travel times at different time periods. The travel time became more or less constant after ten seconds. Therefore, the travel time at the end of the tenth second was taken into consideration for calculating the elastic modulus.

Compression wave (P-wave) velocity was calculated by dividing the thickness of the specimen by the corresponding travel time. The elastic modulus, E, was then calculated using

$$E = \rho V_p^2 \tag{3.1}$$

where

E = elastic modulus of the specimen,
V_p = P-wave velocity, and
ρ = bulk density of the specimen.

For practical use, Equation 3.1 can be written as

$$E = \frac{W}{(\pi \cdot R^2 \cdot H)\, g} \left(\frac{H}{t}\right)^2 \tag{3.2}$$

or

$$E = \frac{WH}{(\pi R^2 g t^2)} \tag{3.3}$$

where

W = weight of specimen,
R = radius of specimen,
H = height of specimen,
g = acceleration of gravity, and
t = travel time.

Indirect Tensile Strength Test

The test setup, which is schematically shown in Figure 3.4, consists of a loading press capable of applying a compressive load at a controlled rate. Two steel loading strips, 13 mm by 20 mm, with the 13 mm surface machined to the curvature of the specimen, were used. One of the loading strips was welded to a metal base plate. To apply the load uniformly along the height, the loading strips were attached to the specimen. Hydrostone cement paste was prepared with a 4:1 hydrostone

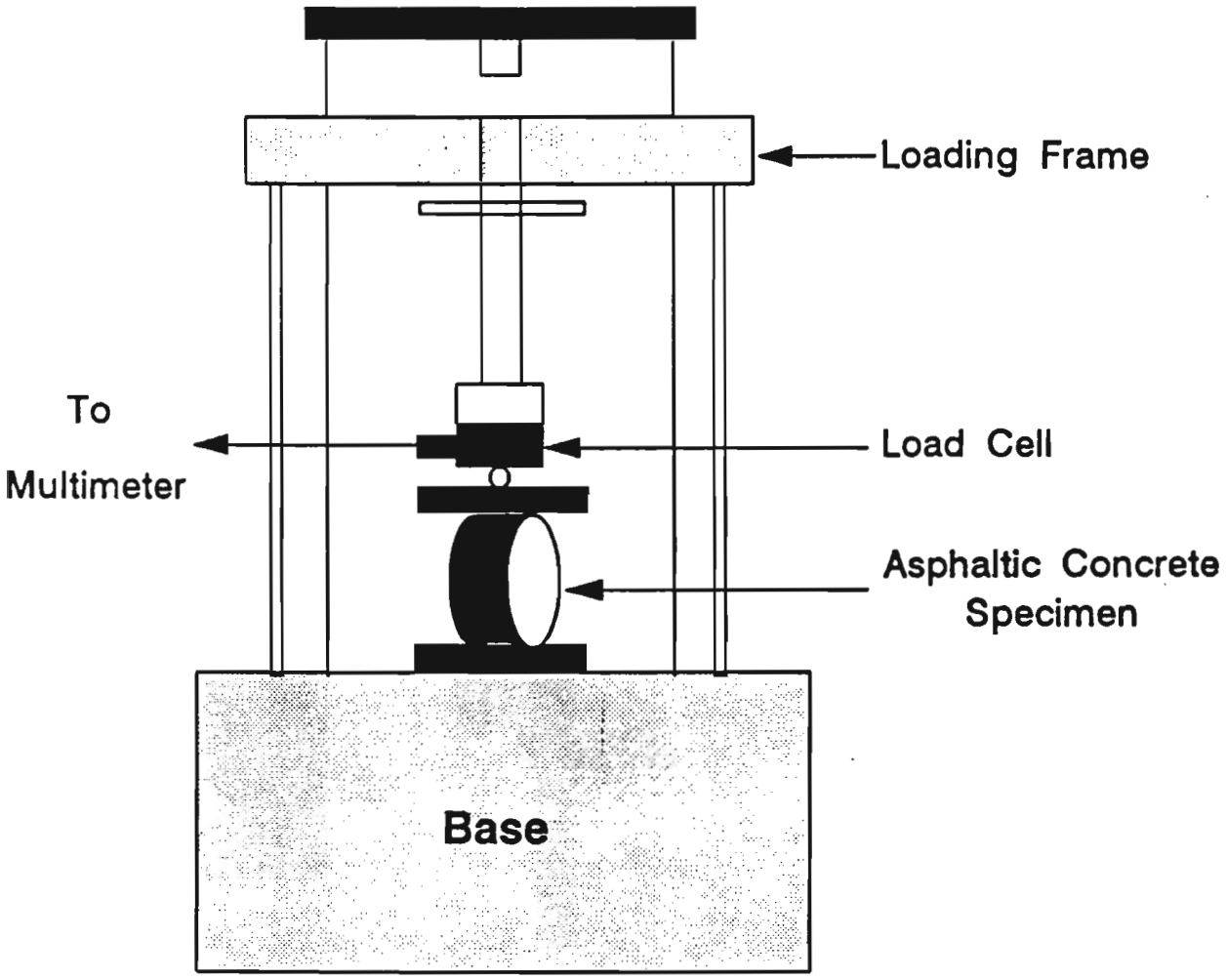

Figure 3.4 - Schematic of Test Setup for IDT Strength Test.

cement-distilled water ratio. The paste was applied to the top and bottom of the diametrical surfaces of the specimen along the loading strips. The paste was allowed to harden for at least twenty minutes, before it was placed within the loading frame to be tested.

While the paste was hardening, the loading setup was placed into a temperature-controlled chamber for about fifteen minutes at a temperature of 25±0.1°C (77±0.1°F). The setup was removed from the chamber and placed into the loading system. The loading rates, common to the procedure, are either 1.65 mm or 51 mm per minute (Ronald et al., 1989). In this study, a loading rate of 1.65 mm per minute was used throughout the experiments. The indirect tensile strength of the specimen was determined from

$$\sigma = \frac{2P}{\pi D H} \tag{3.4}$$

where

σ = indirect tensile strength,
P = load at failure,
D = diameter of specimen, and
H = height of specimen.

After the IDTS tests were performed, on a pair of similar specimens, they were placed in zip-loc bags until the extraction and recovery of asphalt could be carried out.

Extraction and Recovery of Asphalt Cement

The extraction of the asphalt from asphalt-aggregate mixture was carried out, using trichloroethylene (TCE) as a solvent, as per Texas method TEX-210-F (equivalent to ASTM D2172). The asphalt was recovered from the solution containing asphalt and solvent following TEX-211-F (equivalent to ASTM D1856). The asphalt recovered from this method was collected in 90 ml penetration cans. The cans were shaken using a Vortex apparatus to remove air bubbles in asphalt cement. The cans were then allowed to cool down at room temperature.

Penetration Test

Penetration tests (Tex-502-C) were conducted on the recovered asphalt at a temperature of 25±0.1°C (77±0.2°F). The test specimen was kept in a container filled with distilled water and placed in a temperature-controlled chamber set at 25±0.1°C (77±0.2°F) for one hour. The specimen was then removed and tested for its penetration value. The test was repeated three times at three different locations. The average of the three values was considered the penetration of the asphalt cement.

Kinematic Viscosity Test

Kinematic viscosity (Tex-529-C) of the recovered asphalt was then measured at a temperature of 135±0.1°C (275±0.2°F). An oil bath was used to maintain the required temperature. A Zeitfuchs cross arm viscometer was placed in the oil bath. The asphalt specimen was preheated for fifteen minutes in an oven maintained at 150°C (302°F) and then was poured into the viscometer up to the fill mark. The asphalt was then held in the viscometer for fifteen minutes, by closing the narrow opening of the viscometer with a rubber stopper. After fifteen minutes the stopper was released to let the asphalt flow.

Evaluation of Setup

To evaluate the repeatability of the tests, thirty identical specimens were prepared and tested as per testing procedures explained above using the mix from El Paso. The repeatability of each method was evaluated by calculating its coefficient of variation from thirty tests. Table 3.3 shows the statistical parameters for the data collected from testing the thirty specimens.

Given the variation in VTM, the coefficients of variation were relatively moderate for the elastic modulus and IDT strength; however, for the kinematic viscosity and penetration, the variation was high. This was attributed to the presence of solvent and fines in asphalt, after the recovery process. To overcome the above problem, a procedure was conceived as described in Appendix C. The elapsed time, (after the final drop) during the recovery of asphalt cement, was increased from five minutes to fifteen minutes. This change was in agreement with the recommendations of Burr et al. (1990). The necessary precautions were taken to minimize the transfer of fines from extraction procedure to the asphalt-solvent solution, by providing two filters instead of a single filter.

Table 3.3 - Statistical Parameters for Data obtained from Thirty Specimens.

Parameter	VTM (percent)	Elastic Modulus (GPa)	IDT Strength (kPa)	Kinematic Viscosity (Cst)	Penetration (1/10 mm)
Average	3.75	49.3	280	291	85
Standard Deviation	0.17	6.3	29	53	30
Coefficient of Variation	4.5	12.8	10.3	18.3	35.3

The specimens were also centrifuged twice. The specimens were centrifuged for 60 minute during the first stage and for 30 minutes during the second stage. The speed of centrifuge during the first stage was increased from 2000 rpm to 3000 rpm. The speed of centrifuging during the second stage was kept at 2000 rpm.

The modifications in the new test procedure also include better temperature control on specimens during elastic modulus and IDTS measurements.

With the above modifications in the test procedures, better control was achieved on all the tests conducted on asphaltic concrete specimens, as well as, on asphalt binders. As a result of the changes described, the coefficients of variation of modulus, IDT strength, kinematic viscosity, and penetration were reduced to 5, 6, 10, and 9 percent, respectively.

As the coefficients of variation for both modulus and IDT strength are low, the average values of elastic moduli and IDT strengths obtained from the replicate specimens were considered in further chapters to analyze the data.

Chapter 4

Presentation and Discussion of Results

Introduction

As mentioned earlier, oven aging at 85°C was used to prepare the specimens. The specimens were aged for periods of 0, 1, 2, 7, and 28 days. At each aging period, nine pairs of specimens were prepared. Three different asphalt contents and three levels of VTM were used. The elastic modulus, strength, and penetration tests were conducted at 25±0.1°C, and kinematic viscosity was measured at 135±0.1°C (275±0.2°F). Based on the measurements made on all specimens, relationships amongst different parameters were developed. The results from all tests are included in Appendix D for completeness.

Aging Effects on Test Parameters

The variations in elastic moduli with aging period are illustrated in Figure 4.1. This figure contains three graphs corresponding to 4, 5, and 6 percent AC. To estimate the effects of VTM on the modulus during the aging process, three sets of data representing 3, 5, and 7 percent VTM are included in each graph. In all three graphs, the aging period is represented on a logarithmic scale. In all cases, the modulus increases with the aging period. This is expected, because the aging process hardens the mix resulting in an increase in the modulus.

Figure 4.1a, shows that at a given aging period the moduli from specimens with a 3 percent VTM are greater than those with a 5 percent VTM, which in turn are larger than those with a 7 percent VTM. This reveals that modulus decreases with the increase in the VTM of a mix. An increase in the VTM results in a decrease in the bulk density, causing a decrease in the modulus. The Y-intercept and slope of each fitted line correspond to the value of the modulus, after one day of aging and the rate of increase in the modulus with aging period, respectively. Table 4.1 shows the intercept and slope of each fitted line.

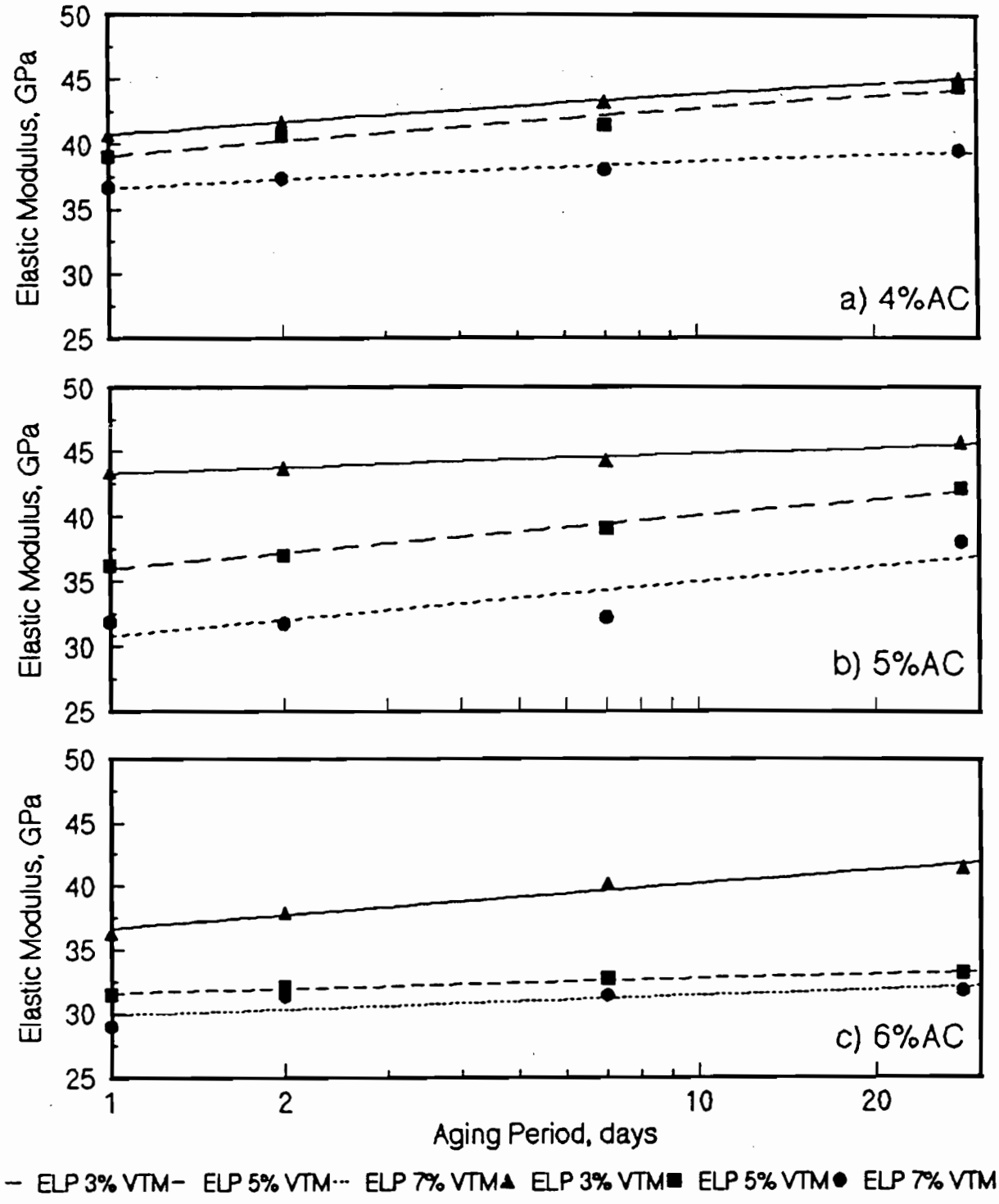

Figure 4.1 - Typical Variation in Elastic Modulus with Aging Period for El Paso Mix.

Table 4.1 - Intercepts and Slopes of Relationship between Elastic Modulus and Aging Period for 4, 5, and 6 percent Asphalt Contents.

Asphalt Content, percent	VTM, percent	Intercept*, GPa	Slope, GPa/log(days)
4	3	40.7	1.34
	5	39.0	1.57
	7	36.6	0.87
5	3	43.3	0.66
	5	35.9	1.80
	7	30.8	1.80
6	3	36.6	1.53
	5	31.6	0.49
	7	29.8	0.67

* Intercept @ 1 day Aging Period.

Considering the slopes, the rate of increase in modulus corresponding to data with a 3 percent VTM is lower than that of a fitted line for a mix with 5 percent VTM. This implies that the rate of change in modulus with the aging period is related to the VTM. However, the slope of the line corresponding to the specimens with a 5 percent VTM is higher than the slope for the specimen with a 7 percent VTM. This can be attributed to the fact that because of high VTM, most of the age hardening occurs within the first 24 hours of oven aging.

Figure 4.1b represents the variation in modulus with aging period for a mix having a 5 percent AC. Trends similar to those observed in the above case, are experienced. Higher moduli are observed for specimens with lower VTM's. As shown in Table 4.1, the rate of increase in modulus is higher for specimens with a 5 percent VTM, as compared to specimens with a 3 percent VTM. The rate of increase in modulus with time is similar for specimens with 5 and 7 percent VTM.

As shown in Figure 4.1c, for specimens with a 6 percent asphalt content the modulus at any aging period increases with a decrease in the VTM of the mix. From Table 4.1, the rate of increase in stiffness for specimens with a 3 percent VTM is faster than the specimens with a 5 percent VTM. However, the rate is lower for specimens with a 5 percent VTM as compared to those with a 7 percent VTM.

In general, it can be concluded that the modulus of any mix increases with aging period, and the moduli decrease with an increase in the VTM. A linear relationship between modulus and the

logarithm of aging period exists; however, the slope of this relationship varies with the VTM and the AC content.

To better quantify the aging effects on stiffness, modulus values at different aging periods were transformed into modulus ratio (M.R.). In a similar way, IDT strength, kinematic viscosity, and penetration, values were also transformed into strength ratio (S.R.), aging index (A.I.), and retained penetration (R.P.). The following equations are used to attain the transformed values:

$$M.R. = \frac{Modulus\ of\ aged\ mix}{Modulus\ of\ original\ mix} \tag{4.1}$$

$$R.P. = \frac{Penetration of\ aged\ asphalt}{Penetration of\ original\ asphalt} \tag{4.2}$$

$$A.I. = \frac{Kinematic viscosity\ of\ aged\ asphalt}{Kinematic viscosity\ of\ original\ asphalt} * 100 \tag{4.3}$$

$$S.R. = \frac{IDT\ strength\ of\ aged\ mix}{IDT\ strength\ of\ original\ mix} \tag{4.4}$$

In the following sections, the effects of aging period on modulus ratio, strength ratio, aging index, and retained penetration for El Paso mix with 5 percent AC content are illustrated as typical examples (see Figures 4.2 through 4.5).

Each figure contains three sets of data corresponding to 3, 5, and 7 percent VTM. The y-axis in each case represents the change in the value of a parameter, due to aging with respect to its virgin value. The slope of each line depicts the rate of increase in the respective parameter, due to aging, i.e. a steeper slope implies a higher sensitivity to aging and vice versa. The intercepts and slopes of lines corresponding to each parameter are shown in Table 4.2.

Modulus Ratio

Figure 4.2 illustrates the variation in the modulus ratio with the aging period. From Table 4.2, the intercept corresponding to specimens with a 3 percent VTM is approximately the same, as the ordinate corresponding to specimens with a 5 percent VTM. These values are smaller than that of the intercept for specimens with a 7 percent VTM. This reveals that the increase in modulus from its virgin value, is slightly higher due to aging, for a mix with a higher VTM. The slope of the line corresponding to data with a 3 percent VTM is less steep as compared to those with a 5 percent and a 7 percent VTM's. However, the slopes of lines from mixes with 5 percent and 7 percent VTM's are similar.

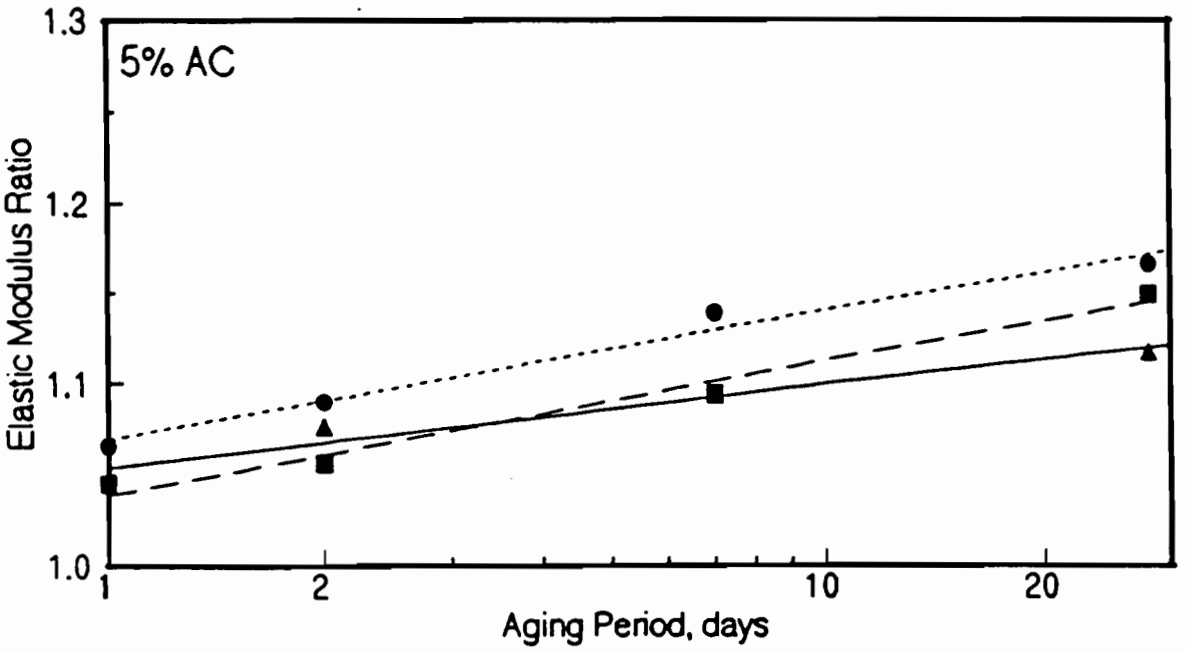

Figure 4.2 - Typical Variation in Modulus Ratio with Aging Period.

Table 4.2 - Intercepts and Slopes of Relationship between Modulus Ratio, Strength Ratio, Aging Index, and Retained Penetration with Aging Period (El Paso Mix, 5 percent AC Content).

Parameter	VTM, percent	Intercept*	Slope
Modulus Ratio	3	1.05	0.002
	5	1.04	0.032
	7	1.07	0.031
Strength Ratio	3	0.96	0.163
	5	1.01	0.290
	7	1.02	0.340
Aging Index	3	0.96	0.210
	5	1.06	0.260
	7	0.93	0.476
Retained Penetration	3	93.63	-9.690
	5	89.40	-10.890
	7	90.16	-14.890

* Intercept @ 1 day Aging Period.

Strength Ratio

Figure 4.3 shows the change in strength ratio, due to the aging period. Also shown is the best fit line to data from each VTM. The lines do not represent the measured data well. It seems that initially the rate of increase in strength is small and after several days the rate increases. In general, the rate of increase in strength for specimens with a 3 percent VTM is smaller than for a 5 percent VTM. Similarly, the effects of aging are more pronounced for specimens with a 7 percent VTM, as compared to those with a 5 percent VTM.

Aging Index

Figure 4.4 exhibits the effects of the aging period on aging index. As in the cases of modulus ratio and strength ratio, the viscosity increases with the increase in aging period. Similar to the strength ratios, the increase in kinematic viscosity accelerates after seven days of aging. During the initial days of aging, the aging index is not related to the VTM, but for longer aging periods, the aging index is larger for mixes with higher VTM's.

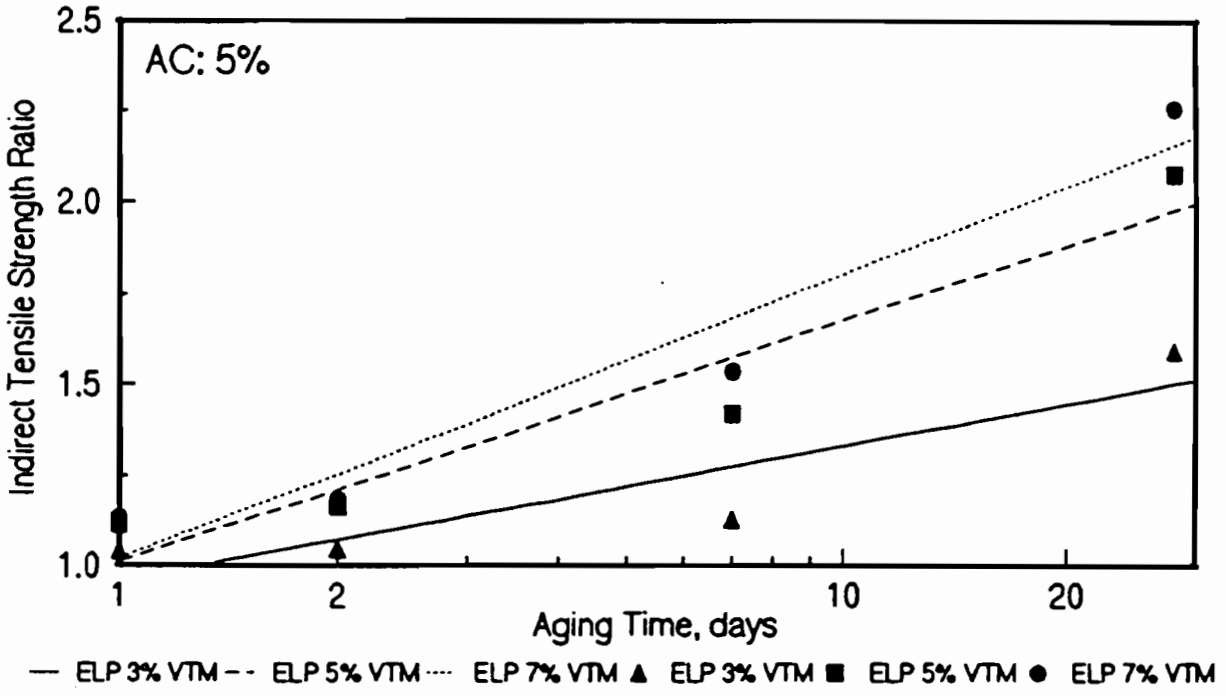

Figure 4.3 - Typical Variation in IDT Strength Ratio with Aging Period.

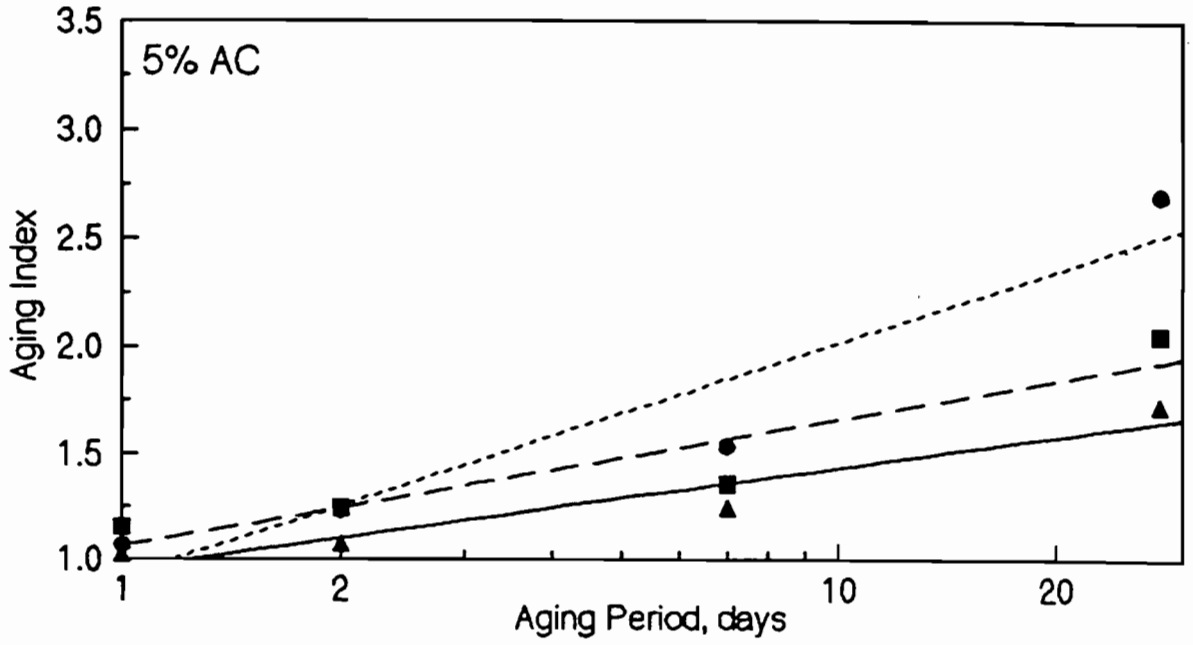

Figure 4.4 - Typical Variation in Aging Index with Aging Period.

Retained Penetration

Figure 4.5 demonstrates the variation in retained penetration with aging period. An inverse relationship exists between those two parameters. The asphalt hardens with age; hence its penetration values become smaller. Similar to the modulus ratio/aging relationship, the intercept decreases with an increase in the VTM of the mix. This shows that the aging effects are more pronounced for mixes with higher VTM's. The slope of the line for a 3 percent VTM is lower, when compared to those for a 5 or 7 percent VTM. The slope corresponding to the mix with a 5 percent VTM is less steep, than that of the mix with a 7 percent VTM.

Relationship Between Mix Properties and Rheological Parameters

Figure 4.6 shows a typical relationship between the elastic modulus and penetration for two specimens prepared similarly. The two specimens exhibit similar behavior. An inverse linear relationship between the elastic modulus and the logarithm of penetration is evident. Due to aging of asphaltic concrete mixture, the asphalt becomes harder; hence the elastic modulus increases with a corresponding decrease in the value of penetration. Practically speaking, the penetration of the asphalt in a mix can be obtained from elastic modulus without a need for the recovery of asphalt.

Figure 4.7 shows the variation in modulus ratio with retained penetration for the two specimens shown in Figure 4.6. The results from the two specimens are quite similar. Similar behavior has been observed for other combinations of VTM and AC content. However, the relation between the modulus and penetration changes with the type, the asphalt content, and the VTM of the mix.

A typical relationship between the elastic modulus and kinematic viscosity is shown in Figure 4.8. A linear relationship more or less exists between the modulus and the logarithm of viscosity. The values in Figure 4.8 are transformed into modulus ratio and aging index, and the relationship is shown in Figure 4.9. A linear relationship exists between the relative values as well. This is expected because the viscosity-aging period shown in Figure 4.4 exhibited this type of relationship. Once again, the trend observed in the two figures are representative of mixes with other VTM's and AC contents.

The data obtained from testing a pair of specimens using El Paso mix with a 5 percent AC and a 5 percent VTM were considered to explain typical relationship between IDT strength and penetration. Figure 4.10 shows the variation in IDT strength with penetration. A bi-linear relationship exists between the strength and the logarithm of penetration as observed in the previous section. Similarly, from the same figure, the penetration of the AC can be estimated knowing the strength of the mix.

The relationship between strength ratio and retained penetration is shown in Figure 4.11. The two specimens exhibit similar behavior; however, the results deviate from a line.

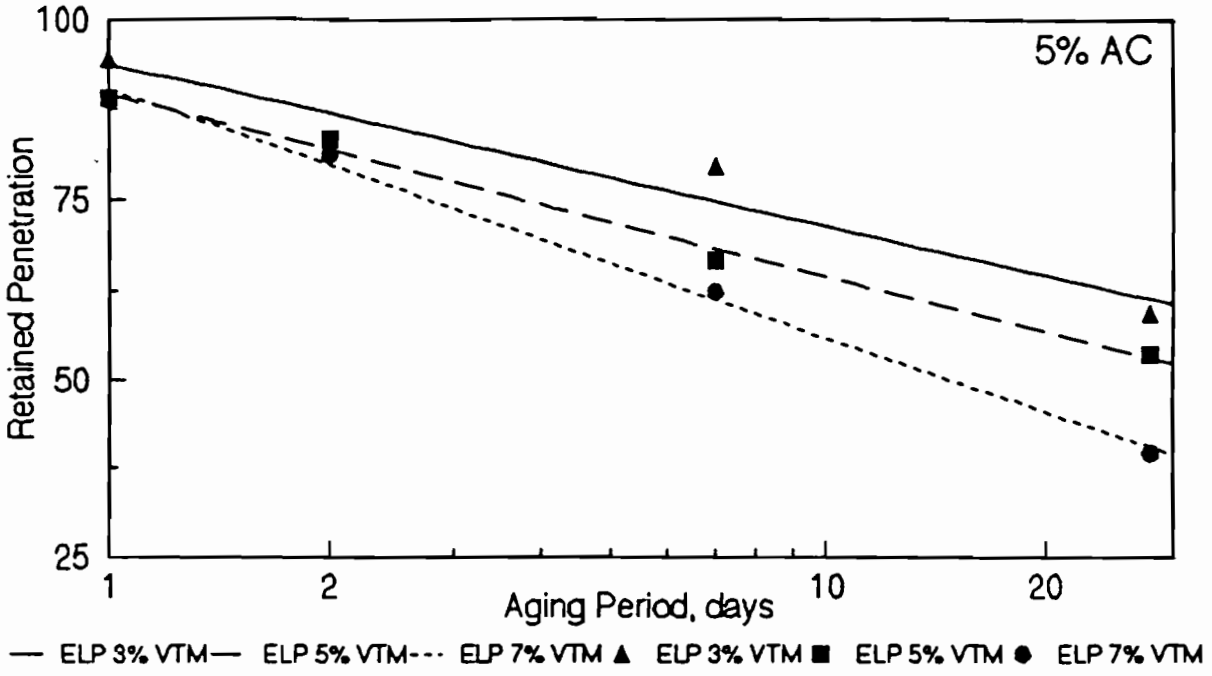

Figure 4.5 - Typical Variation in Retained Penetration with Aging Period.

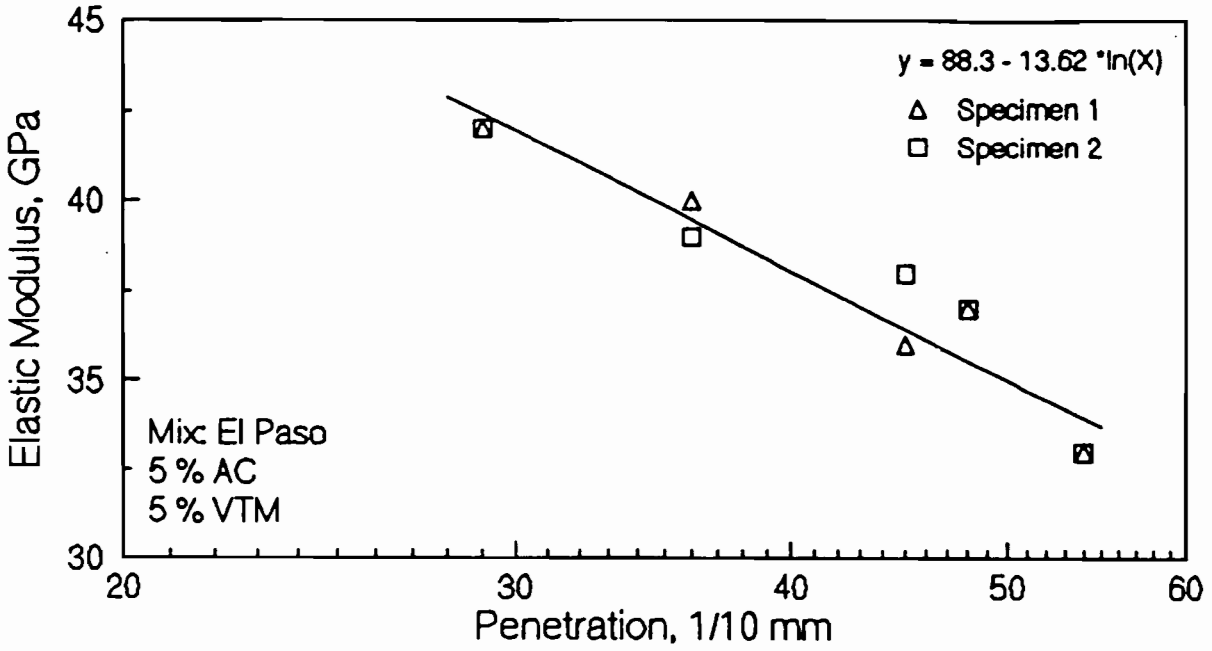

Figure 4.6 - Typical Variation in Elastic Modulus with Penetration for El Paso Mix.

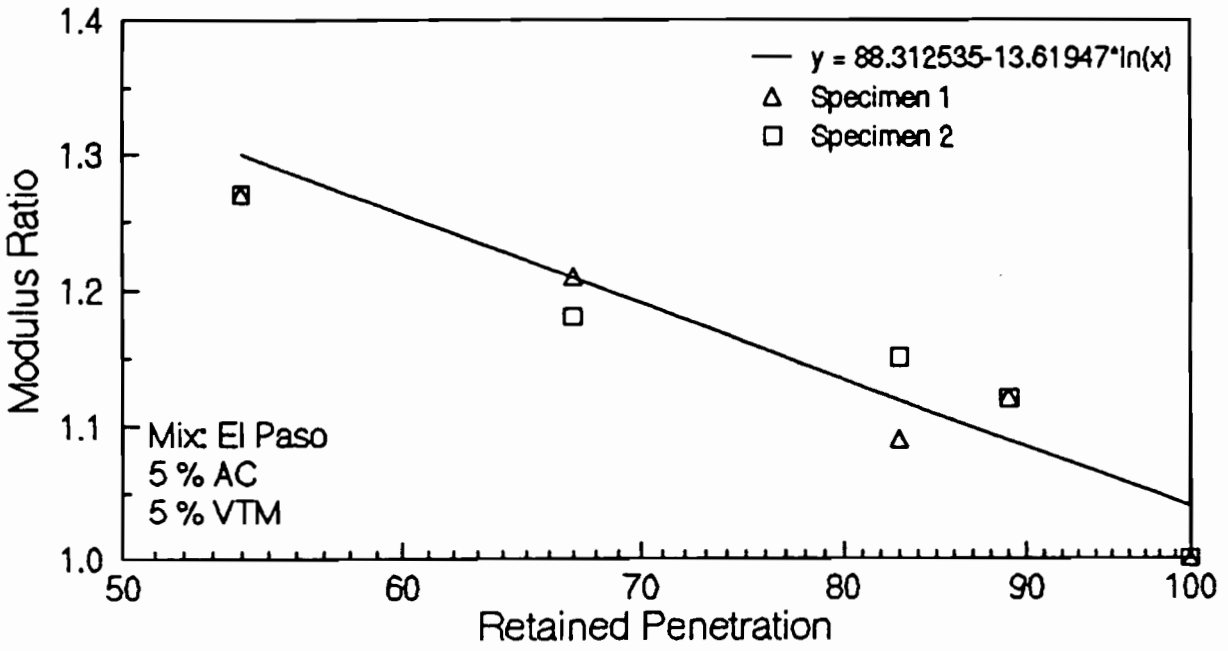

Figure 4.7 - Typical Variation in Modulus Ratio with Retained Penetration for El Paso Mix.

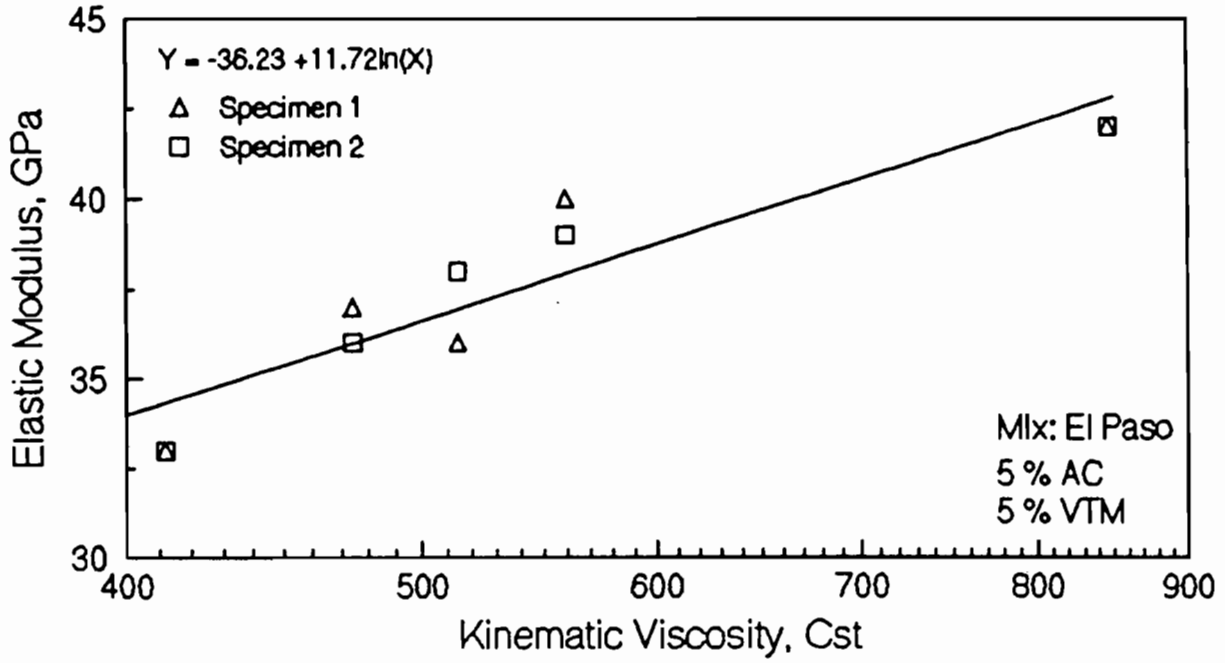

Figure 4.8 - Typical Variation in Elastic Modulus with Kinematic Viscosity for El Paso Mix.

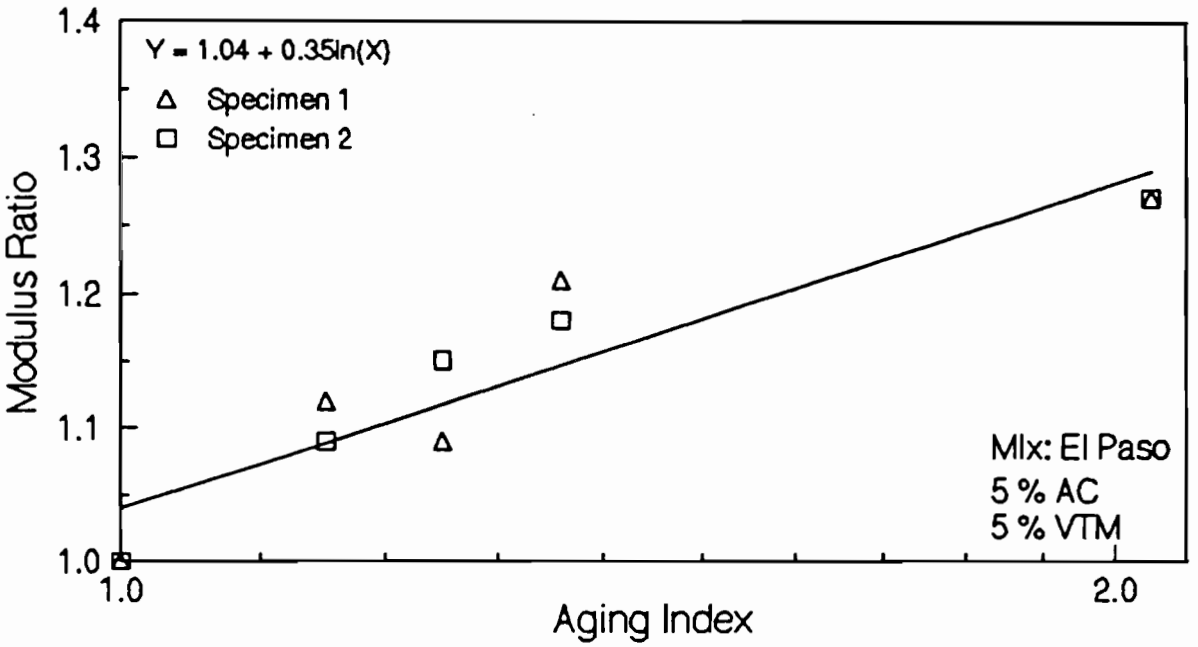

Figure 4.9 - Typical Variation in Modulus Ratio with Aging Index for El Paso Mix.

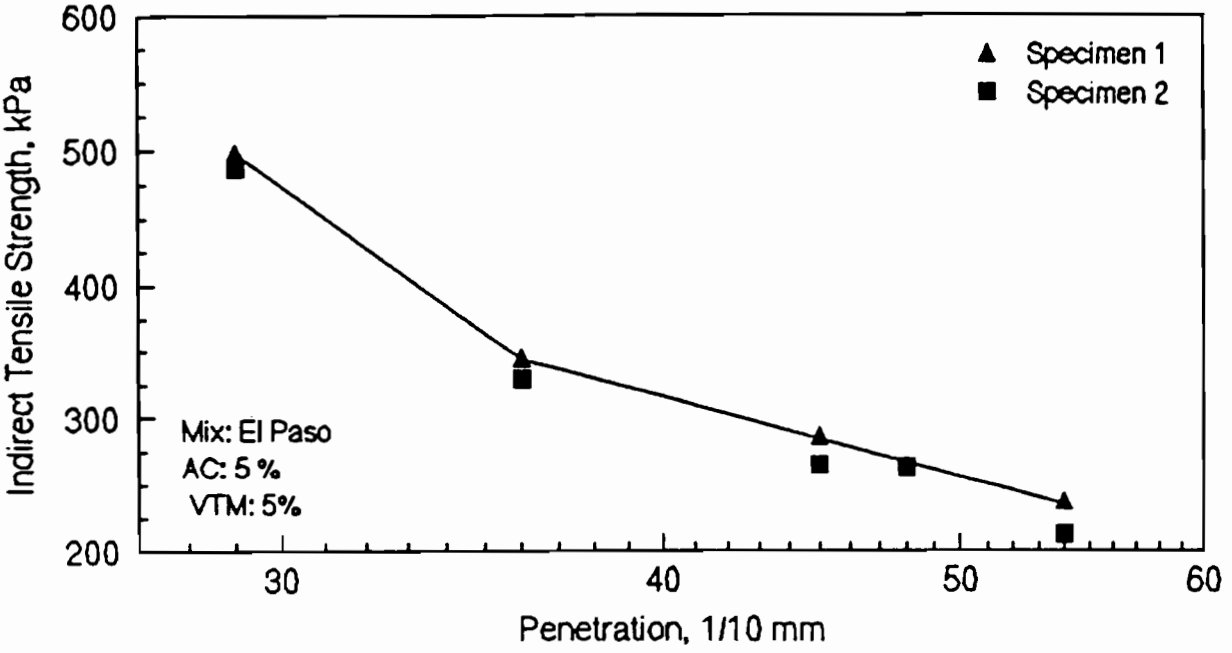

Figure 4.10 - Typical Vairation in IDT Strength with Penetration for El Paso Mix.

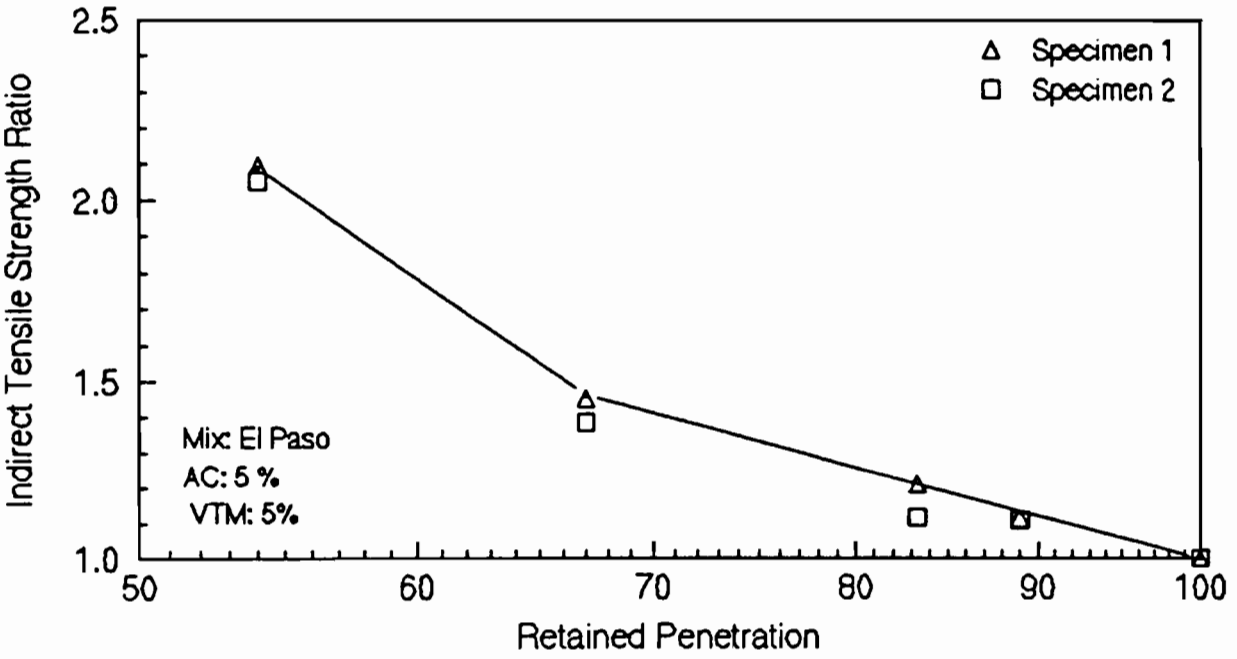

Figure 4.11 - Typical Variation in IDT Strength Ratio with Retained Penetration for El Paso Mix.

A typical relationship between the IDT strength and kinematic viscosity is shown in Figure 4.12 and the relation between the transformed values, i.e. strength ratio and aging index, is shown in Figure 4.13. As in the case of modulus with viscosity, a direct relationship exists between the strength and viscosity and between their transformed values.

Effect of Asphalt Content

In this section, the effects of asphalt content on the relationship between the elastic modulus and penetration are explained. The results corresponding to specimens with a 5 percent VTM are shown here. However, similar trends were found for other VTM's. Figure 4.14 represents the variation in modulus with penetration. Three sets of data corresponding to specimens containing 4, 5, and 6 percent asphalt contents are shown. To evaluate the variation in modulus with penetration, the slopes and intercepts of the lines are shown in Table 4.3. The intercepts corresponding to 4 and 5 percent AC contents are similar. At a given penetration, the moduli from mixes with 4 and 5 percent AC contents are similar; whereas, the modulus for a mix with a 6 percent AC are lower. This reveals that higher modulus can be expected in case of mixes with lower asphalt contents at a given penetration. Basically, a linear relationship exists between modulus and penetration for a given AC content and a given VTM. However, this relationship has to be established through laboratory tests.

The effect of asphalt content can also be examined from the relationship between the elastic modulus and kinematic viscosity for the specimens with 5% VTM. The effect of asphalt content, using the above relationship along with the relationship between IDT strength with rheological parameters for the specimens with 5 percent VTM, are shown in Appendix D. However, similar conclusion as obtained in the case of relationship between modulus and penetration can be drawn.

Table 4.3 - Intercepts and Slopes of Relationships between Elastic Modulus and Penetration for mixes with 5 percent VTM.

Parameter	Asphalt Content, percent	Intercept*, GPa	Slope, GPa/log (penetration)
Elastic Modulus	4	45.81	-11.0
	5	46.08	-13.6
	6	34.00	-4.1

* Intercept Corresponding to a Penetration of 22.

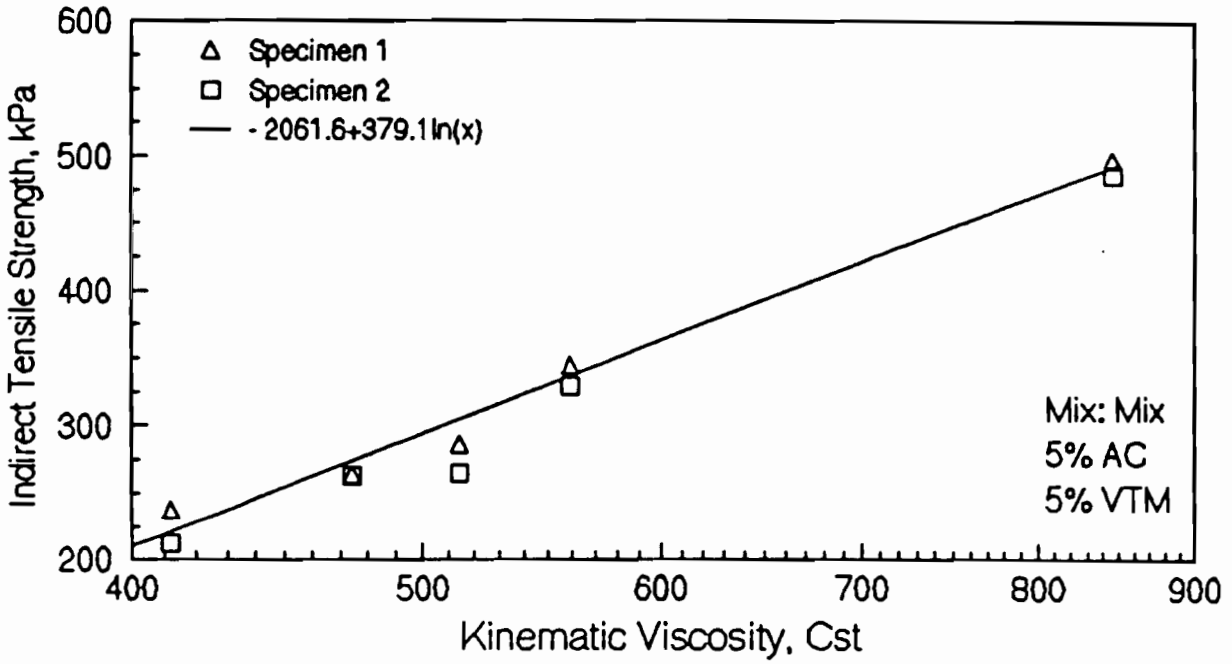

Figure 4.12 - Typical Variation in IDT Strength with Kinematic Viscosity for El Paso Mix.

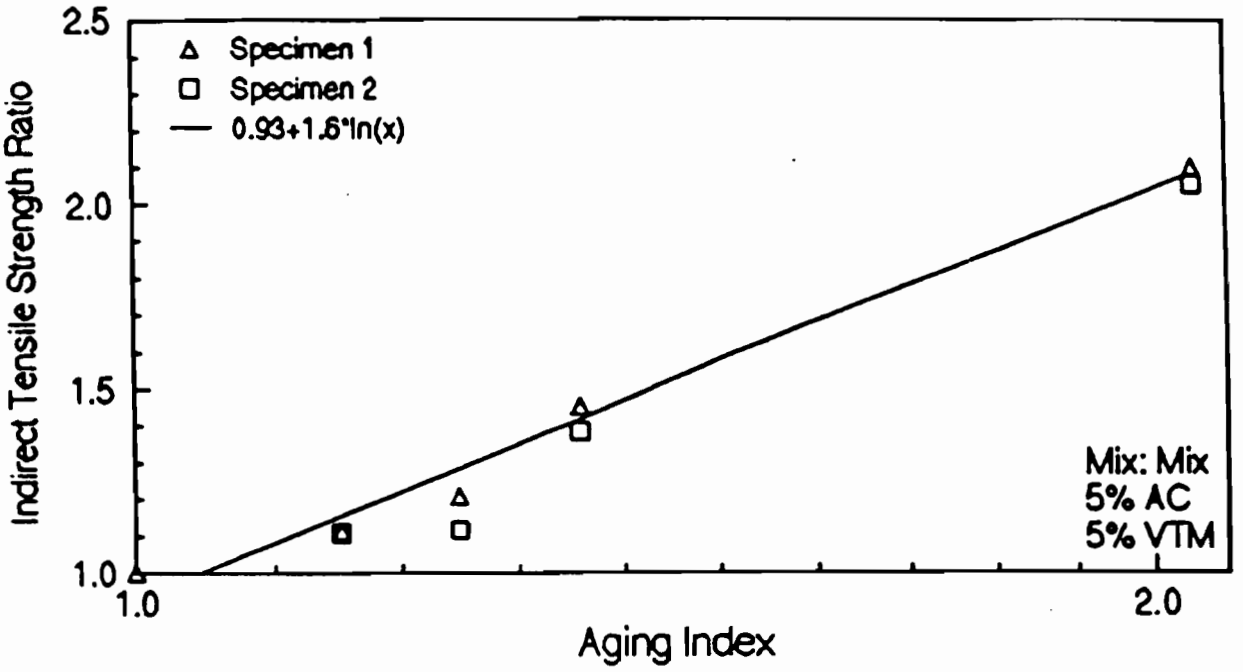

Figure 4.13 - Typical Variation in IDT Strength Ratio with Aging Index for El Paso Mix.

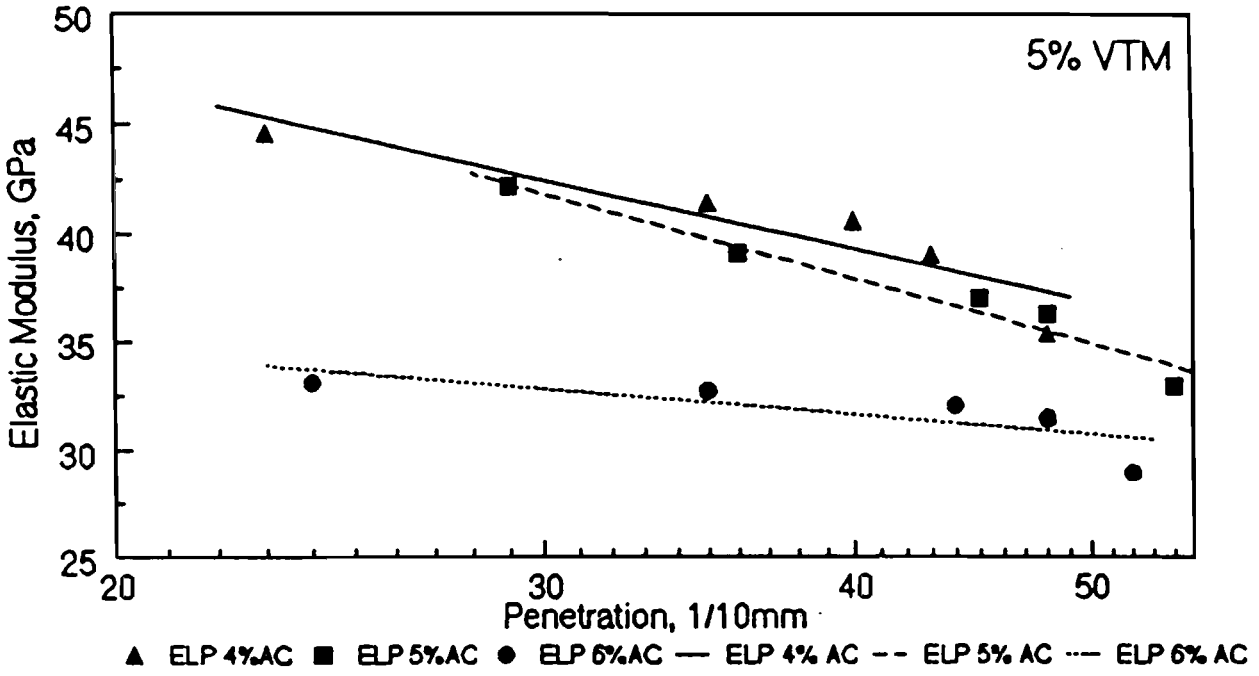

Figure 4.14 - Effect of Asphalt Content on the Relationship of Elastic Modulus and Penetration for El Paso Mix.

Effects of VTM

To illustrate the effects of VTM, data obtained, using El Paso mix for specimens with 5 percent asphalt content and 3, 5, and 7 percent VTM's, are considered in Figure 4.15. It is reasonable to consider a linear relationship for data corresponding to each VTM. The slope and intercept values are presented in Table 4.4. At a given penetration, the modulus corresponding to a higher VTM is lower. Once again, the slopes of the line are not related to the VTM; therefore, each model should be individually calibrated.

Similar observations can be made through the relationships between a) elastic modulus and kinematic viscosity, b) IDT strength and penetration, and c) IDT strength and kinematic viscosity. These relationships are shown graphically in Appendix D. In most cases, modulus/IDT strength corresponding to a higher VTM is lower, for a given value of penetration or kinematic viscosity.

Table 4.4 - Intercepts and Slopes of Relationships between Elastic Modulus and Penetration for mixes with 5 percent Asphalt Content.

Parameter	Percent VTM	Intercept*, GPa	Slope, GPa/log (penetration)
Elastic Modulus	3	49.93	-8.0
	5	47.40	-13.6
	7	38.00	-8.6

* Intercept Corresponding to a Penetration of 20.

Analysis of Parameters

Different parameters, that affect the relationship between modulus or IDT strength with penetration and kinematic viscosity, were analyzed for their correlation coefficients using Statistical Analysis Software (SAS). As explained in Chapter 3, low coefficients of variation were observed in the case of modulus and IDT strength results. After the measurements for modulus and IDT strength were taken, the two replicate specimens were combined to extract enough asphalt for further testing on asphalt, since no replicate specimens were available for penetration and kinematic viscosity values. Due to the above two reasons, the values of modulus and IDT strength from the replicate specimens were averaged. These average values were considered for statistical analysis. To determine the influence of different testing variables, a correlation analysis was performed. The outcome of the correlation analysis for the results obtained using El Paso and Austin mixes are presented in Table 4.5. Similarly, to exemplify the data for any mix, the data for both mixes were treated as one mix and analyzed. The corresponding correlation coefficients are also presented in the table. The values in the tables indicate the significance of the corresponding testing variable. The positive sign symbolizes that the variable is in a direct relationship with modulus/IDT strength, while the negative sign illustrates that the variable is in an inverse relationship.

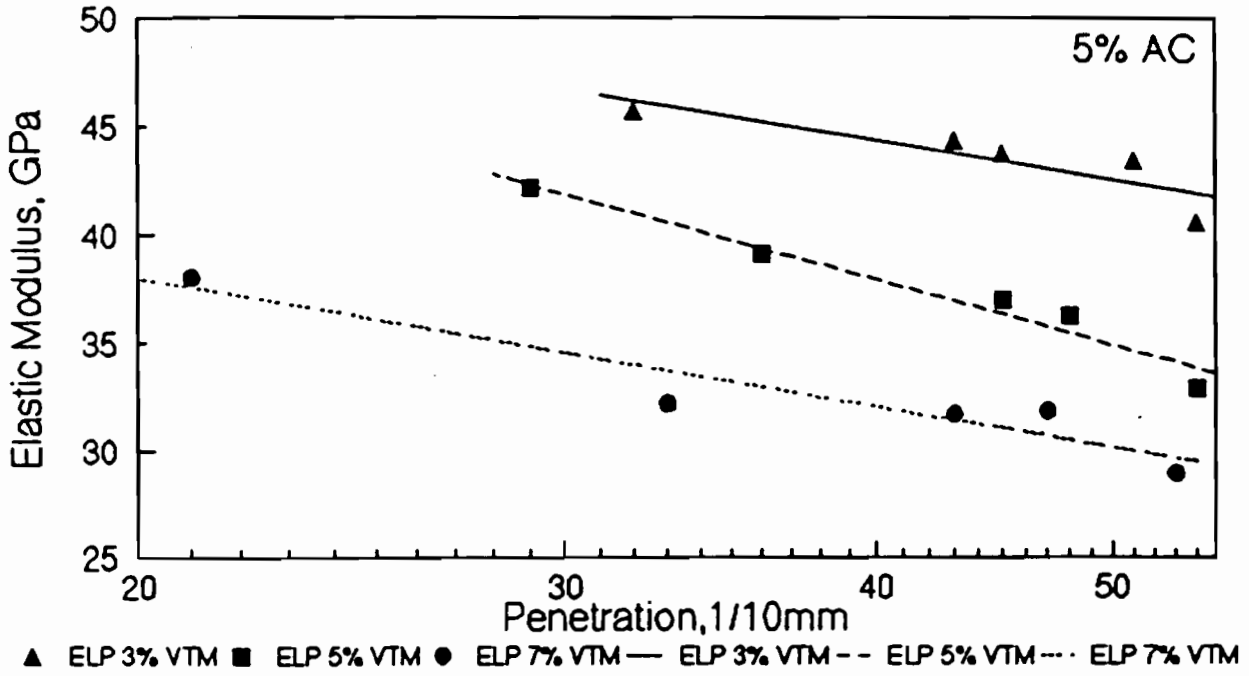

Figure 4.15 - Effects of Voids in Total Mix on the Relationship between Elastic Modulus and Penetration for El Paso Mix

In Table 4.5, the effect of asphalt content and VTM on modulus is more evident from the El Paso mix, than in the case of the Austin mix. However, the combined data also reveals that the elastic modulus is affected by both the percent asphalt content and percent VTM of the mix. In all the three cases, the effect of VTM is more pronounced relative to asphalt content, but the effect of asphalt content was dominant on the results of IDT strength. The relation between modulus/IDT strength with the rheological parameters can also be found in the table. The correlation for penetration and kinematic viscosity with modulus in Austin mix is low compared to that of the El Paso mix. However, the correlation with rheological parameters with IDT strength is moderately high in the case of either mixes and even for the combined data. The aging period clearly affects both the modulus and the IDT strength. From Table 4.5, the asphalt content and VTM more or less influence the relationship between modulus/IDT strength and penetration, or kinematic viscosity. This dependency vary with the type of mix and may have to be determined using multi-regression analyses.

Table 4.5 - Pearson Correlation Coefficients for Modulus and IDT Strength.

Mix Source	Parameter	Percent AC	Percent VTM	Penetration	Kinematic Viscosity	Aging Period
Austin	Elastic	-0.03	-0.22	-0.52	0.59	0.57
	IDT Strength	-0.45	-0.04	-0.78	0.76	0.81
El Paso	Elastic	-0.53	-0.67	-0.29	0.23	0.37
	IDT Strength	-0.59	-0.19	-0.75	0.71	0.71
Austin & El Paso	Elastic	-0.30	-0.50	-0.32	0.37	0.46
	IDT Strength	-0.42	-0.06	-0.81	0.75	0.66

Chapter 5

Development of Prediction Models

Introduction

Based on the relationships observed amongst different testing parameters in the previous chapter, statistical analyses were performed on the experimental data to develop prediction models. These models were also evaluated in terms of predicting the rheological properties of the asphalt cement.

Prediction Models Using Elastic Modulus

Analyses of normality were performed on the data obtained from both mixes used in this study to ensure that the data collected is normal, otherwise many of the statistics used may not be applicable. As a result some of the test parameters were transformed.

To develop the most representative models, a correlation analyss between all parameters was performed, and the significant parameters were selected for use in the models. The data were analyzed for each mix individually as well as by combining them.

The general model that best relates the modulus with the penetration of the binder, asphalt content, and VTM was found to be

$$E = a_1 + a_2 * Log(P) + a_3 * (AC) + a_4 * (VTM) \quad (5.1)$$

where
E = elastic modulus (GPa),
P = penetration (1/10 mm),
AC = asphalt content (percent), and
VTM = voids in the total mix (percent).

Parameters a_1, a_2, a_3, and a_4 are model parameters determined from a multi-variant best fit process.

Similarly, the elastic modulus can be related to the kinematic viscosity, asphalt content, and VTM through

$$E = b_1 + b_2 * Log(\eta) + b_3 * (AC) + b_4 * (VTM) \qquad (5.2)$$

where η = kinematic viscosity (Cst) and b_1, b_2, b_3, and b_4 are once again model parameters.

The above general equations were applied to data from each individual mix, as well as, to those of the combined mixtures. The best-fit parameters are included in Tables 5.1 and 5.2 for penetration and viscosity, respectively.

Table 5.1 - Fit Parameters Relating Elastic Modulus to Penetration, Asphalt Content, and VTM for Specimens Tested.

Mix	Fit Parameters*				Fit Quality		
	a_1	a_2	a_3	a_4	R^2	Root	F
Combined	63920	-6675	-1782	-1724	0.52	3262	31
Austin	53505	-7536	-350	-1028	0.40	3406	9
El Paso	89148	-18189	-2553	-2158	0.85	2051	75

* See Equation 5.1

Table 5.2 - Fit Parameters Relating Elastic Modulus to Kinematic Viscosity, Asphalt Content and VTM for Specimens Tested.

Mix	Fit Parameters*				Fit Quality		
	b_1	b_2	b_3	b_4	R^2	Root MSE	F
Combined	33915	7220	-1802	-1747	0.60	3018	41
Austin	23115	6984	-349	-1033	0.48	3168	12
El Paso	22934	13957	-2837	-2101	0.85	2027	78

* See Equation 5.2

define the quality of the model. Tables 5.1 and 5.2 contain these values for the models relating the elastic modulus to penetration and kinematic viscosity, respectively. The R^2 values are low for the model with combined data and for the model with Austin mix data. However, the value of R^2 for the El Paso mix is high, indicating that the model fits the data well. The root MSE, which is a measure of the spread or dispersion of the data, was found to be large in cases of models with combined data and Austin data, relative to El Paso data. Similarly, F-value, the test of significance, is low for model with Austin data, and moderate for combined data. However, the F-value is considered as large for El Paso data.

Equations 5.1 and 5.2 were then algebraically solved to determine penetration or kinematic viscosity of the asphalt. The new equations for penetration and kinematic viscosity are as follows:

$$P = \frac{10^{E - a_1 - a_3 \cdot (AC) - a_4 \cdot (VTM)}}{a_2} \tag{5.3}$$

$$\eta = \frac{10^{E - b_1 - b_3 \cdot (AC) - b_4 \cdot (VTM)}}{b_2} \tag{5.4}$$

To evaluate the quality of the models, the predicted rheological values from Equations 5.3 and 5.4 are compared with the actual values in Figure 5.1a. To further clarify the extent of errors, a histogram of percent error between calculated and actual values was also developed as shown in Figure 5.1b. The percent error is the ratio of absolute difference in actual and predicted values to the actual value expressed in percent. In Figure 5.1a, few of the data points are enclosed within a 30 percent error band, and most of the data, especially at lower penetrations, fell well outside the 30 percent error band. The histogram, shown in Figure 5.1b, indicates that about 17 percent of the penetrations are predicted within 30 percent of actual values. The data associated with lower penetrations are especially very poorly predicted.

To improve the quality of the models, eight data points were eliminated, assuming that the model cannot satisfactorily predict lower penetrations with respect to the rest of the data in El Paso and Austin mixes. The corresponding fit parameters for the new model are shown in Table 5.3.

Figure 5.2a shows the variation between the actual and predicted penetrations using the new model based on modulus. The number of data points located outside a 30 percent error band are reduced when compared with the previous model. A histogram of the prediction errors corresponding to combined data is shown in Figure 5.2a. About 29 percent of the data could be estimated within 30 percent error. This shows that the quality of the model is slightly improved by excluding data points with low penetration values. The models relating modulus to kinematic viscosity are also considerably improved by eliminating the outliers. This can be observed from Figure 5.3 and Figure 5.4. Figure 5.3 is drawn based on the model developed from combined data of two mixes using Equation 5.4. Similarly, Figure 5.4 is drawn based on the model developed from combined data after eliminating the outliers.

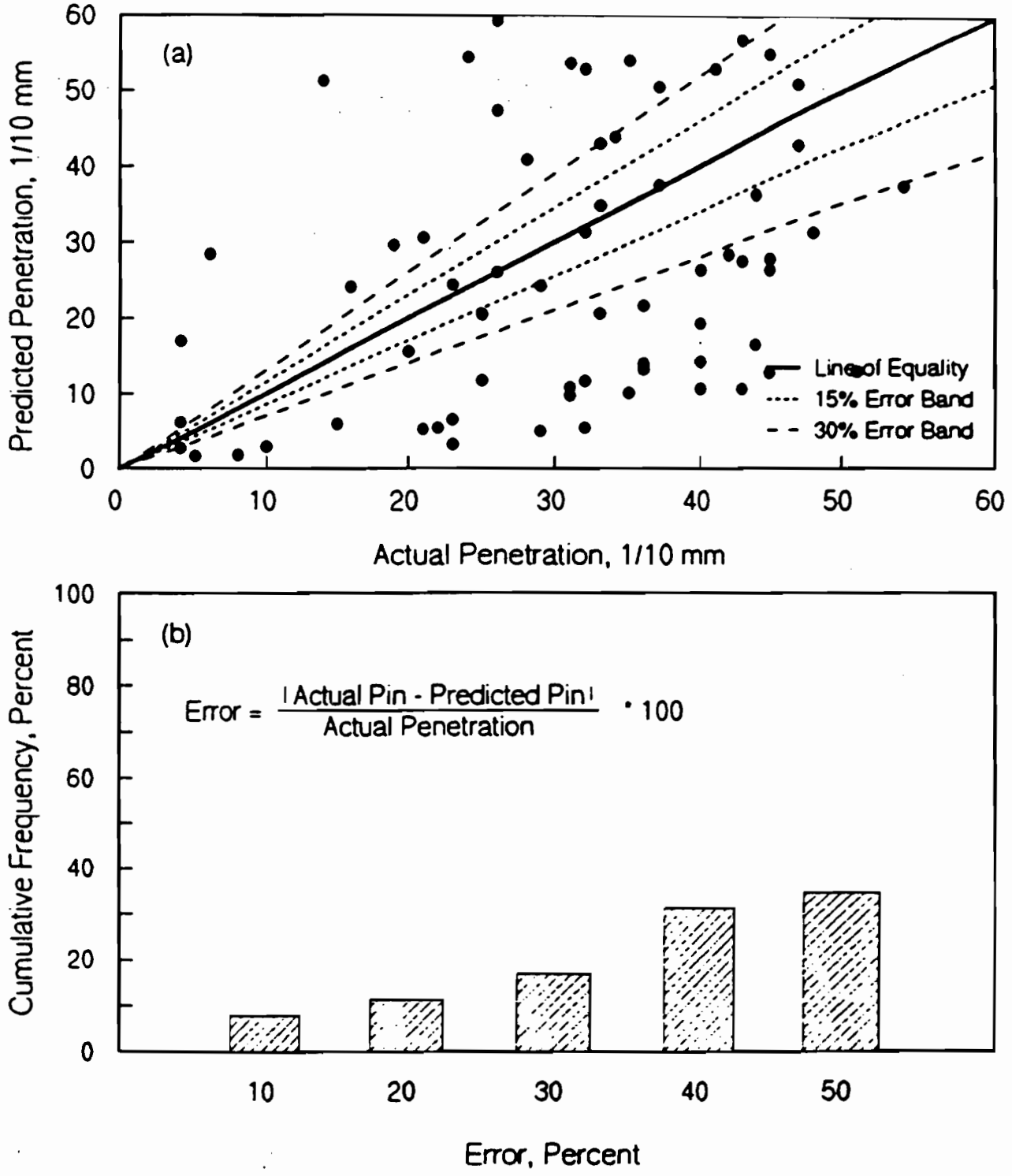

Figure 5.1 - Comparison of Actual and Predicted Penetration Values from Model Presented in Equation 5.1 for All Data a) Scatter Plot b) Cumulative Error.

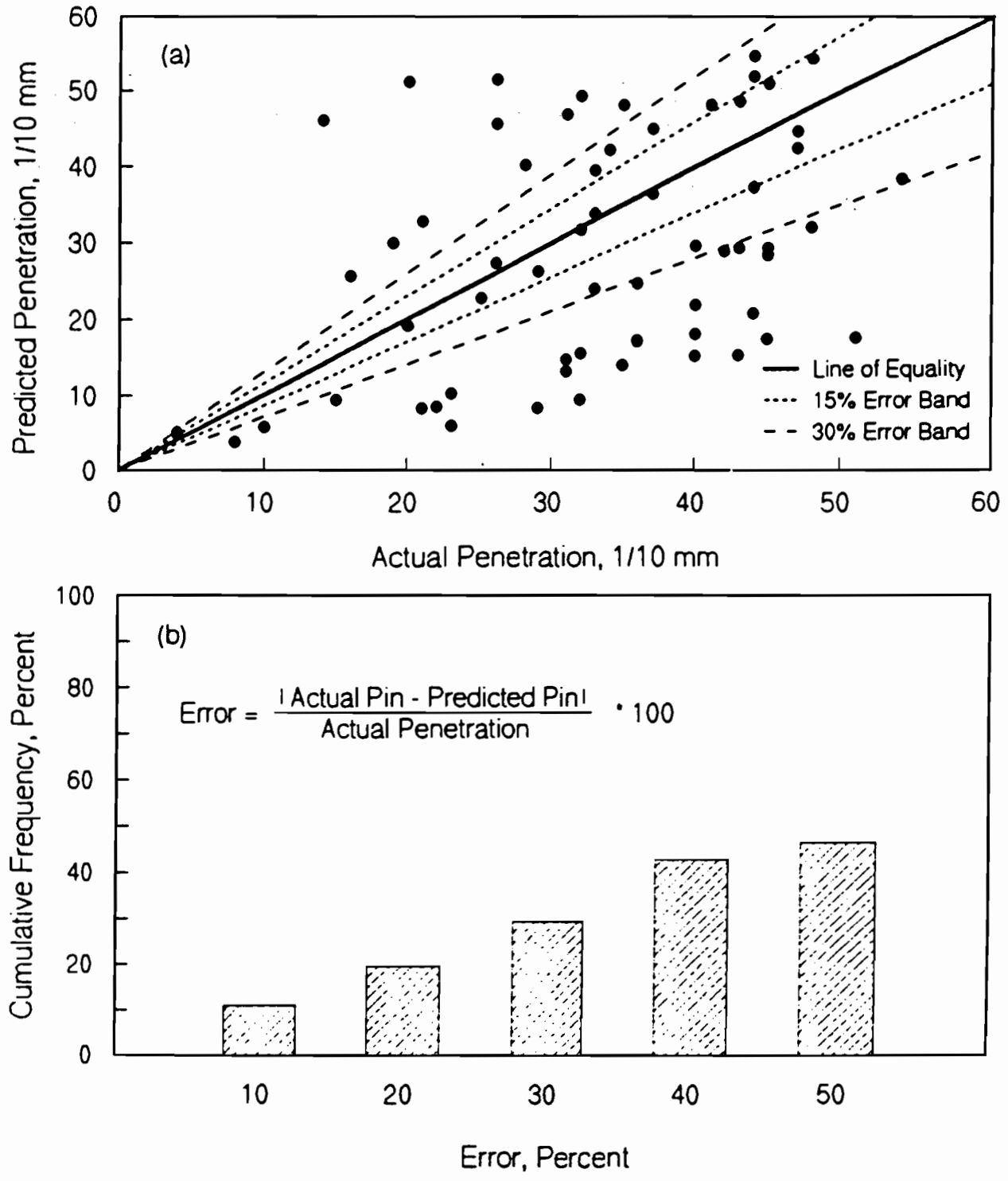

Figure 5.2 - Comparison of Actual and Predicted Penetration Values Using Equation 5.1 for All Data (without Outliers) a) Scatter Plot b) Cumulative Error

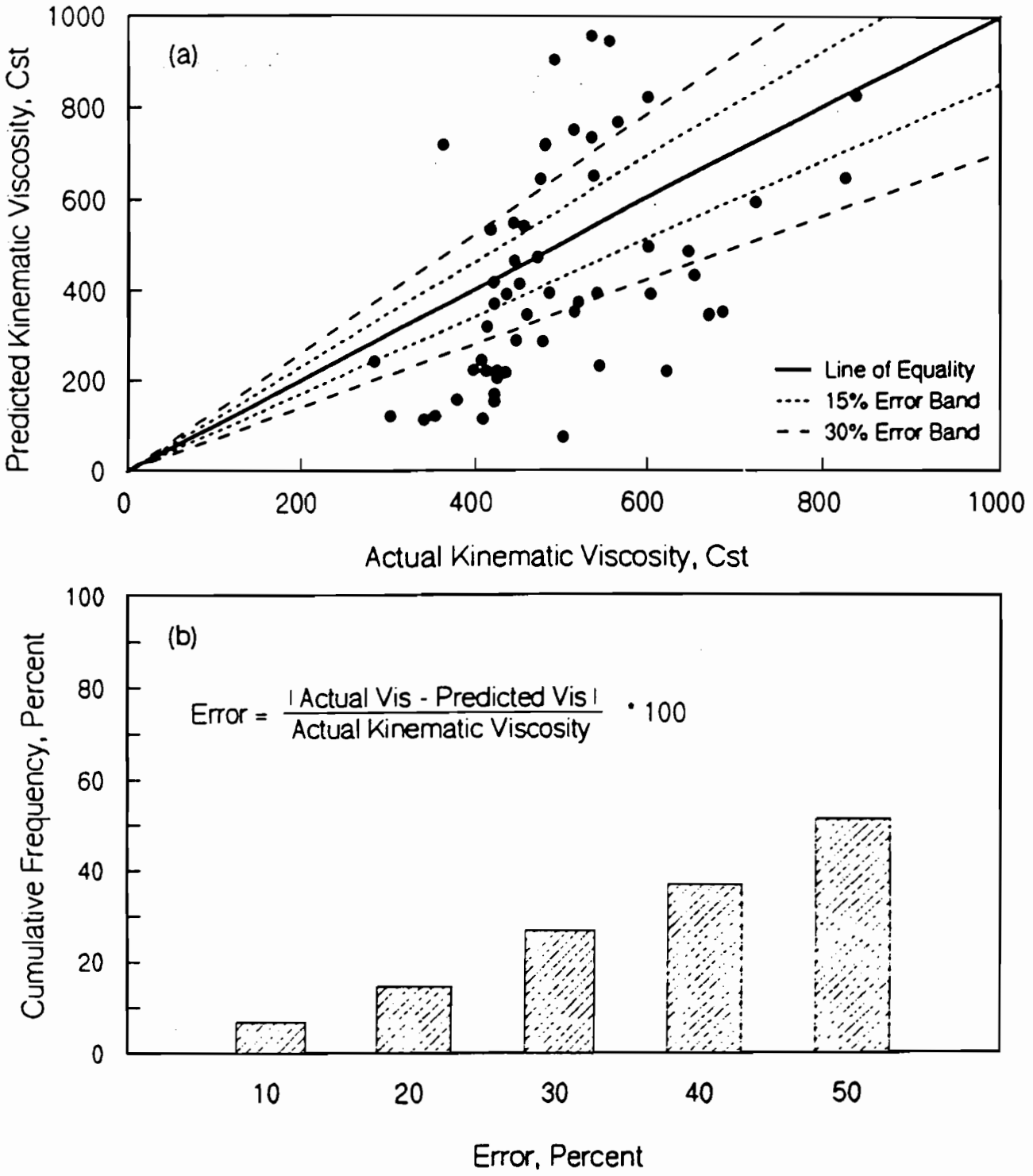

Figure 5.3 - Comparison of Actual and Predicted Kinematic Viscosity Values Using Equation 5.2 for All Data a) Scatter Plot b) Cumulative Error.

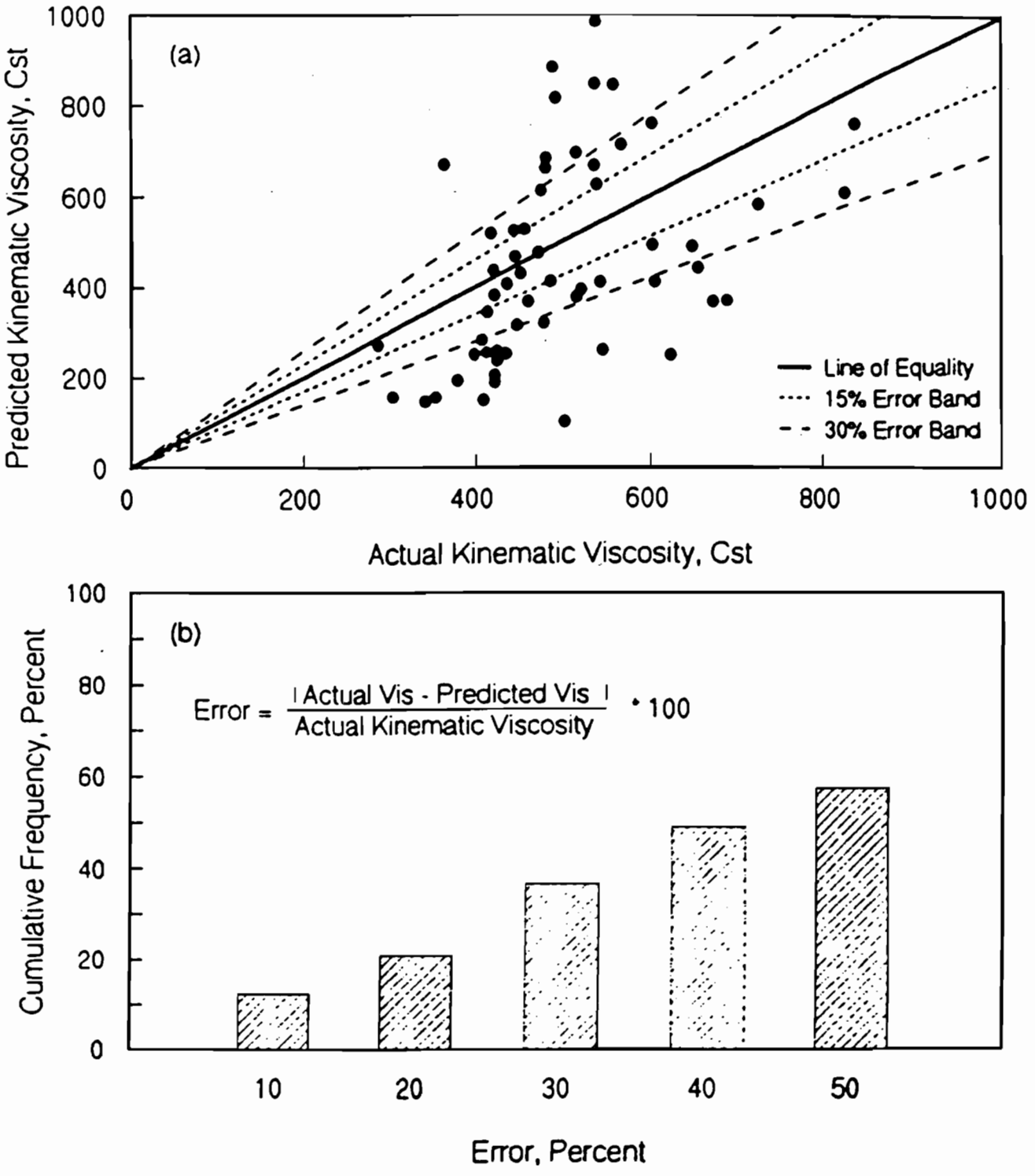

Figure 5.4 - Comparison of Actual and Predicted Kinematic Viscosity Values Using Equation 5.2 for All Data (without Outliers) a) Scatter Plot b) Cumulative Error.

Table 5.3 - Fit Parameters Relating Elastic Modulus to Penetration, Asphalt Content and VTM of Specimens Tested after Eliminating Points with Low Penetration Values.

Mix	Fit Parameters				Fit Quality			Cumulative percent error		
	a_1	a_2	a_3	a_4	R^2	Root MSE	F-value	10	20	3
Combined	67846	-9006	-1777	-1795	0.58	2770	37	11	20	29
Austin	57806	-9961	-377	-1154	0.53	2307	14	15	35	45
El Paso	99013	-25070	-2139	-2286	0.88	1758	97	41	81	95
Austin, 5 % AC	64164	-13017	-	-1761	0.70	2433	13	21	43	50
El Paso, 5 % AC	88704	-23302	-	-2813	0.97	1039	184	60	100	100
Austin, 5 % VTM	41255	-6363	978	-	0.27	2045	2	17	17	33
El Paso, 5 %	94755	-26000	-3307	-	0.91	1561	53	43	93	100

* See Equation 5.1

While 27 percent of the data can be predicted with less than 30 percent error in Figure 5.3, about 37 percent of the data can be predicted with less than 30 percent error as seen in Figure 5.4. Appendix F includes the comparison of actual and predicted values of penetration using the above models corresponding to all cases reported in Tables 5.3. Similar comparisons can be made for all cases reported in Table 5.4.

The statistical parameters in Tables 5.3 and 5.4 show that the models developed for each mix individually are more representative, than those developed by combining the results from both mixes. The percent errors in predicting the data are reduced in cases of both Austin and El Paso mixes, when they are considered separately. More effort was focussed towards evaluating the strengths of the models that were mix-specific rather than considering the combined data.

Table 5.4 - Fit Parameters Relating Elastic Modulus to Kinematic Viscosity, Asphalt Content andVTM of Specimens Tested after Eliminating Points with Low Penetration Values.

Mix	Fit Parameters				Fit Quality			Cumulative percent error		
	a_1	a_2	a_3	a_4	R^2	Root MSE	F-value	10	20	30
Combined	29938	8798	-1838	-1766	0.65	2553	48	12	21	37
Austin	21963	7455	-401	-998	0.56	2249	15	18	28	43
El Paso	8759	18947	-2572	-2210	0.88	1746	98	7	14	31
Austin, 5 % AC	20251	8642	-	-1546	0.77	2151	18	29	43	57
El Paso, 5 % AC	-6593	21099	-	-2806	0.96	1127	155	53	87	100
Austin, 5 % VTM	19519	4848	769	-	0.25	2084	2	50	58	67
El Paso, 5 % VTM	262	19573	-3472	-	0.90	1668	45	29	71	93

* See Equation 5.2

Another approach was followed to further improve the models. Since most of the mix designs for field applications contain an average asphalt content of about 5 percent, additional models were developed to determine rheological parameters considering specimens with only 5 percent AC contents.

To evaluate the quality of different models developed using the above approaches, the fit parameters, fit quality, and cumulative percent errors, obtained from all different models based on penetration and kinematic viscosity from elastic modulus, are shown in Tables 5.3 and 5.4.

Table 5.3 reports the statistical parameters, as well as, the cumulative percent errors. The models are satisfactory, when data related to a 5 percent AC content was used. In the case of the Austin mix, about 43 percent of the penetration results can be predicted within a 20 percent error. In the case

of the model developed with the El Paso data, almost 100 percent of the penetration values can be predicted within a 20 percent error. Models developed for determining kinematic viscosity have more or less the same strength in both the Austin and El Paso mixes, with 5 percent AC content. In Table 5.4, about 43 percent of the Austin mix data can be predicted with less than a 20 percent error; similarly, about 87 percent of the data can be predicted with less than a 20 percent error in the El Paso data.

The same exercise was repeated, but the VTM was maintained at a 5 percent level (as opposed to the AC content). The model representing the data of the Austin mix poorly predicts the penetration values, while the model using the El Paso mix data is strongly representative. The models to predict kinematic viscosity for the Austin and El Paso data, also have more or less a similar increase in strength as in the case of penetration. In both the Austin and El Paso data from Tables 5.1 and 5.2, the fit quality parameters show that the models to predict penetration and kinematic viscosity have more or less equal strength. Similar observation can be made by comparing the fit quality parameters or cumulative percent errors from Tables 5.3 and 5.4, with an exception of the model using El Paso data. The model using El Paso data (after eliminating outliers) is less representative for kinematic viscosity relative to penetration.

Models Using Indirect Tensile Strength

A multi-regression analysis was also performed to develop models using IDT strength, following the above mentioned approaches. The general model, that best relate the IDT strength (σ_t) of the mix with rheological parameters of the asphalt binder, its AC, and its VTM, were found to be:

$$\sigma_t = c_1 + c_2 * Log(P) + c_3 * (AC) + c_4 * (VTM) \tag{5.5}$$

$$\sigma_t = d_1 + d_2 * Log(\eta) + d_3 * (AC) + d_4 (VTM) \tag{5.6}$$

Parameters c_i's and d_i's are the model parameters determined from a multi-variant best fit process. The above equations can be applied to the data from either mix or from the combined data. In the same manner, models were developed by eliminating the eight outlier points identified in the previous section, and by assuming constant AC content and VTM. Tables 5.5 and 5.6 show the corresponding fit parameters, fit quality, and cumulative percent errors for respective cases.

Equations 5.5 and 5.6 were then algebraically solved to determine penetration or kinematic viscosity of the asphalt. The new equations for penetration and kinematic viscosity are;

$$P = 10^{\frac{\sigma_t - c_1 - c_3 * (AC) - c_4 * (VTM)}{c_2}} \tag{5.7}$$

$$\eta = 10^{\frac{\sigma_t - d_1 - d_3 * (AC) - d_4 * (VTM)}{d_2}} \quad (5.8)$$

Figure 5.5 presents the comparisons of predicted (from Equation 5.7) and actual values of penetration by using combined data. In Figure 5.5 and Table 5.5, the model predicts 31 percent of the data with less than a 10 percent error and about 53 percent of the data with less than 20 percent error. The model can also be evaluated from the statistical parameters. The R^2, and F-values of the model are high, and the corresponding root MSE is low, which indicates that the model is moderately representative.

Additional models were developed for each mix individually and by combining the results from both mixes, after eliminating outliers identified in the previous section. The statistical parameters in Tables 5.5 and 5.6 show that the strength of the models in all three cases were slightly reduced by eliminating the outliers; however, the percent error in predicting either penetration or viscosity (from Tables 5.5 and 5.6) reveal that the strength of the models were only slightly afffected.

The models developed for each mix individually are significantly improved by considering data with 5 percent AC content. In Table 5.5, almost 100 percent of the penetration values can be predicted, when using either the El Paso or Austin mix data with less than a 20 percent error. The models developed for each mix individually have even higher strength by considering 5 percent VTM, than those models developed with 5 percent AC content. In Table 5.5, about 100 percent of the penetration values can be predicted using model developed for the Austin mix with less than 10 percent error. From the same table, about 93 percent of penetration values can be predicted using model developed the for El Paso mix with less than 10 percent error.

The strength of the models developed for determining kinematic viscosity using Equation 5.8 can also be evaluated in the similar way. The fit quality and cumulative percent errors are presented in Table 5.6. The statistical parameters in Table 5.6 show that the strength of models were reduced by eliminating outliers; however, the cumulative percent errors show that the strength of the models were improved. The strength of the models to predict the viscosity were improved considerably by considering either 5 percent AC content or 5 percent VTM (seeTable 5.6). More than 80 percent of the viscosity values can be predicted in either the Austin or El Paso mix by considering 5 percent VTM and 5 percent AC conten, for only the El Paso mix. The model poorly predicts the viscosity values for Austin mix with 5 percent AC content.

Table 5.5 - Fit Parameters Relating IDT Strength to Penetration, Asphalt Content and VTM of Specimens Tested after Eliminating Points with Low Penetration Values.

Mix	Fit Parameters				Fit Quality			Cumulative percent error		
	c_1	c_2	c_3	c_4	R^2	Root MSE	F-value	10	20	30
Combined	1975	-751	-88	-	0.81	97	130	33	63	74
Austin	2096	-725	-118	-	0.75	125	49	35	475	6
El Paso	1802	-731	-61	-	0.84	53	73	45	76	98
Austin, 5 % AC	2283	-1074	-	-60	0.96	53	131	57	100	100
El Paso, 5 % AC	1671	-761	-	-27	0.93	26	83	87	100	100
Austin, 5 % VTM	2465	-1059	-91	-	0.99	21	455	100	100	100
El Paso, 5 % VTM	2299	-996	-723	-	0.98	23	231	93	100	100

* See Equation 5.5

Table 5.6 - Fit Parameters Relating IDT Strength to Kinematic Viscosity, Asphalt Content and VTM of Specimens Tested after Eliminating Points with Low Penetration Values.

Mix	Fit Parameters				Fit Quality			Cumulative percent Error		
	d_1	d_2	d_3	d_4	R^2	Root MSE	F-value	10	20	30
Combined	-880	633	-196	-	0.77	97	130	35	52	74
Austin	-550	585	-125	-	0.81	104	79	25	53	65
El Paso	-924	589	-73	-	0.83	48	96	31	69	90
Austin, 5 % AC	-1218	670	-	-42	0.96	49	155	36	79	100
El Paso, 5 % AC	-1493	709	-	-27	0.96	20	141	93	100	100
Austin, 5 % VTM	-1288	856	-125	-	0.97	35	161	83	100	100
El Paso, 5 % VTM	-1377	769	-79	-	0.98	22	254	86	100	100

* See Equation 5.6

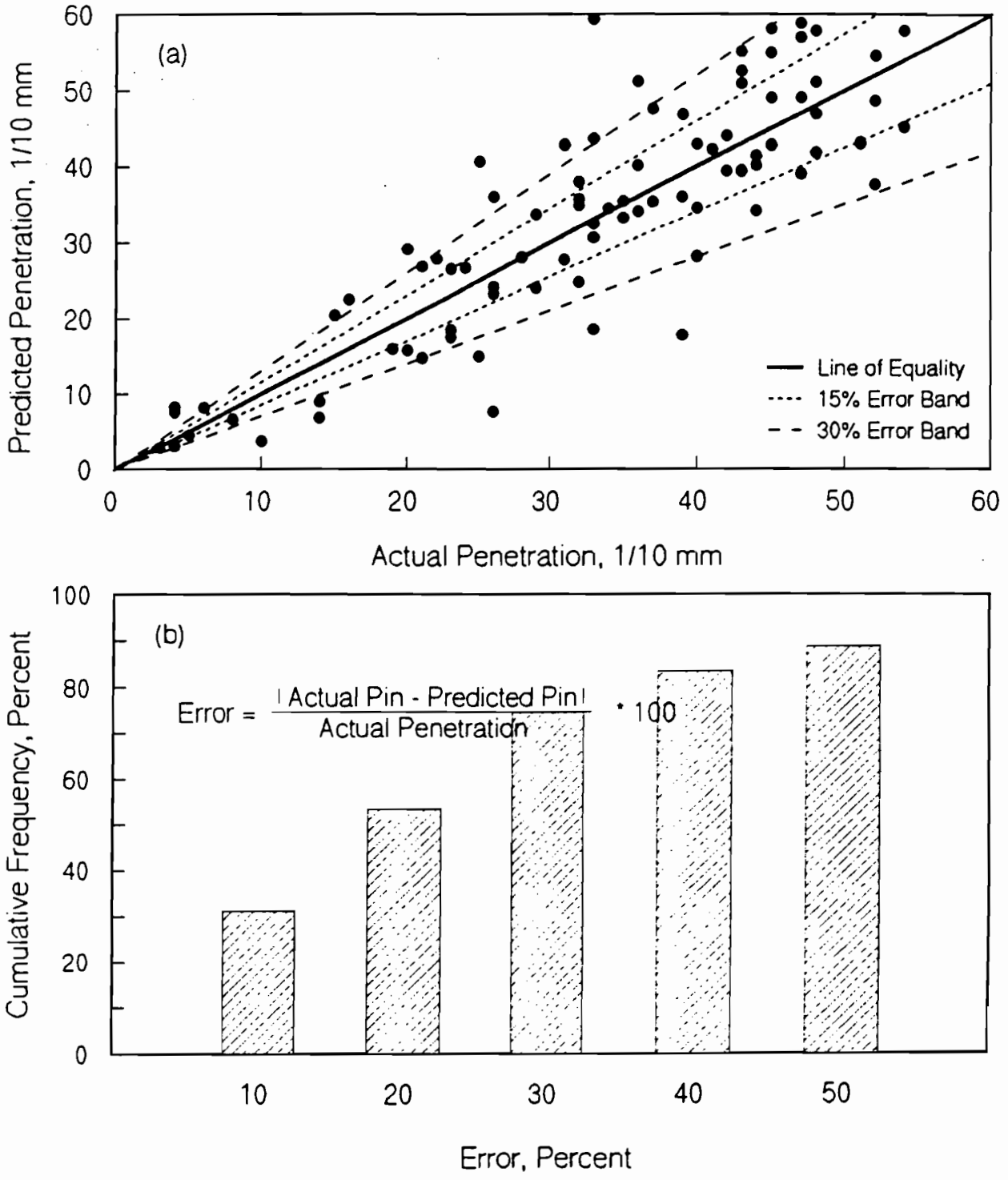

Figure 5.5 - Comparison of Actual and Predicted Penetration Values Using Equation 5.5 for All Data a) Scatter Plot b) Cumulative Error.

Estimation of Asphalt Grade using Prediction Models

In this section, the models developed in the previous sections are represented graphically in a more practical way. The asphalt grade of a particular material is the primary interest, rather than the predicting the exact value of penetration or viscosity. Based on this hypothesis, the models explained above using modulus and IDT strength can be considered to estimate the asphalt grade. Envelops distinguishing the asphalt grades were established using the specifications set by ASTM D3381-83. These specifications are shown in Table 5.7. Prediction charts were prepared by using specification limits, for the El Paso and Austin mixes assuming a 5 percent AC content.

For each of the boundary values (penetration values), modulus values at 3, 5, and 7 percent VTM levels were calculated using Equation 5.1. Figure 5.6 contains fitted lines for the El Paso mix data that differentiate the asphalt grade. It is observed from each of the fitted lines, that modulus decrease with an increase in the percent VTM, because the bulk density decreases; hence, the modulus decreases correspondingly. Similarly, the slope of the fitted lines, i.e. the rate of increase in modulus, is found to be uniform with asphalt grade.

Figure 5.7 shows the prediction chart based on the elastic modulus values from the Austin data with a 5 percent AC content. Similar observations, depicted from Figure 5.6, could also be made using Figure 5.7. The lines (change in elastic modulus with VTM) are more steep in Figure 5.6 (El Paso) than in Figure 5.7 (Austin). This is due to the existence of higher correlation between elastic modulus and VTM for El Paso mix as observed from Table 4.5.

Table 5.7 - Relationship between Viscosity Grade and Rheological Parameters of AC based on Original Asphalt (From ASTM D3381-83).

Viscosity Grade	AC-10	AC-20	AC-30	AC-40
Kinematic viscosity,Cst	250	300	350	400
Penetration,1/10 mm, min.	80	60	50	40

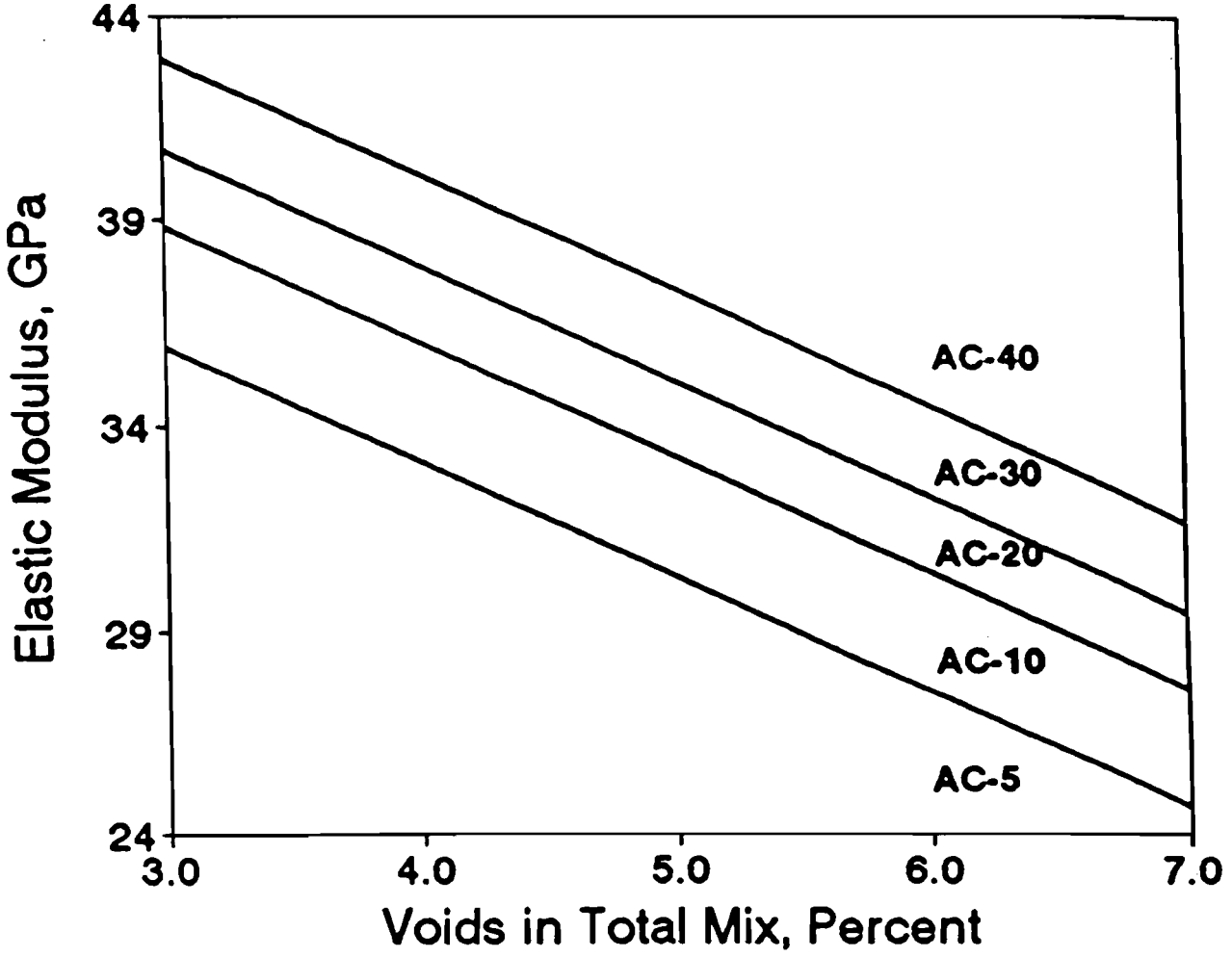

Figure 5.6 - Prediction Chart using Model from Elastic Modulus for El Paso Mix with a 5 percent AC Content.

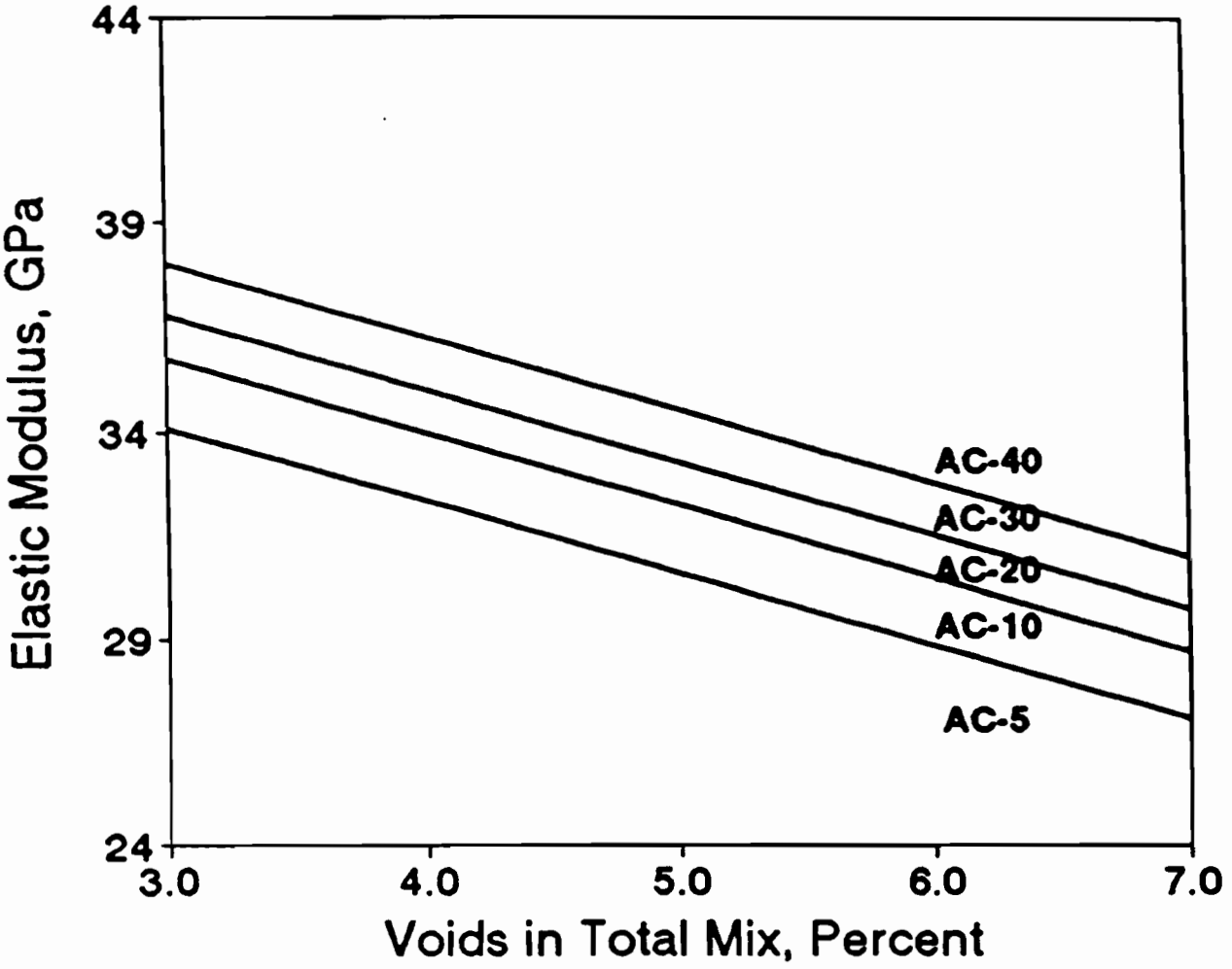

Figure 5.7 - Prediction Chart using Model from Elastic Modulus for Austin Mix with a 5 percent AC Content

In Figure 5.6 or Figure 5.7, the asphalt grade of either the El Paso or Austin mix can be determined without conducting the Abson recovery, providing the modulus and the VTM of the mixes are known. Similar charts could be readily developed for other combinations of parameters. For example, the modulus can be replaced by IDT strength, and penetration with kinematic viscosity.

In summary, the models using the elastic modulus and IDT strength can possibly be used in determining the rheological parameters; however, these models may poorly predict the rheological parameters, if the mix is highly age susceptible. Similarly, the prediction charts developed from elastic modulus can be used effectively in finding the asphalt grade of the mix without opting for the Abson recovery.

An attempt was made to use the chart shown in Figure 5.6 to validate its applicability. Cores from in-service pavement at three sites [San Angelo, TX; El Paso, TX (different than that used in developing model); and Childress, TX] visited for other research purposes were used in this case study. Two cores from each site were selected. The elastic modulus of the mixture was measured on the intact cores. The binder was then recovered to determine the viscosity, penetration and AC content.

Table 5.8 includes the measured moduli, as well as, the measured and predicted penetrations and viscosities of each mixture. Equations 5.3 and 5.4 with the regression coefficients related to the El Paso mix, were used to estimate the penetration and viscosity. Practically speaking, the calculated and predicted values are not that far off, given that none of the mixes were used to develop the model.

Figure 5.8 shows the asphalt grade predicted for the three binders. The asphalt grade is predicted reasonably well for all mixes, except for the El Paso mix, where the grade is marginally missed.

In summary, the models, using the elastic modulus, could possibly be used to get an estimate of the rheological parameters. The prediction charts like the one shown in Figure 5.8 may be used to estimate the grade of the asphalt used in the mix without opting for the Abson recovery.

Table 5.8 - Comparison of Predicted and Measured Rheological Parameters at Several Sites

Site	Mix Properties			Penetration (1/10mm)		Kinematic Viscosity (cSt)		Asphalt Grade	
	Asphalt Content (%)	VTM (%)	Modulus (GPa)	Measured	Predicted	Measured	Predicted	Measured	Predicted
El Paso	5.8	3.5	39.7	20	23	641	674	AC-40	AC-30
Childress	4.3	8.2	28.9	15	11	779	401	AC-40	AC-40
San Angelo	4.8	5.5	44.5	12	18	772	1115	AC-40	AC-40

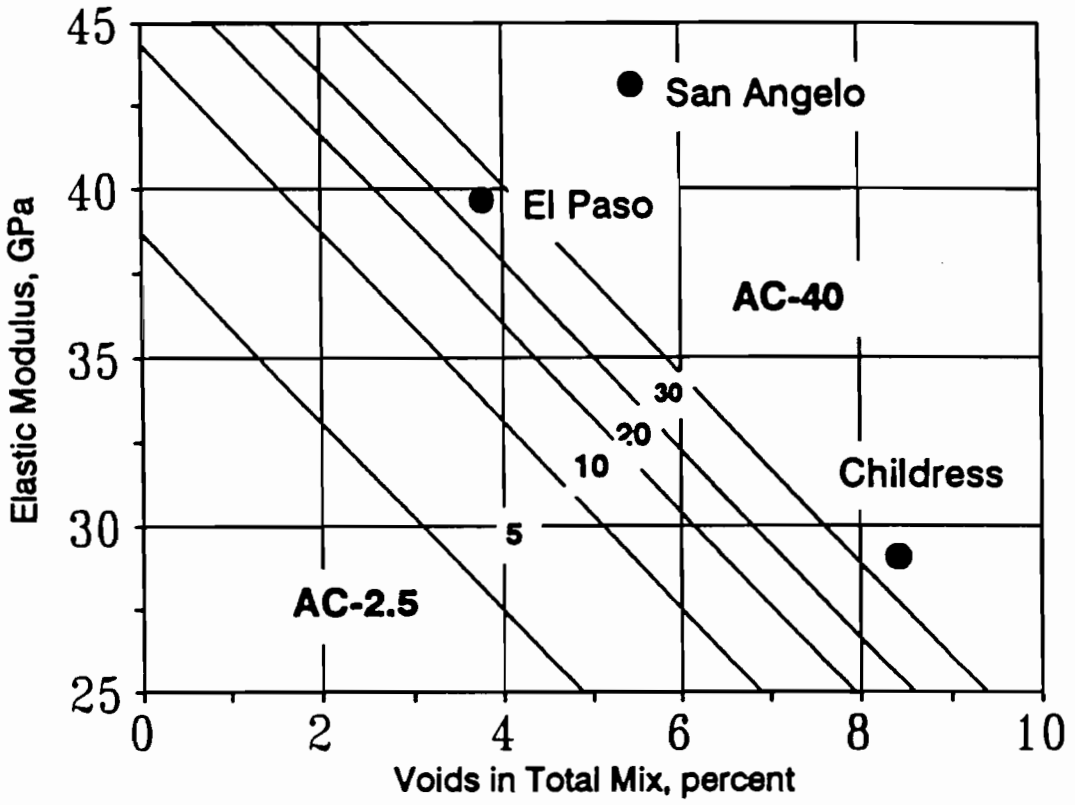

Figure 5.8 - Prediction Charts for Estimating Asphalt Grade of Binder from Elastic modulus of Mix

Chapter 6

Optimization of Ultrasonic Tests

Introduction

In the last chapter, the feasibility and limitations of estimating the asphalt grade from the modulus obtained with the ultrasonic wave propagation methods were discussed. Given the relative success reported in the previous section, an exercise was carried out to determine if the methodology can be further enhanced. The results of this study are presented herein.

In the previous chapters, a V-meter was used to perform tests. To review briefly, a transmitting transducer, connected to a high-voltage electrical pulse generator, was placed on one side of the specimen. A receiving transducer was securely placed on the opposite face of the specimen to monitor compression waves.

In the field, a device developed at UTEP under Project 1966 (Baker et al., 1995) can be used to measure moduli of the asphalt-concrete pavement layer. With the device, shear modulus is determined from shear wave velocity using the ultrasonic surface wave method, and Young's modulus is obtained from the compression wave measured with the ultrasonic body wave method.

At inter-granular level, compression waves introduce a so called push-pull (compression-tension) motion within the specimen; whereas, shear waves produce a shearing motion at the aggregate interfaces. Based on this discussion, the change in the viscosity of asphalt coating aggregates may more significantly affect the inter-granular shear bond and, therefore, the shear modulus.

Another parameter to consider is that the molded specimens or the AC layers placed in the field are assumed to be isotropic. Given the directionality of the compaction effort, the material should at least be considered cross-anisotropic, where the properties in the horizontal and vertical directions are different.

Theoretically speaking, the stiffness parameters of an isotropic material can be defined by two elastic constants, which are Young's modulus and Poisson's ratio. An anisotropic material possesses five elastic constants. Shear and/or compression waves should be measured in five different directions to measure the five constants.

Developing anisotropic constitutive models for asphalt mixes is far beyond the scope of this report; however, at least experimentally, one can take advantage of this principle to define which of the five elastic parameters are more sensitive to the viscosity of the asphalt. The goals of this chapter are the following:

1. Is the viscosity of the asphalt more sensitive to shear or Young's modulus of the specimen?

2. Where are the optimum locations for the source and receiver, so that the viscosity can be determined repeatably and reliably?

Practically speaking, the test procedure will not change from the one defined in Chapter 3. Only the source and receiver are placed in different locations on the specimen (as opposed to the two faces of the briketts).

Methodology

The test factorial is shown in Figure 6.1. A total of forty specimens were prepared from two mixes (twenty specimens per mix). One mix was age-susceptible and one was not (see next section for specifications of each mix).

The specimens were prepared at two nominal VTM's (3 and 6 percent) to assess the effects of the compaction efforts. Based on the results presented in Chapter 5, the asphalt content was maintained at the optimum.

To understand the effects of the specimen height on the resolution of the wave propagation method, half of the specimens were prepared with nominal dimensions of 100 mm by 50 mm, and another half with nominal dimensions of 100 mm by 100 mm. A SHRP gyratory compactor was used to prepare the specimens.

The specimens were oven-aged either for 0, 1, 2 or 7 days to simulate field aging. For each aging period a duplicate specimen was tested to determine the repeatability of the results.

As indicated before, the material should at least be modeled as a cross-anisotropic material, because of the compaction pattern used to lay down asphalt. Such material requires the estimation of five parameters. As such, the rays should be imparted into the material and received along five paths. In this study, more than five paths were used. These paths, which are schematically shown in Figure 6.2, consist of shear and compression waves, along the longitudinal axis of the specimen, shear and compression waves along the diameteral axis of the specimen, and shear or compression waves along

DESIGN OF EXPERIMENT

ASPHALT MIX	AAB-02 & RB				AAK-1 & RL			
SPECIMEN HEIGHT mm	50		100		50		100	
AIR VOIDS, %	3	6	3	6	3	6	3	6
AGING PERIOD, DAYS								
0	BS30	BS60	BL30	BL60 BL60R	KS30	KS60 KS60R	KL30	KL60
1	BS31	BS61	BL31 BL31R	BL61	KS31 KS31R	KS61	KL31	KL61
2	BS32 BS32R	BS62	BL32	BL62	KS32	KS62	KL32	KL62 KL62R
7	BS37	BS67 BS67R	BL37	BL67	KS37	KS67	KL37 KL37R	KL67

Figure 6.1 - Test Factorial for This Study

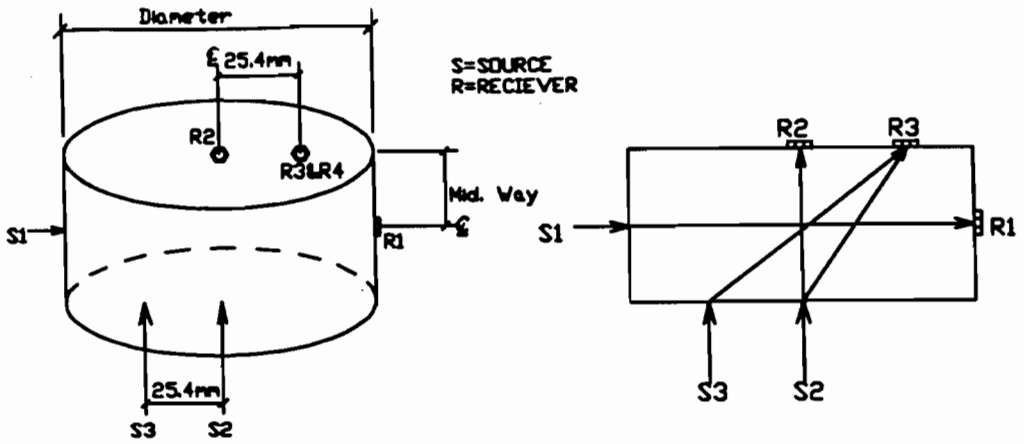

50 mm Specimen

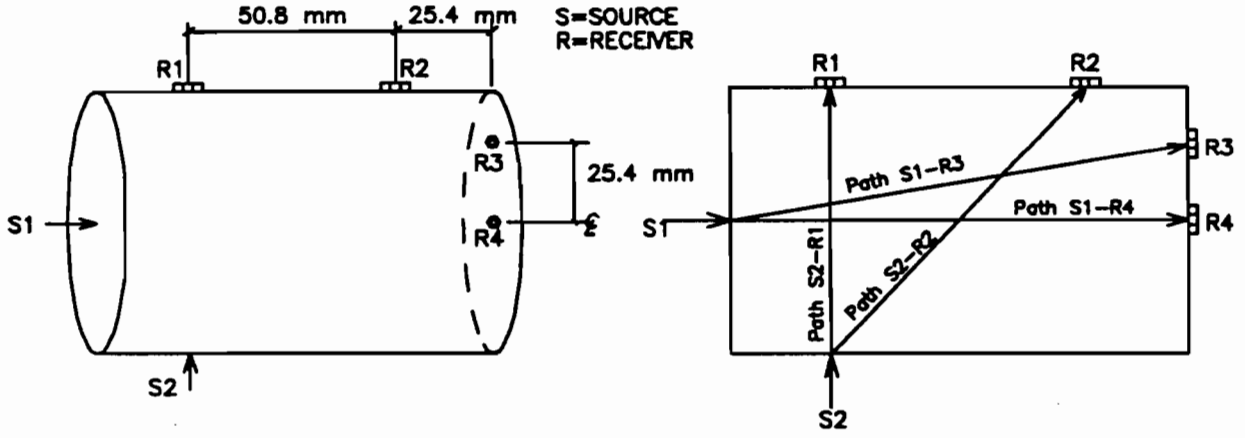

100 mm Specimen

Figure 6.2 - Ray Paths Considered for 100 mm and 50 mm Specimens

one or two oblique path. These measurements can be made easily and rapidly in the laboratory, by following the same procedure described before. Once again, the goal is to determine which of the ray paths and which type of wave are most sensitive to the viscosity of the asphalt.

The test procedure can be summarized in the following steps:

1. Perform wave propagation tests along the paths shown in Figure 6.2 to determine the shear and compression wave velocities.

2. Recover asphalt from the mix using Abson recovery.

3. Perform penetration and test as discussed in Chapter 3.

Test Set Up

Because of the size of the transducers and the nature of the V-meter, an alternative test set up was developed. The set up is shown in Figure 6.3. The source was a piezo-electric shaker, which was connected to an impulse generator through an amplifier. The receiver was a piezo-electric accelerometer, that was connected to an oscilloscope through a signal conditioner. The input impulse to the shaker and the output of the accelerometer were captured by the oscilloscope for determining the traveltime and eventually the modulus.

The source was securely placed on the specimen at the desired locations. To maximize the shear and compression wave energies, the source head was placed at an angle of 45 degrees relative to the longitudinal axis of the shaker. The accelerometer was screwed to a nut glued to the specimen with "crazy glue."

Before each test, the system was calibrated using a series of four aluminum rods 12 mm in diameter and 25, 50, 100 and 200 mm long. In addition, two aluminum specimens similar to the two sizes of specimens tested (i.e. 100 mm by 100 mm, and 100 mm by 50 mm) were extensively tested to understand the effects of the specimen size on the behavior of waves.

This system has several advantages as compared to a V-meter, which include the following:

1. The amplitude and dominant frequency of the input waves can be readily optimized for each specimen.

2. Since the source is smaller (diameter of 12 mm, as compared to 50 mm for the v-meter), it can be more securely connected to the specimen.

3. The receiver is smaller (about 5 mm) which can be more securely attached to the specimen.

Performing tests with the V-meter is more convenient because of its automated nature. However, it is possible to develop an automated system optimized for our use.

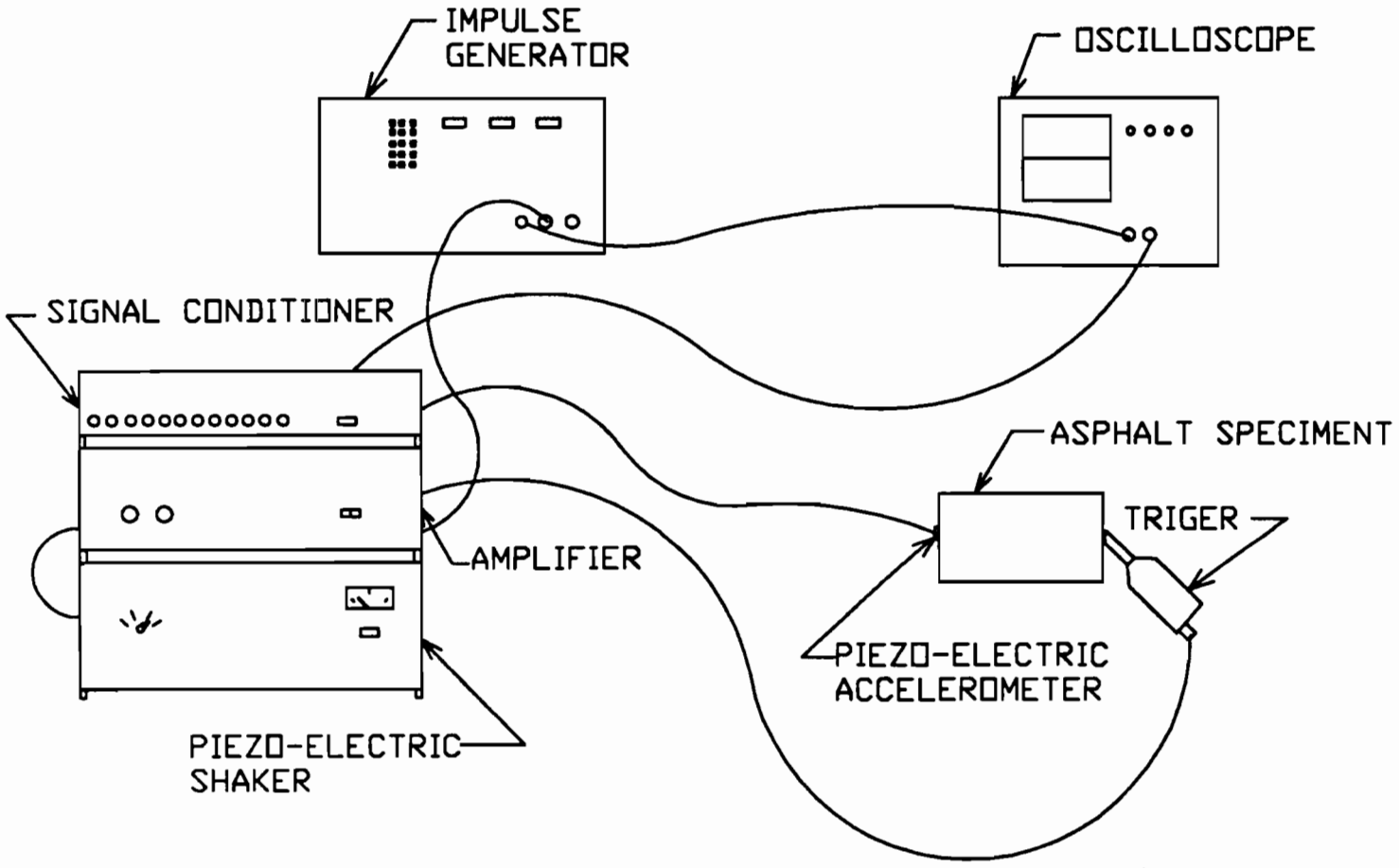

Figure 6.3 - Schematic of Test Set Up

Materials Tested

The asphalt and aggregates, used in this study, were obtained from the Strategic Highway Research Program (SHRP) Asphalt Material Library in Reno, Nevada. The mix design and materials used were those adapted by SHRP Project A-003 for aging studies and were very similar to those used by Bell et al. (1991).

Two types of asphalt and two types of aggregate were used. The asphalts were AR-4000 from California Valley (SHRP designation AAOB-2) and Boscan AC-30 (SHRP designation AAK-1) and the aggregates were designated as RL and RB.

The gradation curve of the mixes is shown in Figure 6.4. The penetration values of the virgin asphalts at 25°C were measured as 58 and 119 for the AAK-1, and the AAOB-2 materials, respectively. The main compositions of the RB and RL aggregates were limestone and sandstone/granite, respectively.

Presentation of Results

In this section, only typical results from the tests mentioned above are included; however, the results from all tests are included in Appendix F for further inspection.

Figure 6.5 shows a typical variation in Young's modulus with penetration for a specimen when a V-meter is used. The trend is much similar to that reported in Chapter 5. Also shown in the figure, is the results obtained with the new setup along the S2-R2 path. This path is equivalent to the V-meter path (see Figure 6.3). The slope of the best fit lines from the two data sets are generally similar, indicating that both test systems are equally sensitive to the modulus-penetration relationships.

The absolute moduli measured with the two systems are different. This is expected for two reasons. First, the size of the sensors and the receivers from the two systems are different. For the V-meter, where the source and the receiver are 50 mm in diameter, the waves generated resemble a plane wave front. For the new set up, where the source and receivers are less than 12 mm in diameter, the waves resemble the propagation of elastic waves in a medium. Secondly, based on our experience with the aluminum blocks, the V-meter typically records faster travel time, which can be translated to faster modulus than normally reported for the material.

Short Specimens (Normal Brikettes)

A typical variation in Young's modulus with penetration along the three paths (i.e. S1-R1, S2-R2 and S3-R3 in Figure 6.3) for 100 mm diameter, 50 mm height are shown in Figure 6.6. Young's moduli measured along various paths are different. This can be contributed to the facts that the material exhibits anisotropic behavior. Even though not shown here, the aluminum specimens yielded almost identical moduli in all three paths.

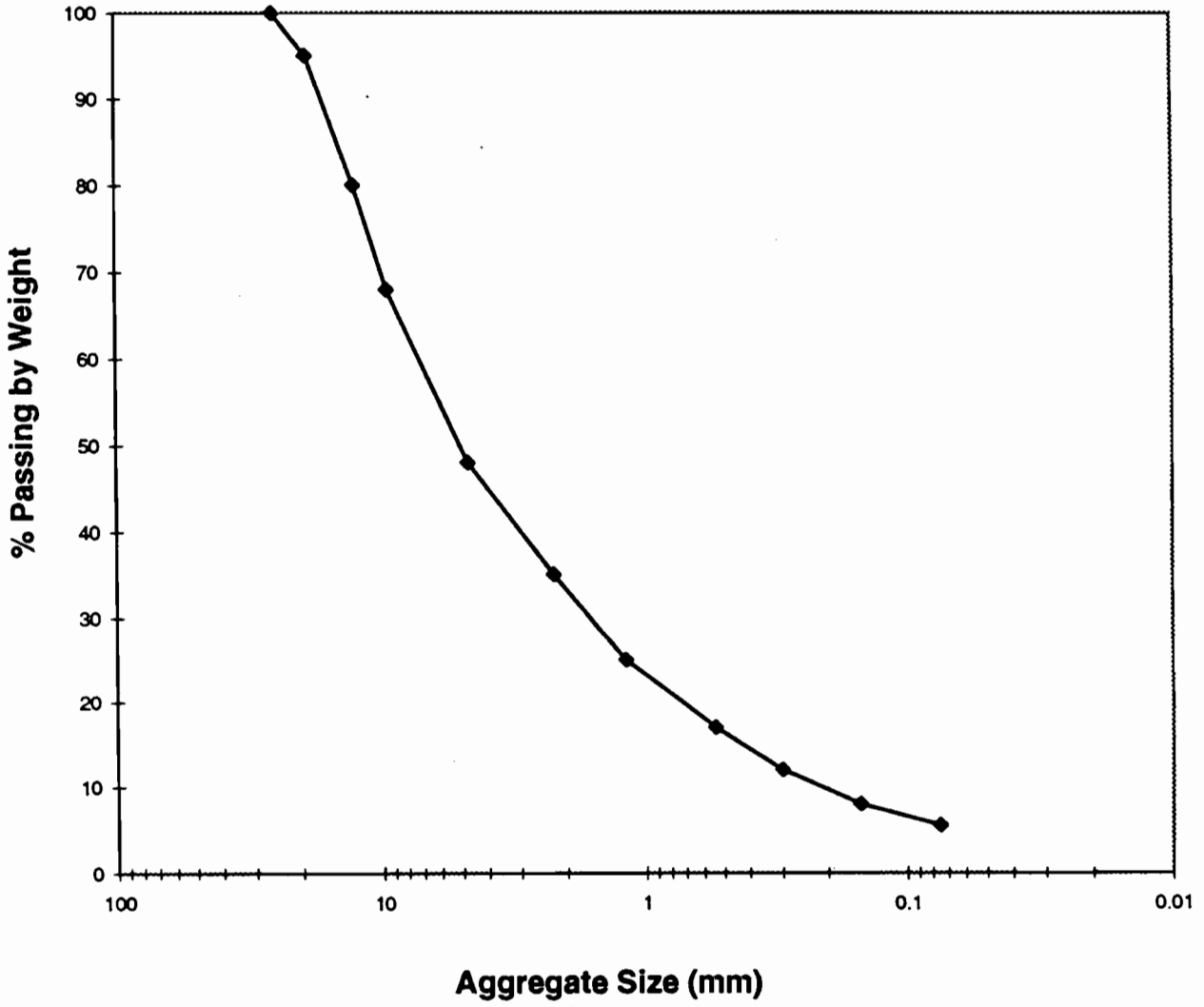

Figure 6.4 - Gradation of Aggregates

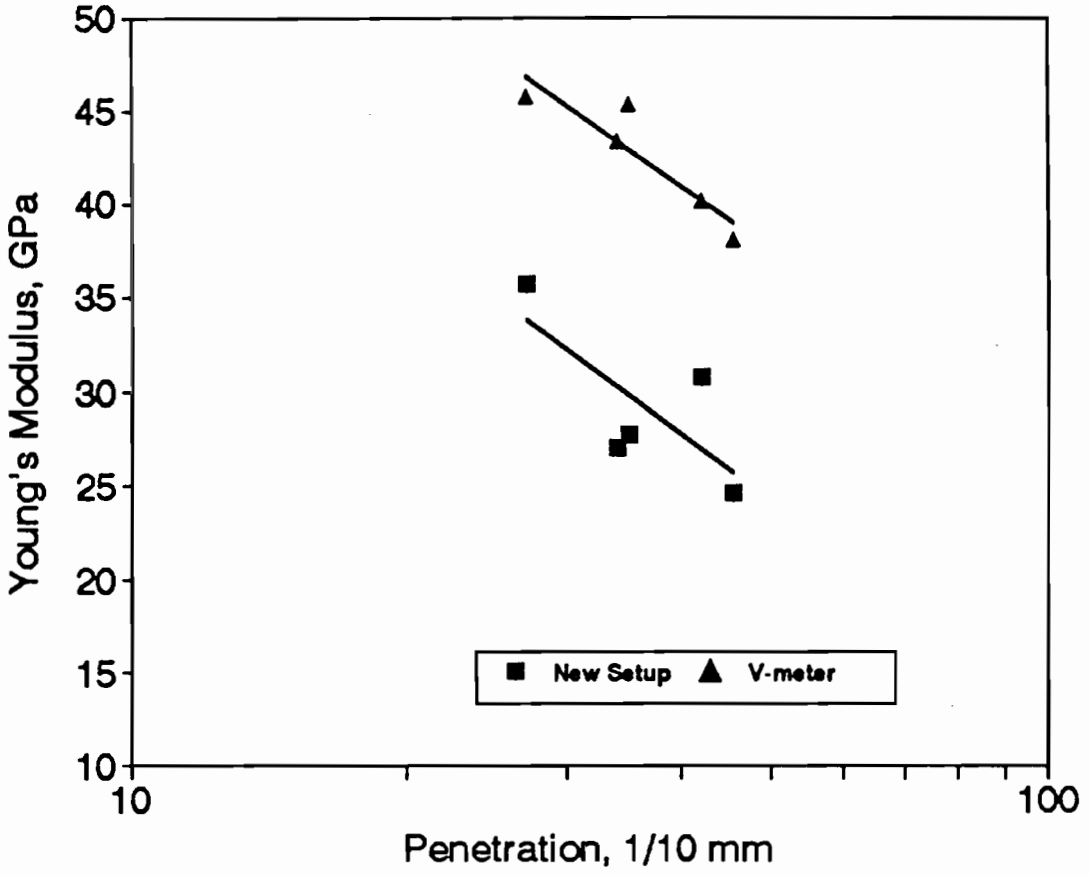

Figure 6.5 - Comparison of Typical Variation in Young's Modulus with penetration from V-Meter and New Set-Up

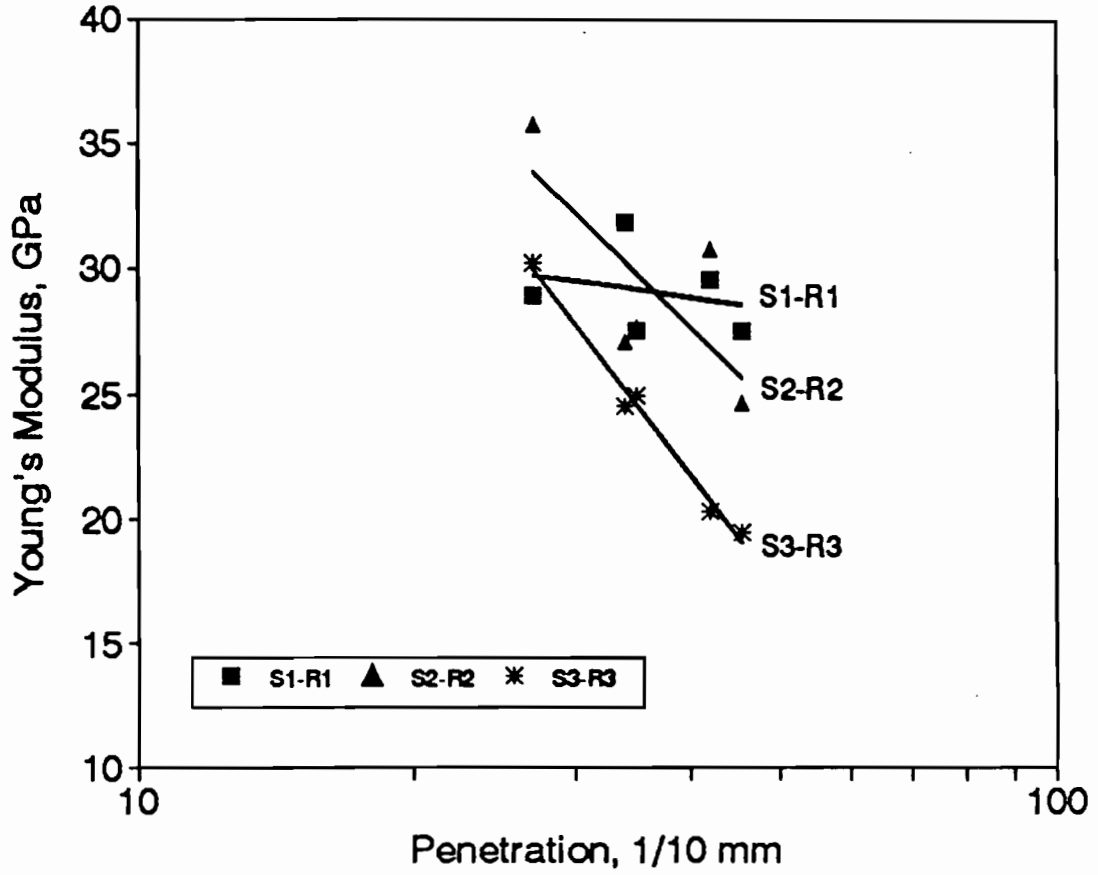

Figure 6.6 - Typical Variation in Young's Modulus with Penetration along Wave Paths Used with New Set Up

The results for all specimens can be summarized in Figure 6.7. For almost all tests, Young's moduli measured along S1-R1 (along the diameter of the specimen) path were not sensitive to the variation in penetration; therefore, this path should not be used for estimating the viscosity.

The Young's modulus-penetration relationships were constructed using the compression wave velocities measured along the S2-R2, except on one occasion in which results provided were similar to those obtained in Chapter 5. However, in most cases, the S3-R3 path provided Young's moduli that were by far more sensitive to the variation in the penetration of the asphalt.

It was mentioned that with the new system shear wave velocities were also measured to obtain shear modulus. When shear modulus was correlated to the penetration, the results were rather different. The variation in shear modulus with penetration for different specimens are shown in Figure 6.8. Once again, the anisotropic nature of the material is quite obvious since the moduli along various directions are quite different.

Contrary to the cases when Young's moduli were used, the S1-R1 path yields the greatest sensitivity of the shear modulus to the penetration. For the S2-R2 or the S3-R3 paths, the shear modulus does not vary much with respect to penetration. For specimens with higher VTM's, the S2-R2 path is relatively sensitive as well.

Long Specimens (100 mm Brikettes)

The longer specimens were used for two practical reasons. A longer raypath would allow compression and shear waves to develop more fully. Therefore, they can be identified more easily.

A longer travel path would also allow us to measure the traveltime more accurately, at a given rate of data acquisition. Since longer raypaths translate to longer traveltime, a less sophisticated (and as such a less expensive data acquisition system) would be necessary.

It should be mentioned that the existing system is quite adequate for testing the typical 50 mm long brikettes. We anticipate that it can be packaged at a cost of about $10,000. The goal was to determine if the system can be packaged at even a cheaper cost.

The variations in Young's modulus with penetration for all specimens are shown in Figure 6.9. Once again, the moduli measured with the V-meter are consistently greater than those measured with the new system. The reasons for the differences were described in the previous section.

Based on the measured penetration and modulus values, it seems that the long specimens (especially when the VTM's are small) do not age as significantly as the shorter specimen. Therefore, either the temperature should be increased or the specimen should be age-conditioned for a longer period.

In Figure 6.9, Young's moduli measured along raypaths S2-R2 and S2-R1 are not sensitive to aging; therefore, it can be concluded that compression waves transmitted and received along the diameter of the specimens should not be used for predicting the penetration of the AC.

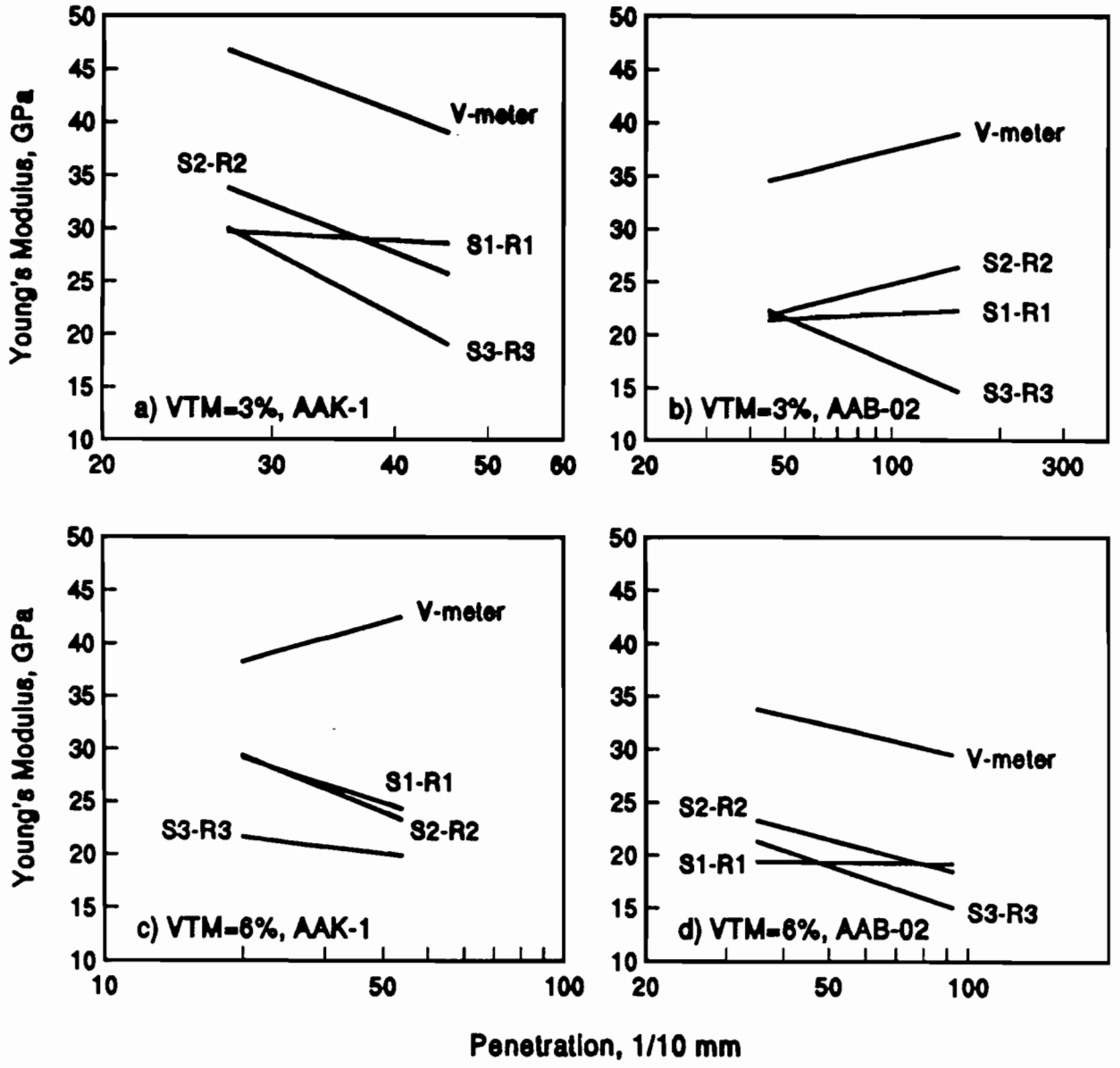

Figure 6.7 - Variation in Young's Modulus with Penetration for Different Wave Paths.

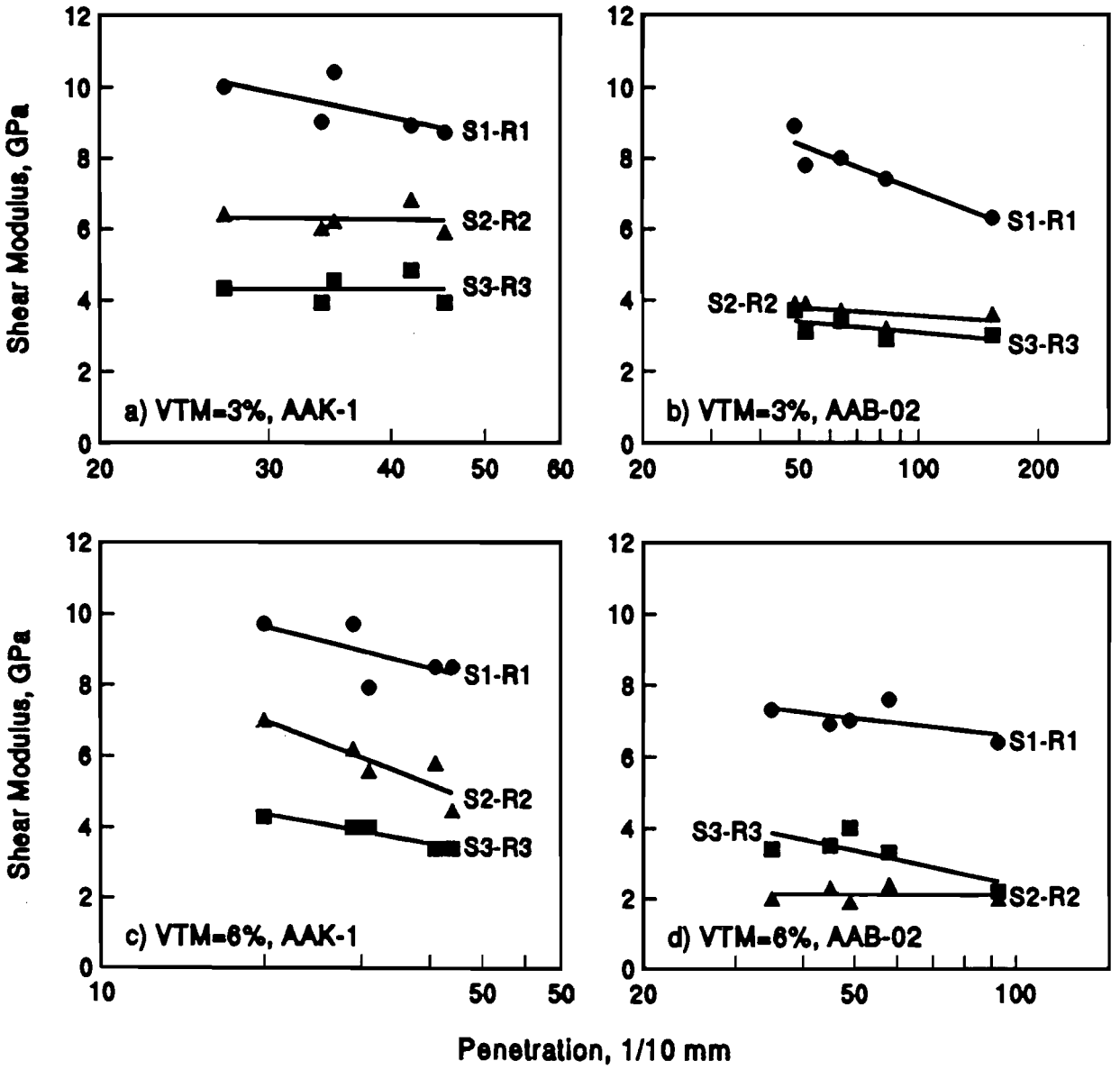

Figure 6.8 - Variation in Shear Modulus with Penetration for Different Wave Paths (Short Specimens).

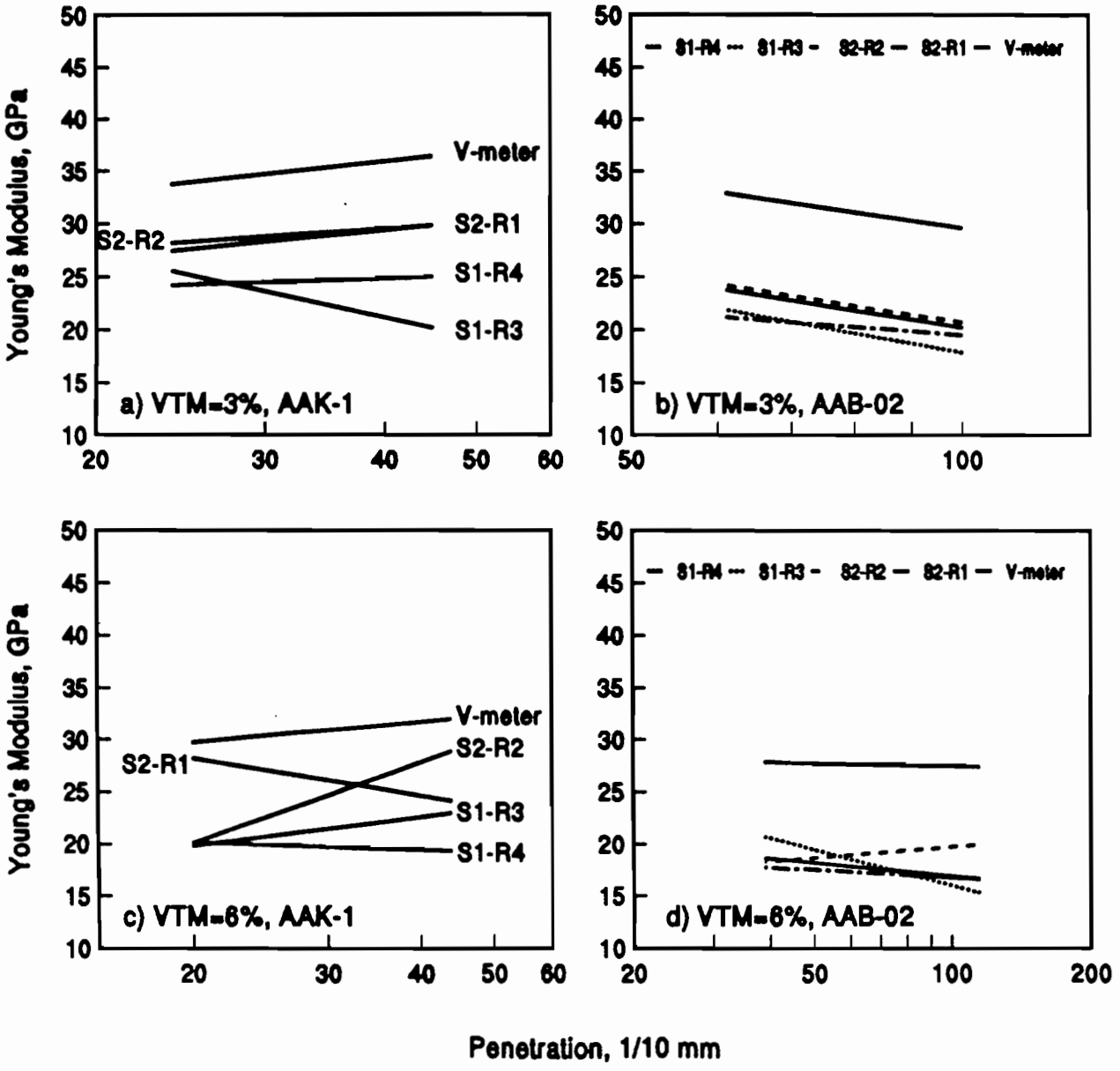

Figure 6.9 - Variation in Young's Modulus with Penetration for Different Wave Paths (Long Specimens).

For the specimens with low VTM's, only Young's moduli along the S1-R3 path seems to be sensitive to the modulus. However, for the specimens with high VTM's, all paths show some sensitivity towards the Young's modulus-penetration relationship, with the S1-R3 path being the most sensitive.

The variations in shear modulus with penetration are shown in Figure 6.10. Similar to the case of the short specimens, the variation in modulus is normally most pronounced for the raypaths transmitted and received along the diameter of the specimen. In all cases, except one, shear moduli along the So-R2 path are most sensitive to the variation in penetration of the AC.

Based upon this study it can be recommended that:

1. At this time, the normal size brikette can be used for determining the stiffening of the binder due to aging. Using longer specimens requires a modification of the aging process.

2. The stiffening of the binder can be best predicted by transmitting and receiving of either compression waves along an oblique path through the height of a specimen, or shear waves along the diameter of a specimen. Both these paths yield results that seem to be more repeatable and sensitive than those determined by a V-meter.

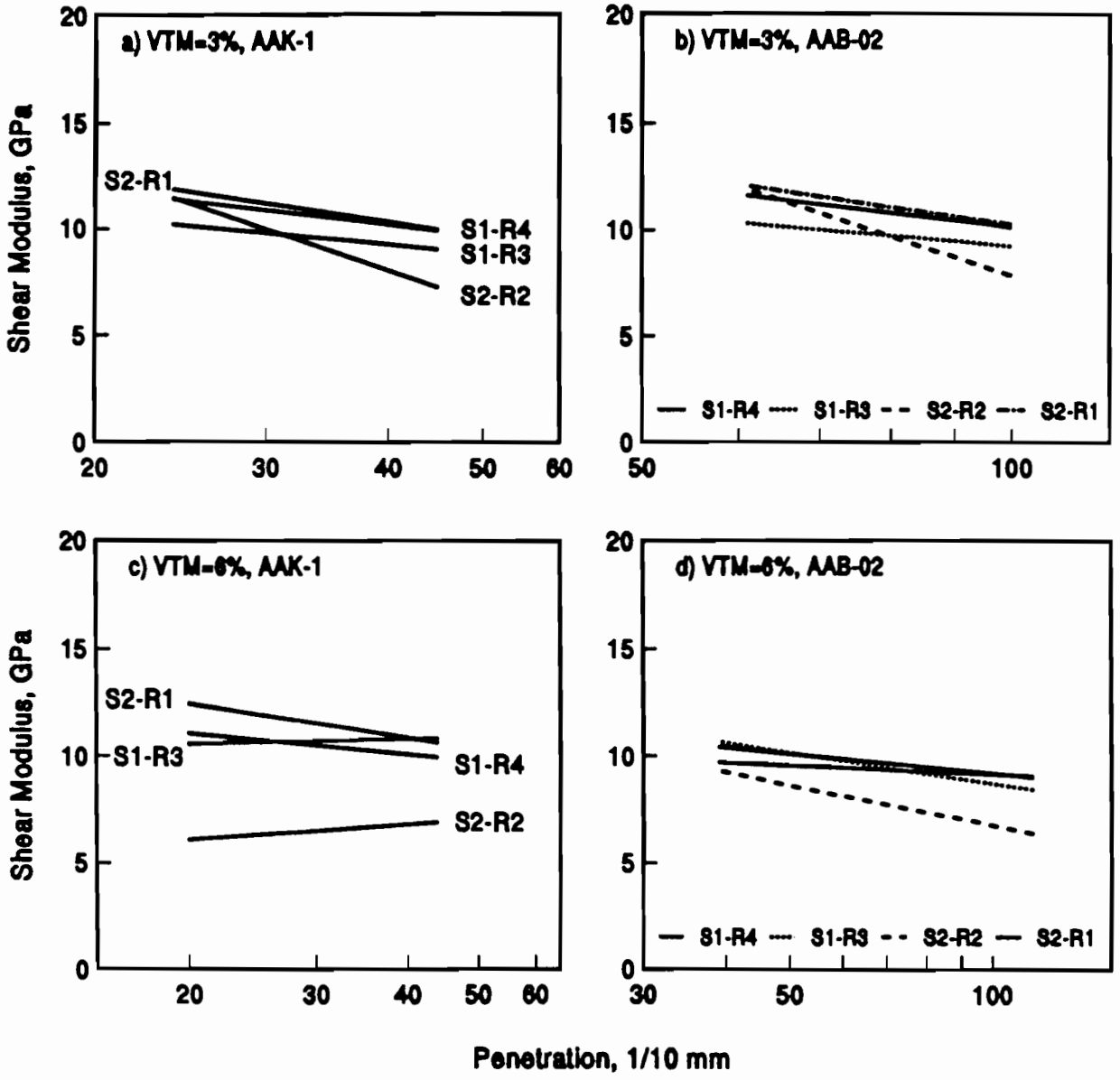

Figure 6.10 - Variation in Shear Modulus with Penetration for Different Wave Paths (Long Specimens).

Chapter 7

Closure

Summary

Due to growing environmental and economical concerns, asphalt recycling has become an attractive rehabilitation alternative technique. As the rheological parameters of asphalt change with time due to aging, its constituent properties have to be measured, before it can be blended with virgin materials. This would ensure high-quality pavement and avoid excessive maintenance cost. The existing methods, using Abson recovery, includes many problems like utilization of hazardous solvents. The wave propagation techniques can be used to determine the rheological parameters of asphalt without using the hazardous solvents in extraction and recovery process.

A laboratory study was conducted from two different mix designs with three different asphalt contents and VTM's. Specimens were aged for 0, 1, 2, 7, and 28 days at 85°C in an oven. All specimens were tested for their elastic moduli and IDT strengths. A V-meter was used to measure the elastic moduli of specimens. The asphalt binder contained in the specimens were extracted and recovered to measure their rheological parameters.

Analysis were conducted to identify mix parameters that best correlate to modulus and IDT strength. Based on the correlation amongst the parameters, models were developed for predicting the penetration and the kinematic viscosity using the elastic modulus or IDT strength.

Using these models along with ASTM specifications for different grades of asphalt, prediction charts were generated to estimate the asphalt grade of RAP materials knowing their moduli or strengths.

Conclusions

Based on the results of this study, the following conclusions were drawn:

1. The use of wave propagation techniques can be extended to predict the rheological parameters, thereby avoiding Abson recovery.

2. A linear relationship exists between the modulus and logarithm of penetration (or kinematic viscosity), for a given AC and VTM.

3. Elastic modulus is affected by both the asphalt content and the VTM in the mix. However, the effects of the VTM are more prominent, on the modulus as compared to the asphalt content of the mix.

4. The models developed are mix-specific; that is the model should be calibrated for a given mix.

5. Practically speaking, when the asphalt content is known, models based on elastic modulus can be used to predict the rheological parameters.

6. Prediction charts can be generated to estimate the asphalt grade.

7. Models developed based on the IDT strength can be used as well, to predict the rheological parameters.

References

1. Baker R.M., Crain, K., and S. Nazarian, *Determination of Pavement Thickness with a New Ultrasonic Device*, Report 1966-1F, Center for Geotechnical and Highway Materials Research, The University of Texas at El Paso, El Paso, TX, 1995.

2. Bell, C.A. *Summary Report on Aging of Asphalt-Aggregate Systems*: Report SHRP A/IR-89-004, Strategic Highway Research Program, National Research Council, 1990.

3. Bell, C.A., Y. AbWahad and M.E. Cristi. *Investigation of Laboratory Aging Procedures for Asphalt-Aggregate Mixtures*. In Transportation Research Record 1323, TRB, National Research Council, Washington, 1991, pp. 32-46.

4. Bell, C.A., Y. AbWahab, J.E. Kliewer, D. Sosnovske and Wieder. *Aging of Asphalt-Aggregate Mixtures*. Proceedings, 7th International Conference on Asphalt Pavements, Nothingham, U.K., 1992.

5. Bell, C.A., A.J. Wiedder and M.J. Fellin. *Laboratory Aging of Asphalt-Aggregate Mixtures: Field Validation.* Report SHRP-A-390, Strategic Highway Research Program, National Research Council, 1994.

6. Burr, B.L., R.R. Davision, C.J. Glover, and J.A. Bullin. *Solvent Removal from Asphalt.* In Transportation Research Record 1269, TRB, National Research Council, Washington, 1990, pp. 1-8.

7. Cipione, C.A., R.R. Davison, B.L. Burr, C.J. Glover, and J.A. Bullin. *Evaluation of Solvents for Extraction of Residual Asphalt from Aggregates.* In Transportation Research Record 1323, TRB, National Research Council, Washington, pp. 47-52.,1991.

8. Consuegra, A., D.A. Little, D.A., H.L., Von Quintas, and J. Burati. *Compactive Evaluation of Laboratory Compaction Devices Based on Their Ability to Produce Mixtures with Engineering Properties Similar to Those Produced in the Field.* In Transportation Research Record 1228, TRB, National Research Council, Washington, pp. 80-87, 1989.

8. Harvey, J. and C.L. Monismith. *Effects of Laboratory Asphalt Concrete Specimen Preparation Variables on Fatigue and Permanent Deformation Test Results Using SHRP A-003A Proposed Testing Equipment.* Proceedings, In Transportation Research Board, TRB, 72th Annual Meeting, National Research Council, Washington, 1992.

9. Huang, S., Mang Tia, Byron E. Ruth and Gale C. Page. *Effects of Modifiers on the Temperature Susceptibility and Aging Characteristics of Typical Asphalt Cements Used in Florida.* Preprint, TRB, National Research Council, Washington, 1993.

10. Kim, O., C.A. Bell, J.E. Wilson and G. Boyle. *Effect of Moisture and Aging on Asphalt Pavement Life.* Oregon State Highway Division HP & R Study: 083: 5157, Final Report, Part 2 - Effect of Aging, 1986.

11. Lee, D.Y., *Asphalt Durability Correlation in Iowa.* Highway Research Board, Record 468, National Research Council, Washington, 1973.

12. Nazarian, S., M. Baker and R.C. Boyd. *Determination of Pavement Aging by High-Frequency Body and Surface Waves.* Proceedings, 7th International Conference on Asphalt Pavements, Nothingham, U.K., 1992.

13. Norman, W. Garrick and R.R. Biskur. *Effects of Asphalt Properties on Indirect Tensile Strength.* In Transportation Research Record 1269, TRB, National Research Council, Washington, D.C., pp. 26-39, 1990.

14. Noureldin, A.S., L.E. Wood. *Variations in Molecular Size Distribution of Virgin and Recycled Asphalt Binders Associated with Aging.* In Transportation Research Record 1228, TRB, National Research Council, Washington, D.C., pp.191-197, 1989.

15. Noureldin, A.S. and L.E. Wood. *Laboratory Evaluation of Recycled Asphalt Pavement Using Nondestructive Tests.* In Transportation Research Record 1269, TRB, National Research Council, Washington, D.C. pp. 92-100, 1990.

16. Roberts, F.L., P.S. Khandal, E.R. Brown, D.Y. Lee and T.W. *Kennedy Hot Mix Asphalt Materials, Mixture Design, and Construction.* NAPA Education Foundation, 1991.

17. Sosnovake, D., Y. AbWahad and C.A. Bell. *The Role of Asphalt and Aggregate in the Aging of Bituminous Mixtures.* Proceedings, Transportation Research Board, 72nd Annual Meeting, National Research Council, Washington, 1992.

18. The Asphalt Institute. *Asphalt Hot-Mix Recycling*. Manual Series No.20 (MS-20), August, 1981.

19. Tia., B.E. Ruth, C.T. Charai, J.M. Shiau, D. Richardson and J. Williams. *Investigation of Original and In-Service Asphalt Properties for the Development of Improved Specifications - Final Phase of Testing and Analysis*. Final Report, Engineering and Industrial Experiment Station, University of Florida, Gainseville, FL, 1988.

20. Vallegra, B.A., C.L. Monismith and K. Granthem. *A Study of Some Factors Influencing the Weathering of Paving Asphalt.* Proceedings, Association of Asphalt Paving Technologies, Volume 26, 1957.

21. Verhasselt, A.F., and F.S. Choquet. *Comparing Field and Laboratory Aging of Bitumens on a Kinematic Basis*. In Transportation Research Board 72nd Annual Meeting, National Research Council, Washington, 1992.

22. Von Quintus, H.L., J.A. Scherocman, C.S. Hughes and T.W. Kennedy. *Asphalt-Aggregate Mixture Analysis System (AAMAS)*. In Transportation Research Record 338, TRB, National Cooperative Highway Research Program Report, 1991.

23. Yibin Li. *Evaluation of Aging Effects of Asphaltic Concrete using Wave Propagation Techniques*. M.S. Thesis, The University of Texas at El Paso, El Paso, Tx. 1994.

APPENDIX A

Mix Design Details

a) Mix Design Details including Aggregate Gradation for El Paso Mix Design

Sieve No. (inches)	Cumulative Percent Passing
1/2 - 3/8	9
3/8 - # 4	31
# 4 - # 10	19.1
< # 10	40.9
Optimum Asphalt Content	5 %
Maximum Bulk Density	95.9 %

b) Mix Design Details including Aggregate Gradation for Austin Mix Design

Sieve No. (inches)	Cumulative Percent Passing
1/2 - 3/8	4.4
3/8 - # 4	33.8
# 4 - # 10	63
# 10 - # 40	81.8
# 40 - # 80	92.7
# 80 - # 200	96.7
< # 200	3.3
Optimum Asphalt Content	5.3 %
Maximum Bulk Density	96 %

APPENDIX B

Data Sheets

RESEARCH PROJECT 1369
TESTING METHODS FOR RECLAIMED ASPHALT PAVEMENTS
FORM 1/2: PROPERTIES OF ASPHALT CONCRETES

Specimen ID	Diameter (mm)	Height (mm)	Date/Time prepared

Prepared by:

Revised by:

Approved by:

[1] Weight (g)	[2] Weight Submerged (g)	[3] Weight at SSD (g)	[4]=[3]-[2] Bulk Volume (cm3)	[5]=[1]/[4] Bulk Density (g/cm3)	[6] Max Density (g/cm3)	[7]=1-[5]/[6] Air Voids (%)

Date/Time placed in oven	Date/Time removed from oven	Period in oven at 85°C

COMMENTS:

Specimen ID	WAVE PROPAGATION TEST			INDIRECT TENSILE TEST		
	Temperature (°C)	Travel Time (μs)	Modulus (MPa)	Temperature (°C)	Load(max) (N)	Strength (KPa)

DIAMETRAL RESILIENT MODULUS TEST

Temperature (°C)	Load(vert) (N)	Gag. Length (mm)	ΔHT (mm)	ΔVT (mm)	Poisson's ratio	Modulus (MPa)

RESEARCH PROJECT 1369
TESTING METHODS FOR RECLAIMED ASPHALT PAVEMENTS
FORM 2/2: PROPERTIES OF RECLAIMED ASPHALT CEMENTS

Specimen ID	Specimen ID	Method of Extraction	Date/Time prepared

Prepared by:

Revised by:

Approved by:

[1] Sample Initial Weight (g)	[2] Final Dry Filter Weight (g)	[3] Initial Dry Filter Weight (g)	[4]=[3]-[2] Fines in Filter (g)	[5] Pan and Extracted Agg Weight (g)	[6] Pan Weight (g)	[7]=[5]-[6] Extracted Agg Weight (g)

[8] Ash/100ml Weight (g)	[9] Total Solution Used (ml)	[10]=$\frac{[8]*[9]}{100}$ Total Ash Weight (g)	[11]=[4]+[7]+[10] Total Agg Weight (g)	[12]=[1]-[11] Asphalt Weight (g)	[13]=$\frac{[12]*100}{[1]}$ Asphalt Content (%)

PENETRATION TEST		VISCOSITY TEST		COMMENTS:
Temperature (°C)	Penetration (0.1mm)	Temperature (°C)	Viscosity (cst)	

Appendix C

Laboratory Testing Procedure

PROTOCOL FOR THE LABORATORY TESTING

I. OBJECTIVE

The purpose of this memorandum is to document the protocol to be followed for all the testing being performed in laboratory during the course of Project 1369.

II. PROTOCOL

(1) PREPARATION OF SPECIMENS (~1 hour and 45 minutes)

(a) Place the asphalt cement into the brown oven which should be set at 150C ± 1C for exactly 1 hour. Resist the temptation of playing with the temperature settings. If the asphalt is left in the oven for more than 1 hour, disregard the asphalt cement.

(b) Place the dry aggregate with its proper gradation on a steel bowl into the brown oven which should be always set at 150C ± 1C.

(c) Place the mixing bowl (including the whip) and the gyratory mold (including the base plate) into the brown oven for at least 15 minutes to ensure proper temperature during specimen preparation.

(d) Take the mixing bowl out from the oven and place the mixing bowl onto the precision balance. Then, zero the balance.

(e) Close to the time for the asphalt cement to be 1 hour into the oven, you should take the aggregate out from the oven and put it on the mixing bowl, making a small hole in the middle and checking the proper weight of the aggregate. Then zero the balance to accommodate for the asphalt.

(f) Take the asphalt out (right after 1 hour from the oven) and pour it into the mixing bowl. The amount of asphalt poured into the mixing bowl has to be the amount specified by the experimental design.

(g) Mix the hot mix asphalt for 30 sec., and make sure that all the aggregates particles are coated with asphalt.

(h) Place the hot mix asphalt into the brown oven and reheat it for 15 minutes.

(i) Take the gyratory mold and base plate out of the brown oven to prepare the mold ready for compaction i.e., spray light oil to prevent stickiness, place paper on top of base plate, fix cone on top of mold, etc.

(j) Take the hot mix asphalt out of the brown oven after 15 minutes. Then, place the hot mix asphalt into the gyratory mold and compact it to the desired compacting effort. This should take no more than 4 minutes.

(k) Take the specimen out from the gyratory mold and let it cool to room temperature (23C) for 1 hour. Measure its dry, submerged, and SSD weights in order to calculate its air voids. If the air voids are within the desired range, the specimen should be labeled for testing; otherwise, it will be thrown away. If accepted, proceed to measure its dimensions (diameter and thickness).

(l) Finally, place the specimen inside the blue temperature chamber which should be at 25C ± 0.1C. The specimen should also be placed into a water bath to make sure that all-around the specimen is at the desired temperature. The specimen should be inside the temperature chamber for 15 minutes at 25C ± 0.1C.

(2) LABORATORY TESTING — V-METER AND INDIRECT TENSILE TESTS (~2 hours)

(a) Before taking the specimen out of the temperature chamber, make sure that the V-meter is calibrated and working properly by using the calibration steel rod. Also, every single element or device of this testing set-up that will be in contact with the specimens should be at 25C ± 0.1C.

(b) Take the specimen out of the blue temperature chamber and dry it with a clean clothing. Then, set it into the V-meter set-up. Record the reading from the V-meter after 10 seconds of having completed the testing set-up. Once this is done, take the specimen out of this set-up, and proceed with the indirect tensile testing.

(c) Prepare a hydrostone paste with a 0.27 ± 0.1 water/hydrostone cement ratio. This paste should be placed on top and bottom of the diametral surfaces of the specimen that will be in contact with the loading strips. Place the specimen inside the indirect tensile set-up and lower the top loading strip so that it will squeeze the paste to ensure proper contact and bondage. Remove the excess paste from the specimen, and let the paste set for no less than 20 minutes to ensure hardening before applying any load on the specimen.

(d) While the paste is hardening, place the entire indirect tensile set-up into the blue temperature chamber which is at 25C ± 0.1C for no less than 15 minutes to ensure the specimen is at the right temperature. Thereafter, take the set-up out of the blue temperature chamber, and place it into the loading system.

(e) Before proceeding to perform the indirect tensile test, make sure that the ball of the device is properly aligned with the center of the loading piston and load cell. Once satisfactory position is achieved, do not attempt to move or slide the device.

(f) Check the loading rate of the indirect tensile set-up, turn on the power supply and multimeter of the recording device, and record the initial voltage reading. After this, you are ready for testing.

(g) Start loading the specimen, and make sure that you can catch the reading of the peak value. Report the peak value in voltages and convert it into engineering units. Then, use the formula [$s_t = 2P_u / (p\ d\ h)$] to estimate the indirect tensile strength.

(h) Once the specimen has reached the peak value, you can stop the test and release the load so that the specimen can be recovered. Even though, it would be advisable to let the specimen undergo larger strain amplitudes so that the failure crack is easily identified.

(i) Upon test completion, clean the contact surfaces of the specimens so that no hydrostone paste can be taken as a part of the mix. Now you are ready for asphalt extraction.

(3) EXTRACTION AND RECOVERY OF ASPHALT CEMENT (~4 hours)

(a) Place two companion specimens (already being tested) into a steel bowl. Label the bowl and then, place it into the brown oven (set at 150C ± 1C) for 15 minutes. This is mainly done to soften the asphalt mix and make it more workable.

(b) Take the two specimens out of the oven, brake them down, and weigh the mix. Then, place the mix into the centrifuge bowl and cover it with 600 ml of TCE to soak for 15 minutes.

(c) Dry two paper filters into the brown oven for 15 minutes, and then weigh them. The two filters should then be placed on top of the centrifuge bowl. Afterwards, the top should be placed and tightly bolted.

(d) Start the centrifuge revolving slowly, gradually increasing the speed to a maximum of 3000 rpm [dial set at 30] until solvent ceases to flow from the drain — this will take roughly 5 minutes. Then, add 200 ml of TCE allowing the solution to soak for two minutes and repeat the centrifuge procedure until the ratio TCE/asphalt content of 20:1 is obtained. (This means that 1600 ml of TCE are used for a mix of

4% asphalt, 2000 ml of TCE for a 5% asphalt, and 2400 ml of TCE for a 6% asphalt). Also make sure that the color of the final solution is a light straw color.

(e) Upon completion of the extraction, take the TCE-asphalt solution into clean bottles for high speed centrifuge. It is advisable to always leave some solution into the reservoir to somehow reduce the carrying over of fines into the high speed centrifuge, and to leave 100 ml of solution to determine asphalt and fine content.

(f) Place the bottles with TCE-asphalt solution into the high speed centrifuge for 30 minutes at 3,000 rpm. This constitutes the primary removal of fines. Then, take bottles out from the high speed centrifuge, and carefully tilt the bottles to the opposite side of the dust accumulation area pouring the solution into a clean reservoir. Again, you don't need to pour all the solution, since your objective is not to recover all the asphalt, but rather to recover an amount of asphalt that is completely free of fines.

(g) Thereafter, pour the TCE-asphalt solution (free of most of the fines) again into clean bottles, and place them into the high speed centrifuge for 60 more minutes at 3,000 rpm. This constitutes the secondary removal of fines. By the end of this procedure, the fines have been virtually removed from the TCE-asphalt solution.

(h) In the meantime, set the variable temperature transformer of the primary distillation set-up to 35 units to ensure that the mantle is already at 40C by the time the flask with the TCE-asphalt solution is placed on it. This should be done about 15 minutes before the secondary removal of fines procedure is completed.

(i) Upon completion, take the bottles out from the high speed centrifuge and carefully tilt the bottles to the opposite side of the dust accumulation area pouring the solution into the primary distillation flask. Then, place the flask into the mantle.

(j) Fix all the set-up features (i.e., install the thermometer, CO_2 conducts, distillation tube, water supply, and seals). Then, supply CO_2 at very small rate until primary distillation is completed. Completion of the primary distillation is defined as the moment when about 250 ml remains in the flask. This will take roughly 1 hour and 30 minutes.

(k) In the meantime, set the variable temperature transformer of the secondary distillation set-up to 35 units to ensure that the mantle is already at 40C by the time the flask with the TCE-asphalt solution is placed on it. This should be done about 15 minutes before the primary distillation procedure is completed.

(l) Immediately, upon completion of the primary distillation, place the remains (roughly 250 ml) of the TCE-asphalt solution into the secondary distillation flask, and place this flask into the secondary distillation set-up.

(m) Gradually raise the temperature of the solution to 130C (target rate < 2C/min) by using the variable temperature transformer in the procedure presented in the table below.

Time	Setting	Duration	Temperatur e	Observations
Preheati ng	35	------	40C	Mantle is preheated to reach 40C before receiving the TCE-asphalt solution.
0	45	Leave it for 20 min.	<110C	By the end, temperature will be less than 110C.
20 min.	55	Leave it for 20 min.	<120C	By the end, temperature will be less than 120C.
40 min.	50	Leave it for 5 min.	<125C	By the end, temperature will be less than 125C.
45 min.	45	Leave it for 2 min.	<130C	By the end, temperature will be less than 130C.
47 min.	40	Leave it for 8 min.	<132C	Since the temperature continues to raise; by the time when it reaches 130C, supply CO_2 at a rate of 100 ml/min; that is, set the flow meter to 5.
55 min.	45	Leave it for 15 min.	<160C	By the end, temperature will be less than 157C-160C. By then, increase the CO_2 supply at a rate of 900 ml/min; that is, set the flow meter to 27.
70 min.	0	Leave it for 15 min.	160C	Maintain the temperature at roughly 160-162C and the CO_2 supply until the TCE dripping ceases plus 5 extra minutes.

(n) As stated in the table above, upon reaching 130C, supply the CO_2 at a rate of 100 ml/minute [flow meter reading 5]; but, upon reaching 157C-160C increase the CO_2 supply rate to 900 ml/minute [flow meter reading 27]. Then, maintain the

temperature and CO_2 supply rate constant until the TCE dripping ceases plus 5 extra minutes. That will constitute the completion of the secondary distillation.

(o) Place the remaining asphalt into a tin can and then, put it on top of a vibrator (set at Vertek 5) for 3 minutes to eliminate any entrapped air. Thereafter, cap the tin can and label it. Now you are ready for the next step, penetration and viscosity testing.

(4) LABORATORY TESTING — PENETRATION AND VISCOSITY TESTS (~1 hour)

(a) Let the recovered asphalt cool down at room temperature for at least 2 hours. Then, place it inside a container filled with distilled water. Then, place the container and asphalt into the blue temperature chamber, which is at 25C ± 0.1C. Leave it there for 15 minutes to allow the specimen reach such temperature.

(b) In the meantime, make sure that the penetration needle is perfectly cleaned and dry. If not, clean it with TCE, and then dry it.

(c) Once the asphalt has reached the desired temperature, take the set-up out from the blue temperature chamber to perform the penetration test three times. Once done, cover it with the cap.

(d) Upon completion of the penetration tests, put the can into the brown oven, which is set at 150C ±0.1C; and leave it there for 15 minutes.

(e) Simultaneously, the CANNON temperature bath should be maintained at 135C ± 0.1C, as well as the crossarm viscometers.

(f) Remove the asphalt from the brown oven and place it into the viscometer through the bigger opening until reaching the filling mark. Then close the small opening for 15 minutes to prevent the asphalt to flow, as well as to ensure that the temperature of the asphalt is at the desired temperature; that is, 135C ± 0.1C.

(g) Open the small opening to let the asphalt flow into the viscometer tube, and perform the viscosity test. Record the time spent by the asphalt in travelling from one mark to the other mark. Then, calculate the viscosity of the asphalt by multiplying this travel time (in seconds) with the constant of the viscometer used.

(h) Finally, proceed to clean all the apparatus and tools used.

APPENDIX D

Results

Source of Mix : Austin
Aging Temperature : 85 C

Asphalt Content: 4%
VTM : 3%, 5%, and 7%

Specimen ID	Asphalt Content %	VTM %	Aging Time in days	Bulk Density gm/cm^3	Dimensions Diameter mm	Dimensions Height mm	Elastic Modulus Before Age GPa	Elastic Modulus After Age GPa	IDT Strength kPa	Kin. Viscosity Cst	Penetration 1/10 mm
430	4	3.6	0	2.372	101.96	52.27	41	41	460	286	52
431	4	3.8	1	2.364	101.93	52.40	34	34	456	286	52
432	4	3.4	2	2.376	101.93	52.40	31	33	701	501	39
433	4	3.8	7	2.365	101.77	51.91	33	34	670	501	39
434	4	3.8	28	2.365	101.98	52.30	32	35	683	545	33
435	4	3.9	0	2.364	102.05	52.11	34	39	662	545	33
436	4	3.5	1	2.373	101.97	51.86	33	37	940	623	26
437	4	3.7	2	2.369	102.03	52.06	33	37	942	623	26
438	4	3.8	7	2.366	101.91	52.40	32	38	1203	3315	3
439	4	3.8	28	2.360	101.93	52.45	28	39	1285	3315	3
450	4	5.4	0	2.326	102.00	53.32	32	32	365	304	43
451	4	5.5	1	2.320	102.00	53.21	32	32	367	304	43
452	4	5.5	2	2.320	101.91	53.53	34	36	485	455	37
453	4	5.5	7	2.320	101.94	53.62	34	37	469	455	37
454	4	5.5	28	2.324	102.01	53.93	33	35	609	687	26
455	4	4.9	0	2.336	102.00	53.33	33	36	598	687	26
456	4	5.4	1	2.327	101.99	53.29	31	35	896	1243	14
457	4	5.5	2	2.323	102.02	53.30	33	37	890	1243	14
458	4	5.3	7	2.330	102.00	53.59	33	40	1274	9275	4
459	4	5.4	28	2.327	102.03	53.52	33	39	1165	9275	4
470	4	6.6	0	2.290	101.96	54.50	31	31	281	342	48
471	4	6.6	1	2.290	101.93	54.47	29	29	320	342	48
472	4	7	2	2.290	101.94	54.46	33	36	437	536	25
473	4	7	7	2.290	101.97	54.74	30	36	431	536	25
474	4	7.1	28	2.280	101.97	54.52	30	33	548	671	20
475	4	7	0	2.290	101.97	54.42	29	32	525	671	20
476	4	6.9	1	2.289	102.04	53.89	32	35	701	1390	19
477	4	6.9	2	2.292	102.12	54.25	31	35	736	1390	19
478	4	7.2	7	2.280	101.93	55.07	33	41	930	6055	4
479	4	7.2	28	2.280	101.98	54.97	35	42	963	6055	4

Source of Mix : Austin
Aging Temperature : 85 C

Asphalt Content 5%
VTM : 3%, 4%,and 7%

Specimen ID	Asphalt Content %	VTM %	Aging Time in days	Bulk Density gm/cm^3	Dimensions		Elastic Modulus		IDT Strength kPa	Kin. Viscosity Cst	Penetration 1/10 mm
					Diameter mm	Height mm	Before Age GPa	After Age GPa			
530	5	3.6	0	2.336	101.93	53.06	34	34	279	354	39
531	5	3.6	1	2.336	101.85	53.39	33	33	301	354	39
532	5	3.9	2	2.329	101.83	53.30	36	37	365	444	34
533	5	4	7	2.326	101.83	53.50	35	38	361	444	34
534	5	3.7	28	2.335	101.93	54.00	34	38	451	602	28
535	5	3.6	0	2.332	101.73	53.25	35	37	439	602	28
536	5	3.3	1	2.345	101.89	53.75	36	42	509	825	21
537	5	3.4	2	2.341	101.86	53.01	35	37	680	825	21
538	5	3.7	7	2.335	103.63	54.58	37	47	1050	4000	10
539	5	3.6	28	2.336	103.63	52.76	35	44	1065	4000	10
550	5	5.2	0	2.290	101.87	54.36	37	37	241	364	45
551	5	5.2	1	2.300	101.90	54.19	36	36	241	364	45
552	5	5.1	2	2.301	101.88	54.30	38	39	367	422	32
553	5	5	7	2.304	101.97	54.00	39	40	391	422	32
554	5	5.3	28	2.296	101.94	54.06	37	40	462	600	31
555	5	5	0	2.303	101.94	54.14	36	39	436	600	31
556	5	5.4	1	2.293	101.91	54.20	37	40	610	998	20
557	5	5.3	2	2.294	101.93	54.14	37	38	630	998	20
558	5	5.1	7	2.299	101.82	54.29	37	45	1016	6940	5
559	5	5.1	28	2.299	101.81	54.07	37	44	976	6940	5
570	5	6.8	0	2.260	101.85	55.30	30	30	221	434	33
571	5	6.8	1	2.260	101.81	55.22	30	30	214	434	33
572	5	6.4	2	2.270	101.86	55.43	31	32	332	542	31
573	5	6.4	7	2.270	101.85	55.70	32	33	303	542	31
574	5	6.7	28	2.260	101.81	55.75	30	33	359	566	26
575	5	6.7	0	2.260	101.81	55.37	31	35	365	566	26
576	5	7	1	2.250	101.84	55.57	30	34	503	837	16
577	5	7	2	2.250	101.86	55.15	29	33	522	837	16
578	5	6.6	7	2.270	101.84	54.85	30	42	862	4437	8
579	5	6.5	28	2.270	101.88	54.92	31	42	903	4437	8

Source of Mix : Austin
Aging Temperature : 85 C

Asphalt Content 6%
VTM : 3%, 5%, and 7%

Specimen ID	Asphalt Content %	VTM %	Aging Time in days	Bulk Density gm/cm^3	Dimensions		Elastic Modulus		IDT Strength kPa	Kin. Viscosity Cst	Penetration 1/10 mm
					Diameter mm	Height mm	Before Age GPa	After Age GPa			
630	6	2.8	0	2.320	101.83	53.67	34	34	245	379	42
631	6	2.8	1	2.320	101.85	53.64	34	34	236	379	42
632	6	2.7	2	2.330	101.86	53.54	34	36	263	446	39
633	6	2.7	7	2.325	101.84	53.62	35	37	273	446	39
634	6	3.1	28	2.320	101.86	54.00	34	36	276	435	32
635	6	3.1	0	2.310	101.83	54.03	34	36	265	435	32
636	6	2.9	1	2.320	101.82	54.13	34	37	398	654	26
637	6	2.9	2	2.320	101.82	54.36	34	37	379	654	26
638	6	2.8	7	2.320	101.85	54.00	31	35	751	1919	14
639	6	2.8	28	2.330	101.86	53.89	30	35	793	1919	14
650	6	4.4	0	2.285	101.86	54.74	34	34	224	485	41
651	6	4.4	1	2.284	101.86	54.66	34	34	215	485	41
652	6	4.7	2	2.280	101.86	54.76	34	36	265	491	36
653	6	4.8	7	2.270	101.90	55.22	35	37	304	491	36
654	6	4.4	28	2.285	101.87	54.61	35	37	322	557	33
655	6	4.4	0	2.285	101.90	54.46	35	37	313	557	33
656	6	4.6	1	2.280	101.87	54.89	35	41	485	829	23
657	6	4.6	2	2.280	101.88	54.74	34	39	489	829	23
658	6	4.5	7	2.280	101.87	54.74	35	40	735	2086	4
659	6	4.5	28	2.280	101.88	54.67	35	40	697	2086	4
670	6	6.1	0	2.240	101.85	56.28	32	32	186	420	37
671	6	6.4	1	2.240	101.90	56.40	31	31	181	420	37
672	6	6.1	2	2.240	101.90	55.93	32	33	246	536	32
673	6	6.1	7	2.240	101.90	56.07	31	33	258	536	32
674	6	6	28	2.246	101.86	56.03	32	33	291	601	29
675	6	6	0	2.247	101.86	55.42	32	34	286	601	29
676	6	5.9	1	2.248	101.90	55.40	32	37	435	971	15
677	6	5.9	2	2.248	101.90	55.88	32	39	446	971	15
678	6	6.3	7	2.238	101.85	56.90	28	33	766	4338	6
679	6	6.3	28	2.238	101.80	55.90	27	32	651	4338	6

Source of Mix : El Paso
Aging Temperature : 85 C

Asphalt Content 4%
VTM : 3%, 5%, and 7%

Specimen ID	Asphalt Content %	VTM %	Aging Time in days	Bulk Density gm/cm^3	Dimensions Diameter mm	Dimensions Height mm	Elastic Modulus Before Age GPa	Elastic Modulus After Age GPa	IDT Strength kPa	Kin. Viscosity Cst	Penetration 1/10 mm
430	4	2.5	0	2.447	102.11	50.11	39	39	324	398	47
431	4	2.5	1	2.447	102.47	50.46	39	39	319	398	47
432	4	2.5	2	2.446	101.87	50.46	39	41	327	421	45
433	4	2.7	7	2.441	101.96	50.73	40	41	323	421	45
434	4	2.8	28	2.436	101.85	50.67	39	41	434	443	44
435	4	2.7	0	2.442	101.74	50.95	40	43	423	443	44
436	4	2.4	1	2.449	101.72	50.63	40	43	467	535	40
437	4	2.4	2	2.44	101.89	50.58	39	43	501	535	40
438	4	2.6	7	2.444	102.1	50.8	39	46	749	1040	25
439	4	2.6	28	2.394	102.02	50.91	38	44	726	1040	25
450	4	4.6	0	2.394	101.62	51.62	35	35	323	424	48
451	4	4.6	1	2.388	101.8	51.77	36	36	331	424	48
452	4	4.8	2	2.39	101.78	51.96	34	39	347	479	43
453	4	4.7	7	2.387	101.69	52.29	35	39	365	479	43
454	4	4.9	28	2.383	101.91	52.29	35	41	419	495	40
455	4	5	0	2.382	101.8	52.06	35	40	417	495	40
456	4	5.1	1	2.383	101.66	52.08	35	41	451	617	35
457	4	5	2	2.381	101.85	51.69	36	42	502	617	35
458	4	5.1	7	2.382	102.06	52.02	38	45	694	1225	23
459	4	5.1	28	2.343	102.07	52.09	38	45	655	1225	23
470	4	6.6	0	2.344	102.4	53.21	34	34	266	413	44
471	4	6.6	1	2.34	102.41	53.36	33	33	268	413	44
472	4	6.7	2	2.341	102.29	53.04	34	37	336	488	40
473	4	6.7	7	2.335	102.24	53.23	33	36	282	488	40
474	4	6.9	28	2.337	102.29	53.5	33	37	351	546	36
475	4	6.9	0	2.33	102.39	53.71	34	38	378	546	36
476	4	7.1	1	2.33	102.34	53.14	34	39	422	681	31
477	4	7.1	2	2.331	102.19	53.59	32	37	413	681	31
478	4	7.1	7	2.33	102.07	53.17	34	39	544	1337	22
479	4	2.3	28	2.414	102.18	53.25	34	40	555	1337	22

Source of Mix : El Paso
Aging Temperature : 85 C

Asphalt Content 5%
VTM : 3%, 5%, and 7%

Specimen ID	Asphalt Content %	VTM %	Aging Time in days	Bulk Density gm/cm^3	Dimensions		Elastic Modulus		IDT Strength kPa	Kin. Viscosity Cst	Penetration 1/10 mm
					Diameter mm	Height mm	Before Age GPa	After Age GPa			
530	5	2.3	0	2.414	101.83	51.26	40	40	304	417	54
531	5	2.3	1	2.413	101.86	51.63	41	41	297	417	54
532	5	2.4	2	2.411	101.85	51.42	41	43	310	428	51
533	5	2.4	7	2.412	101.8	51.32	42	44	322	428	51
534	5	2.3	28	2.415	101.75	51.27	41	44	328	447	45
535	5	2.2	0	2.418	101.73	51.07	40	43	307	447	45
536	5	2.2	1	2.417	101.83	51.4	40	44	358	520	43
537	5	2.2	2	2.417	101.78	51.85	41	45	327	520	43
538	5	2.6	7	2.407	102.01	51.7	42	46	488	719	32
539	5	2.5	28	2.409	101.98	51.55	40	45	479	719	32
550	5	5.1	0	2.345	101.77	53.27	33	33	237	412	54
551	5	5.1	1	2.344	101.69	53.13	33	33	212	412	54
552	5	5.1	2	2.344	101.73	53.25	35	37	264	474	48
553	5	5.1	7	2.344	101.82	53.12	34	36	263	474	48
554	5	5	28	2.347	102.07	53.45	34	36	287	514	45
555	5	4.9	0	2.349	102.05	53.7	36	38	266	514	45
556	4	4.9	1	2.351	102.08	53.11	35	40	345	559	36
557	5	4.9	2	2.351	102.11	53.5	36	39	329	559	36
558	5	4.8	7	2.352	102.09	52.68	37	42	498	846	29
559	5	4.7	28	2.355	102.05	52.75	36	42	487	846	29
570	5	6.7	0	2.306	101.7	54.94	30	30	203	421	53
571	5	6.7	1	2.306	101.82	54.54	28	28	183	421	53
572	5	6.9	2	2.299	101.8	55.4	29	31	223	450	47
573	5	6.7	7	2.305	101.85	54.54	31	33	237	450	47
574	5	6.7	28	2.304	101.82	54.71	28	31	239	520	43
575	5	6.7	0	2.306	101.82	55.11	30	33	241	520	43
576	5	7	1	2.299	101.9	54.46	28	32	306	647	33
577	5	6.8	2	2.302	101.8	54.41	29	33	314	647	33
578	5	7.2	7	2.293	101.8	54.71	33	36	445	1136	21
579	5	6.9	28	2.3	101.75	54.63	33	36	471	1136	21

Source of Mix : El Paso
Aging Temperature : 85 C

Asphalt Content 6%
VTM: 3%, 5%, and 7%

Specimen ID	Asphalt Content %	VTM %	Aging Time in days	Bulk Density gm/cm^3	Dimensions		Elastic Modulus		IDT Strength	Kin. Viscosity	Penetration After Age
					Diameter mm	Height mm	Before Age GPa	After Age GPa	kPa	Cst	1/10 mm
630	6	3	0	2.359	101.51	53.6	34	34	213	421	51
631	6	3	1	2.36	101.77	53.07	34	34	213	421	51
632	6	2.9	2	2.363	101.82	53.09	36	39	224	459	46
633	6	2.9	7	2.363	101.82	52.3	32	34	222	459	46
634	6	2.5	28	2.373	101.6	52.85	35	38	244	471	47
635	6	2.7	0	2.366	101.83	52.65	35	38	243	471	47
636	6	2.9	1	2.362	101.85	52.85	35	41	297	537	44
637	6	2.9	2	2.363	101.88	52.85	34	40	272	537	44
638	6	2.9	7	2.363	101.8	52.91	36	42	363	632	40
639	6	2.8	28	2.365	101.81	53.02	35	41	323	632	40
650	6	5.3	0	2.304	101.8	53.67	28	28	179	406	52
651	6	5	1	2.312	101.88	53.82	30	30	175	406	52
652	6	4.9	2	2.314	101.9	54.01	29	31	188	424	48
653	6	4.9	7	2.313	101.85	54.21	30	31	187	424	48
654	6	5.4	28	2.302	101.78	54.15	30	33	235	515	44
655	6	5.4	0	2.302	101.78	54.2	29	31	234	515	44
656	6	5.2	1	2.308	101.86	54.27	29	32	279	604	35
657	6	5.2	2	2.306	101.8	54.73	30	33	307	604	35
658	6	5	7	2.312	101.81	53.94	28	32	393	1058	24
659	6	4.9	28	2.313	101.75	53.96	30	34	325	1058	24
670	6	7.3	0	2.256	101.83	56	29	29	150	407	52
671	6	7.3	1	2.256	101.85	55.5	27	27	133	407	52
672	6	6.7	2	2.269	101.85	55.21	28	30	176	477	47
673	6	6.9	7	2.266	101.85	55.15	26	28	173	477	47
674	6	7	28	2.263	101.73	55.62	27	31	209	480	42
675	6	7.2	0	2.257	101.7	55.65	28	31	205	480	42
676	6	6.7	1	2.271	101.83	55.45	27	31	318	723	33
677	6	6.7	2	2.269	101.8	55.37	27	32	281	723	33
678	6	7.1	7	2.259	101.78	55.24	27	31	368	1155	23
679	6	7.1	28	2.259	101.88	55.51	26	32	353	1155	23

APPENDIX E

Effects of AC and VTM on El Paso Mix

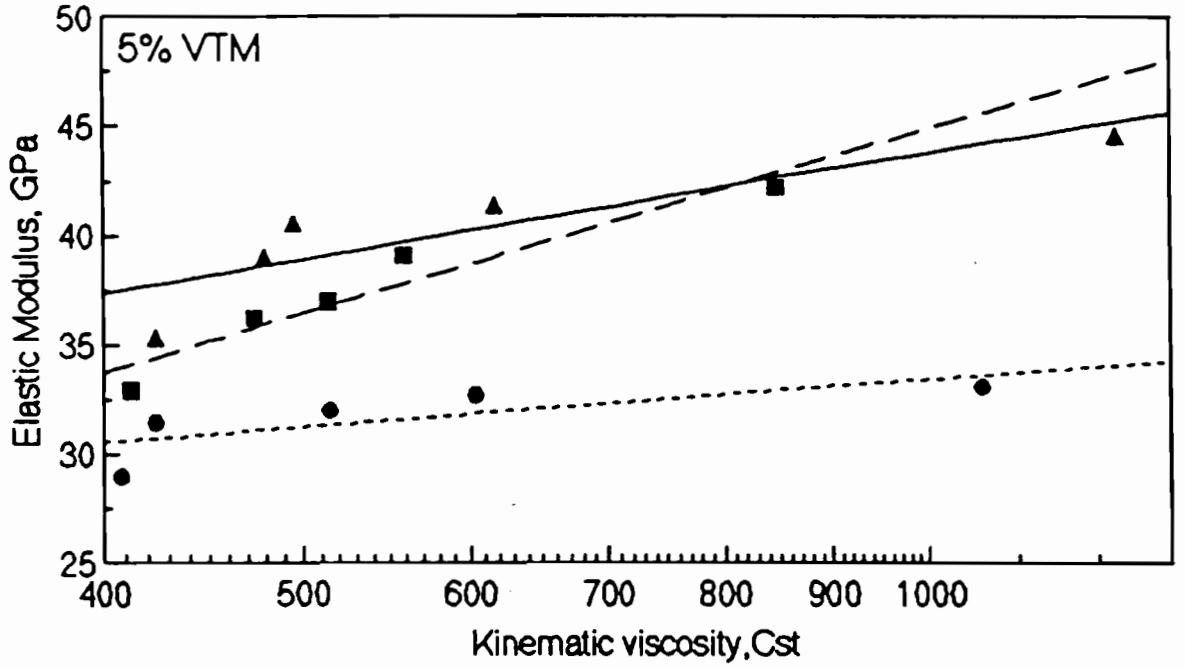

E.1 Effect of Asphalt Content on the Relationship between Elastic Modulus and Kinematic Viscosity for El Paso Mix.

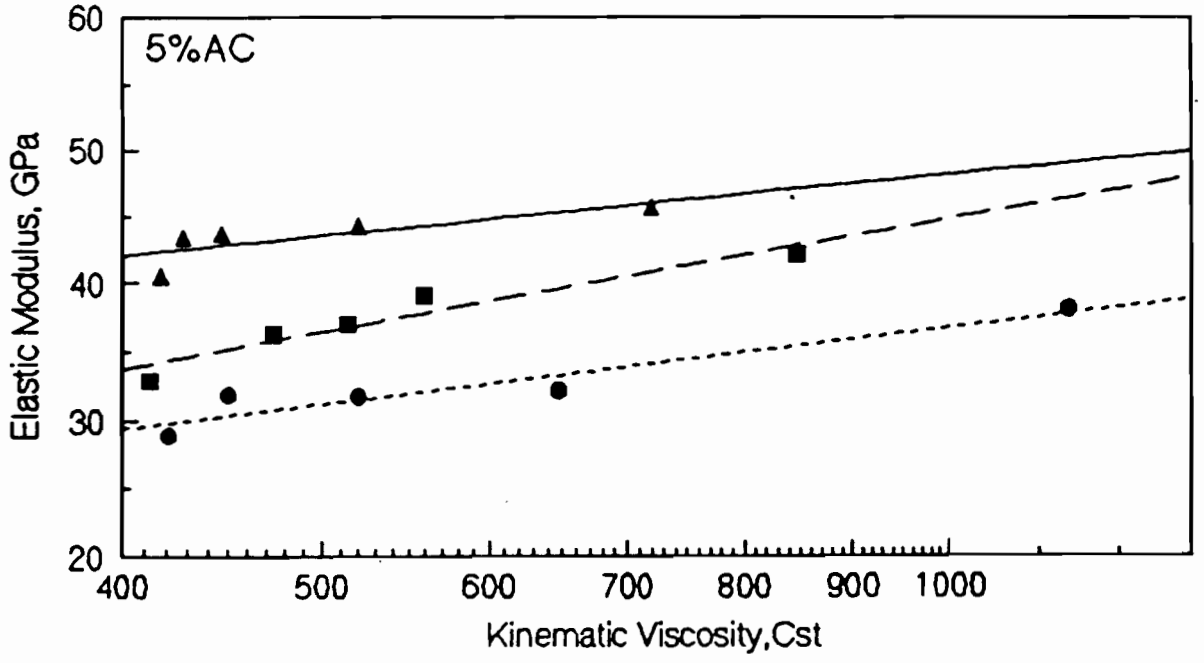

E.2 Effect of Voids in Total Mix on the Relationship between Elastic Modulus and Kinematic Viscosity for El Paso Mix.

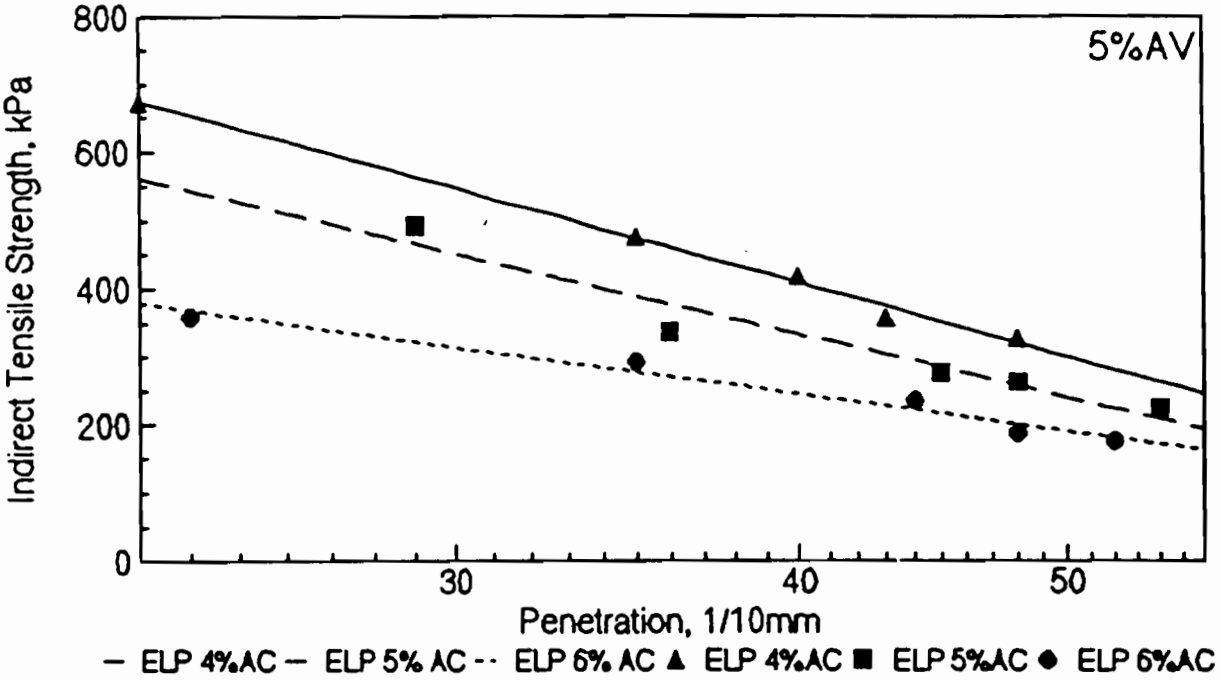

E.3 Effect of Asphalt Content on the Relationship between IDT Strength and Penetartion for El Paso Mix.

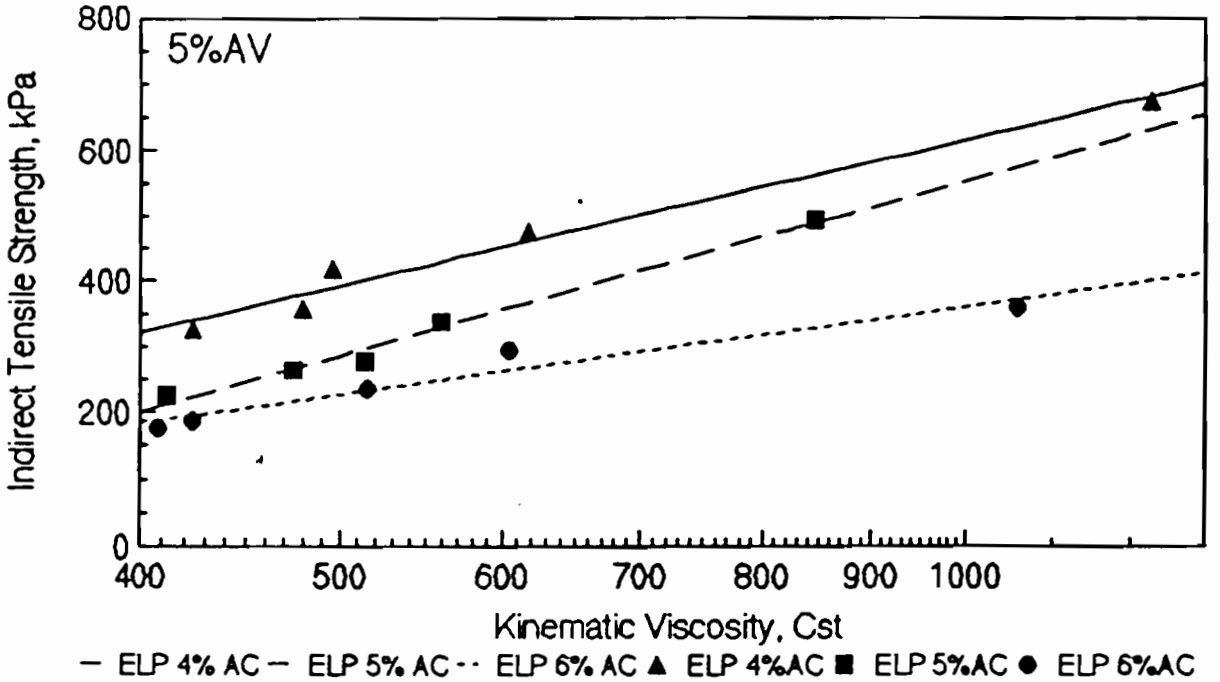

E.4 Effect of Asphalt Content on the Relationship between IDT Strength and Kinematic Viscosity for El Paso Mix.

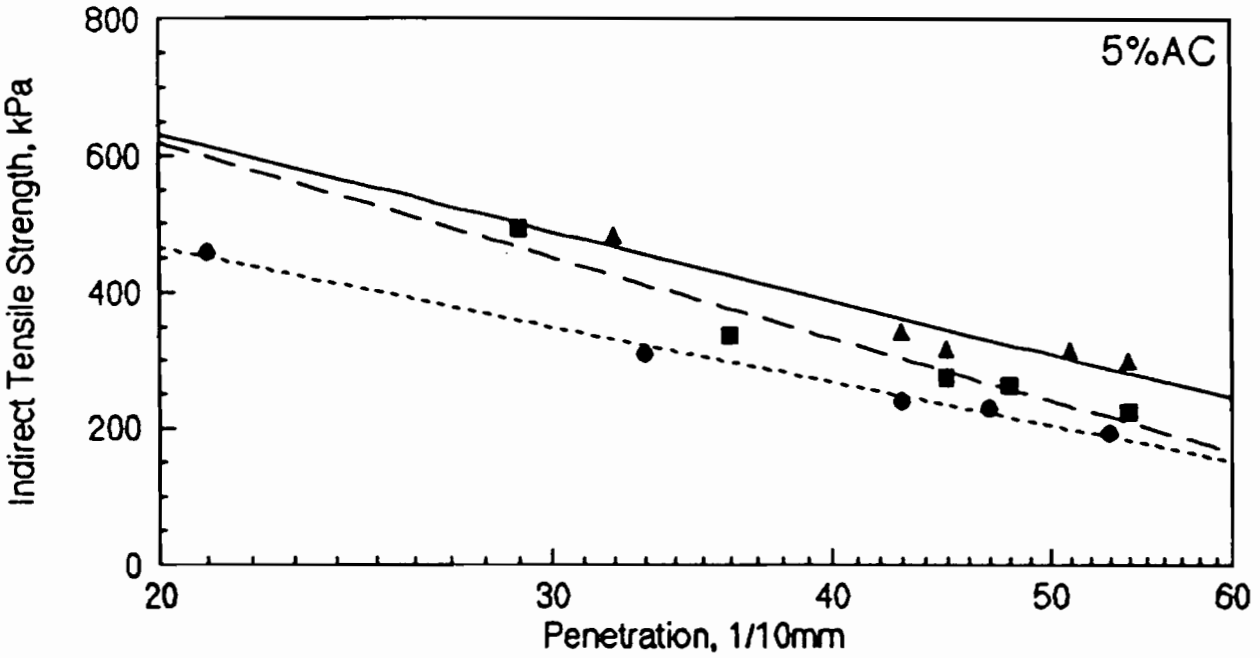

E.5 Effect of Voids in Total Mix on the Relationship between IDT Strength and Penetartion for El Paso Mix.

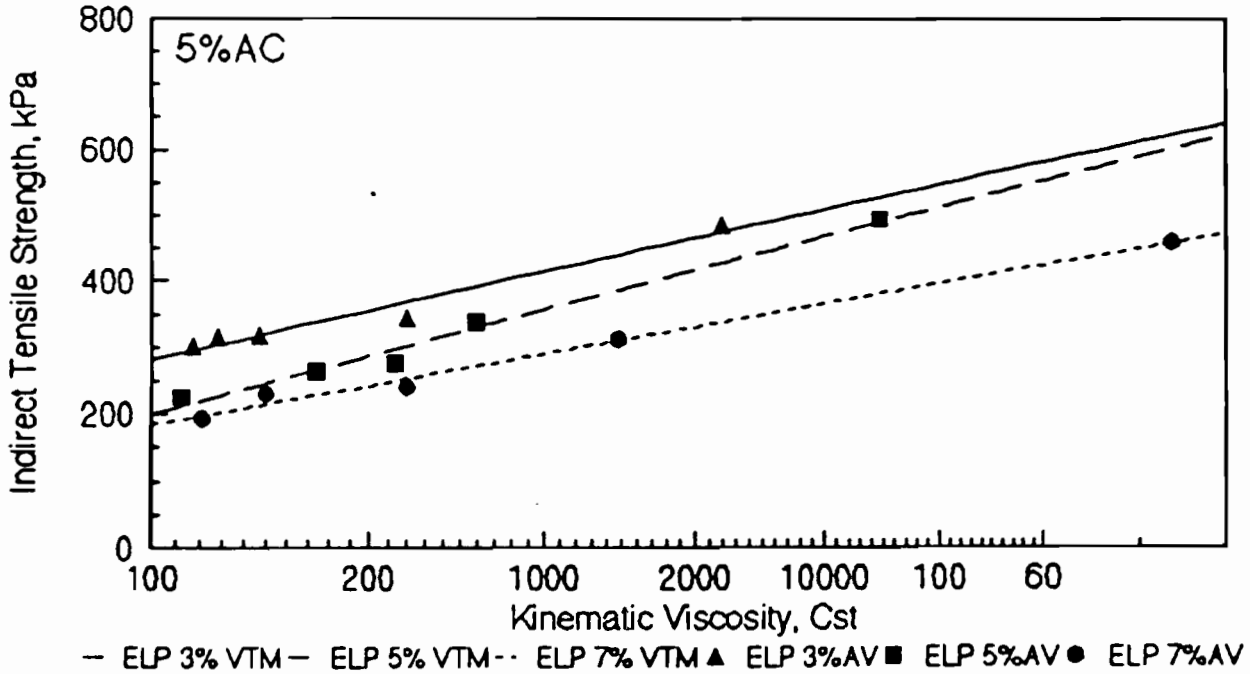

E.6 Effect of Voids in Total MIx on the Relationship between IDT Strength and Kinematic Viscosity for El Paso Mix.

APPENDIX F

Comparison of Actual and Predicted Penetration & % Error

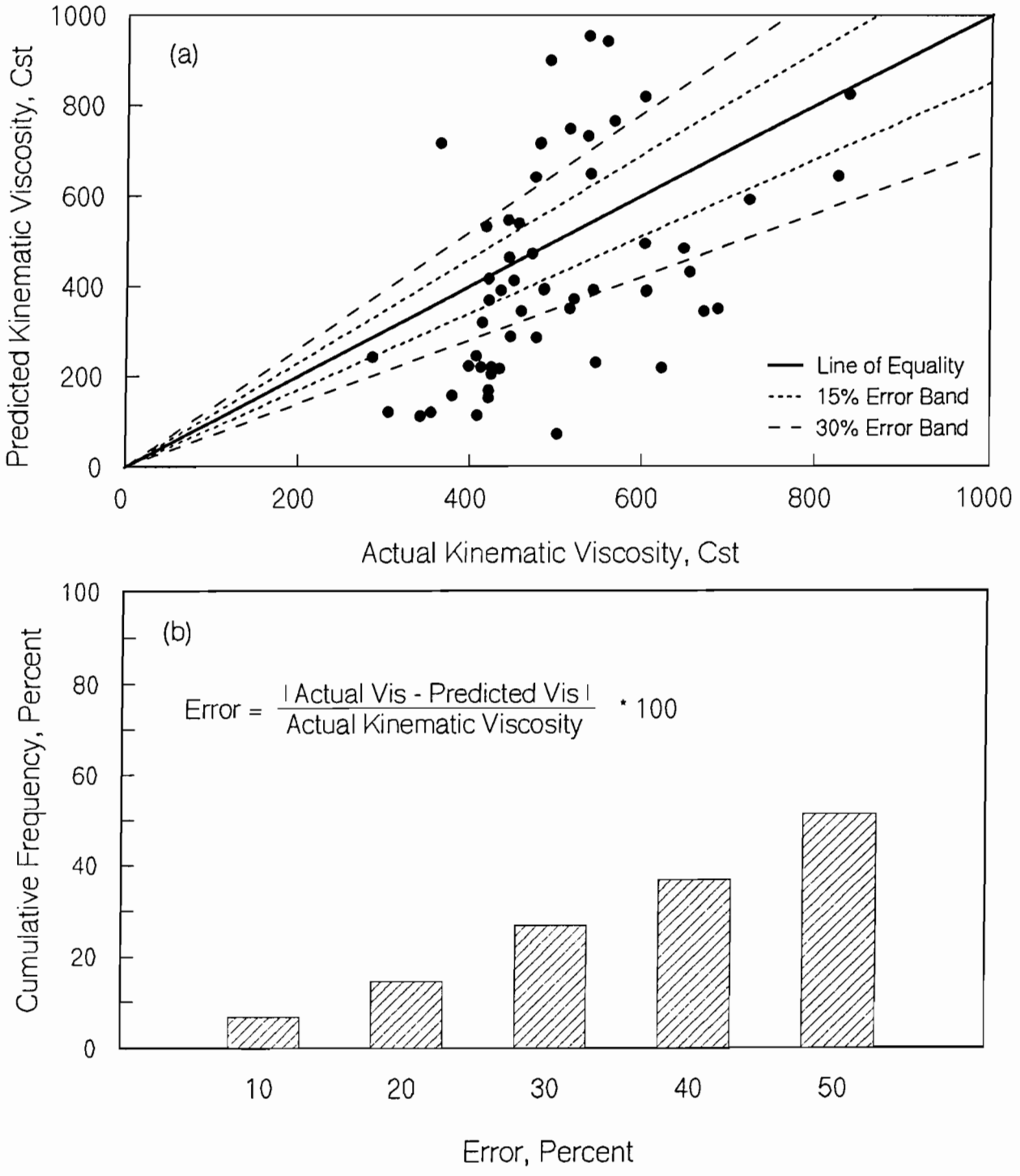

Figure F.1 Comparison of Actual and Predicted Penetration Values Using Equation 5.1 for Austin Data (without Outliers) a) Scatter Plot, b) Cumulative Percent Error.

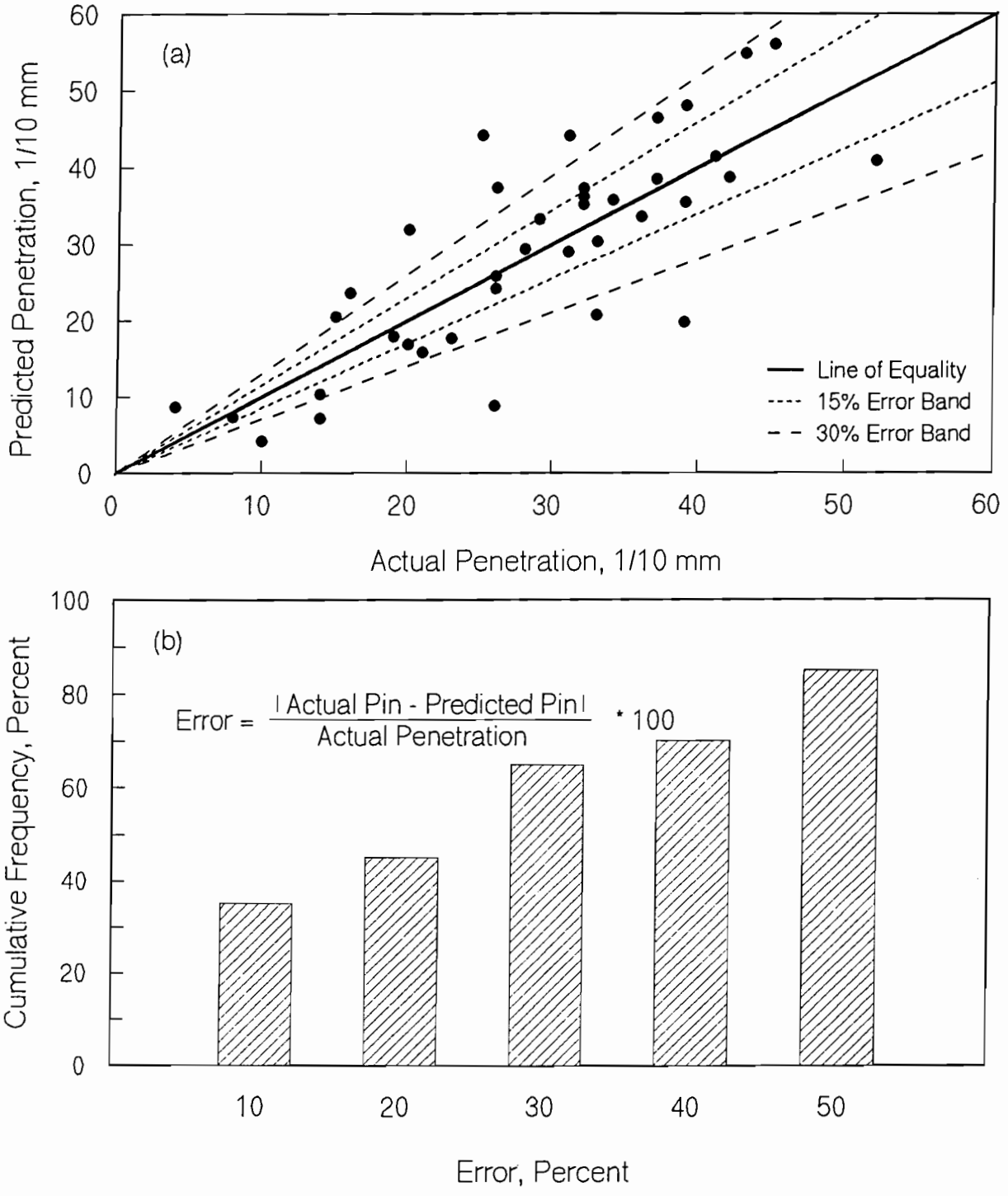

Figure F.2 Comparison of Actual and Predicted Penetration Values Using Equation 5.5 for Austin Data (without Outliers) a) Scatter Plot, b) Cumulative Percent Error.

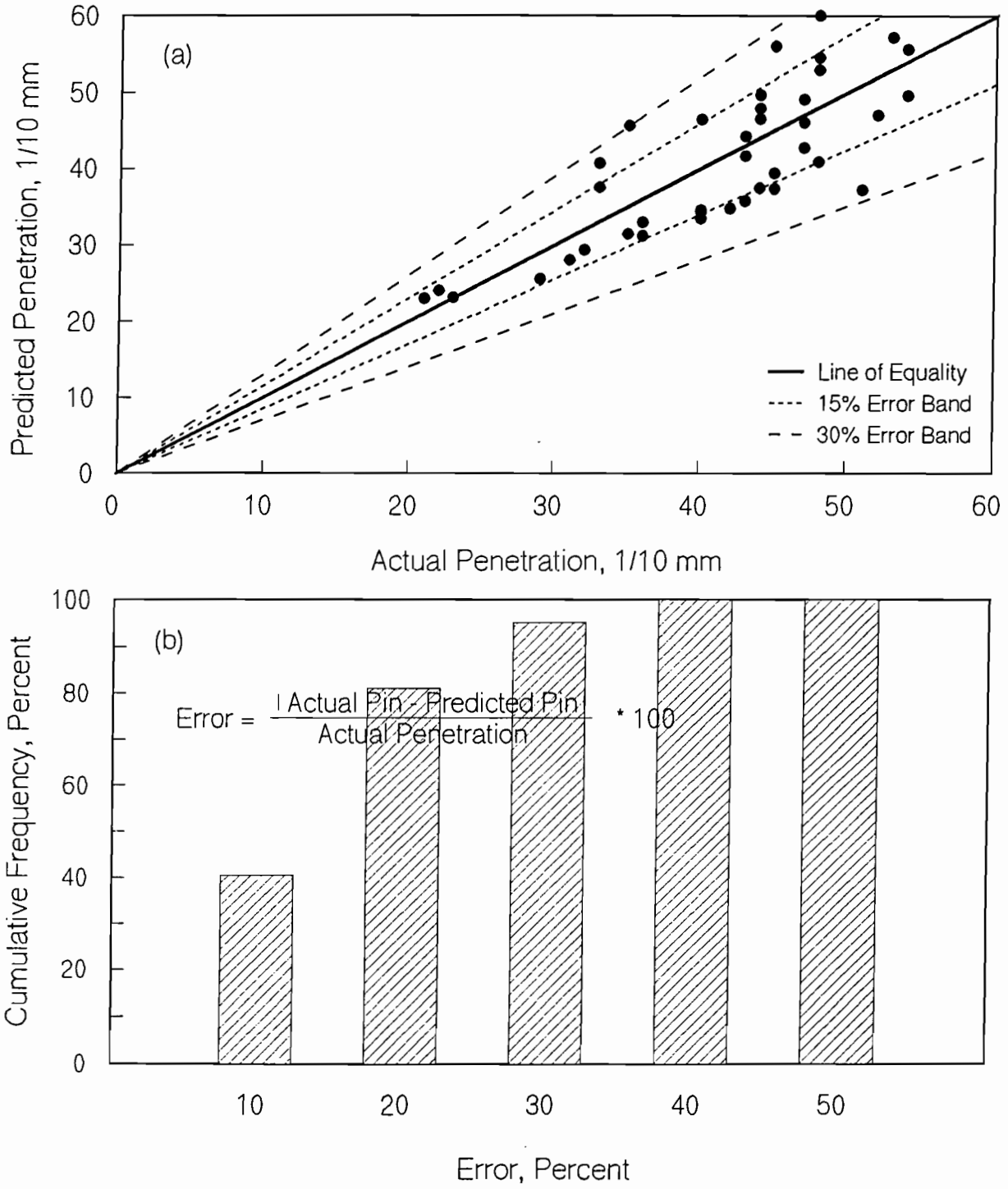

Figure F.3 Comparison of Actual and Predicted Penetration Values Using Equation 5.1 for El Paso Data (without Outliers) a) Scatter Plot, b) Cumulative Percent Error.

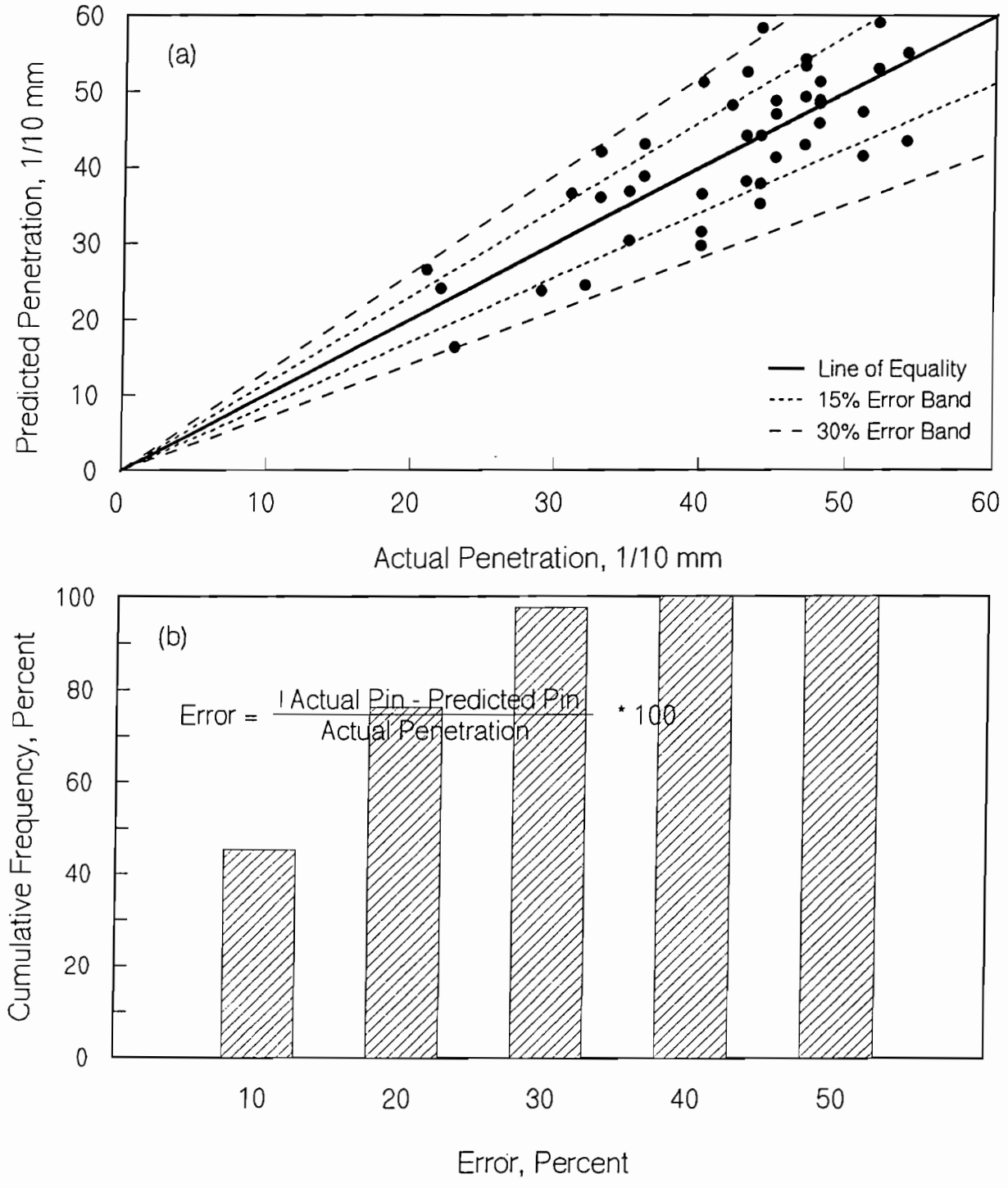

Figure F.4 Comparison of Actual and Predicted Penetration Values Using Equation 5.5 for El Paso Data (without Outliers) a) Scatter Plot, b) Cumulative Percent Error.

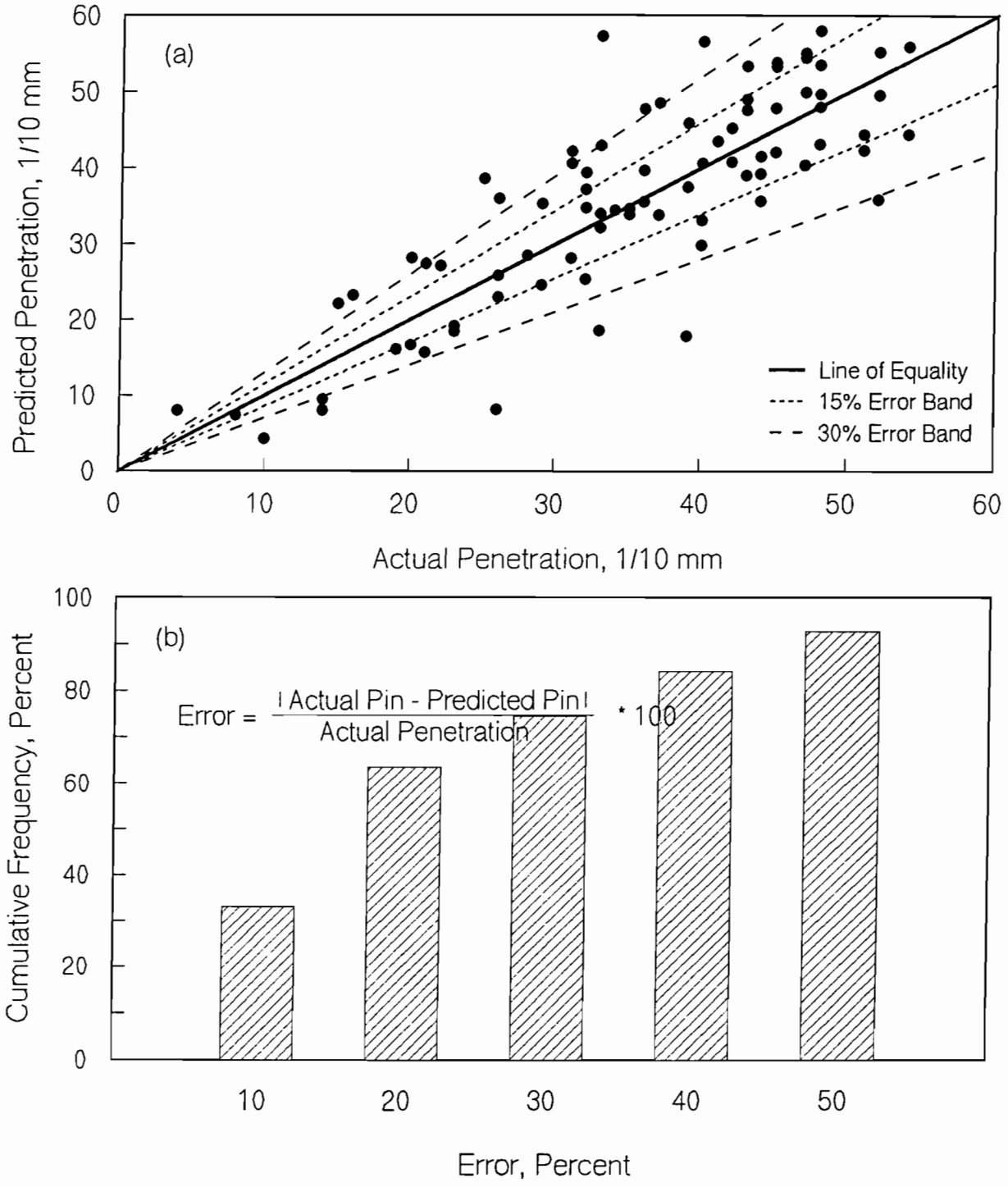

Figure F.5 Comparison of Actual and Predicted Penetration Values Using Equation 5.5 for All Data (without Outliers) a) Scatter Plot, b) Cumulative Percent Error.

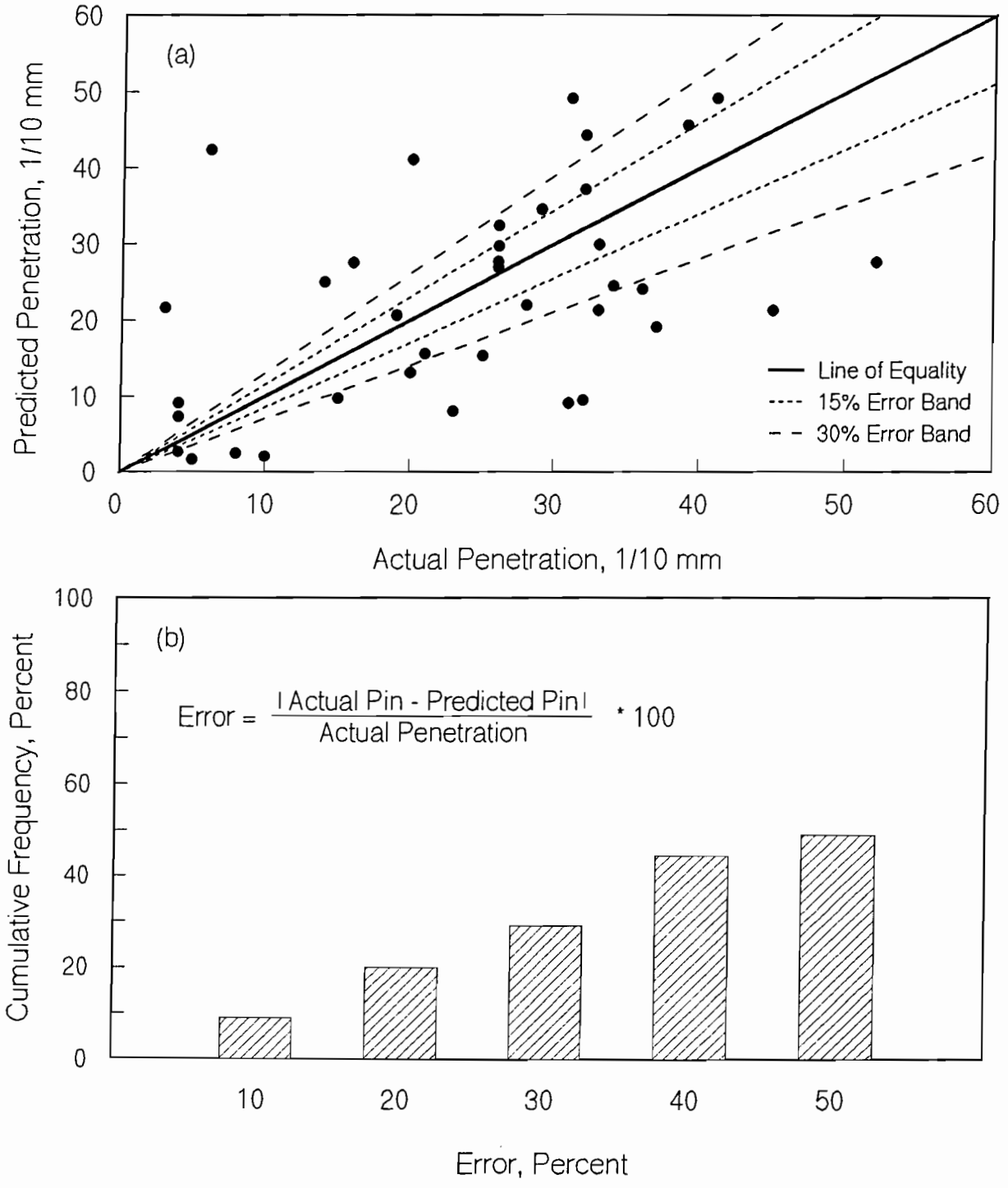

Figure F.6 Comparison of Actual and Predicted Penetration Values Using Equation 5.1 for Austin Data a) Scatter Plot, b) Cumulative Percent Error.

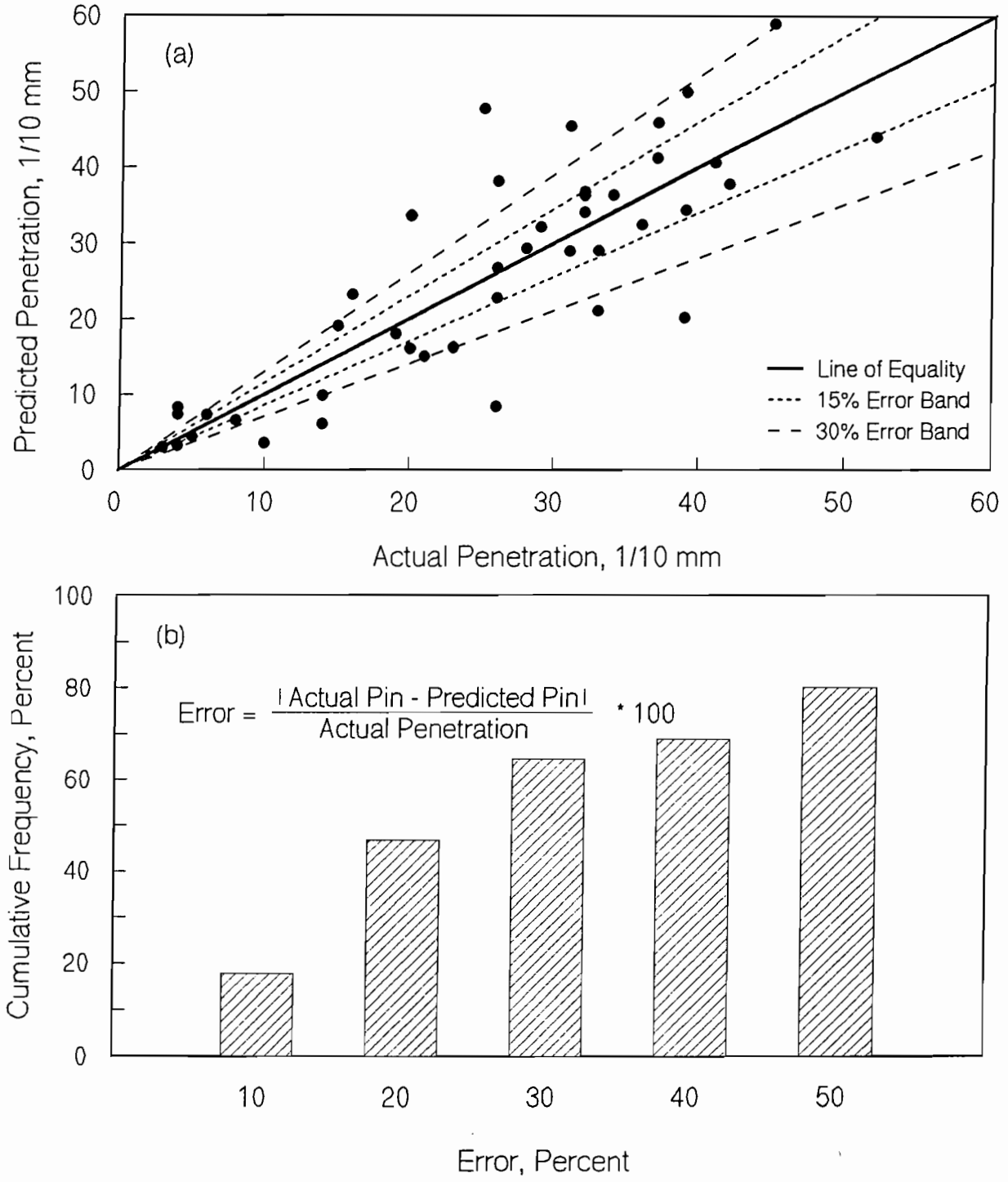

Figure F.7 Comparison of Actual and Predicted Penetration Values Using Equation 5.5 for Austin Data a) Scatter Plot, b) Cumulative Percent Error.

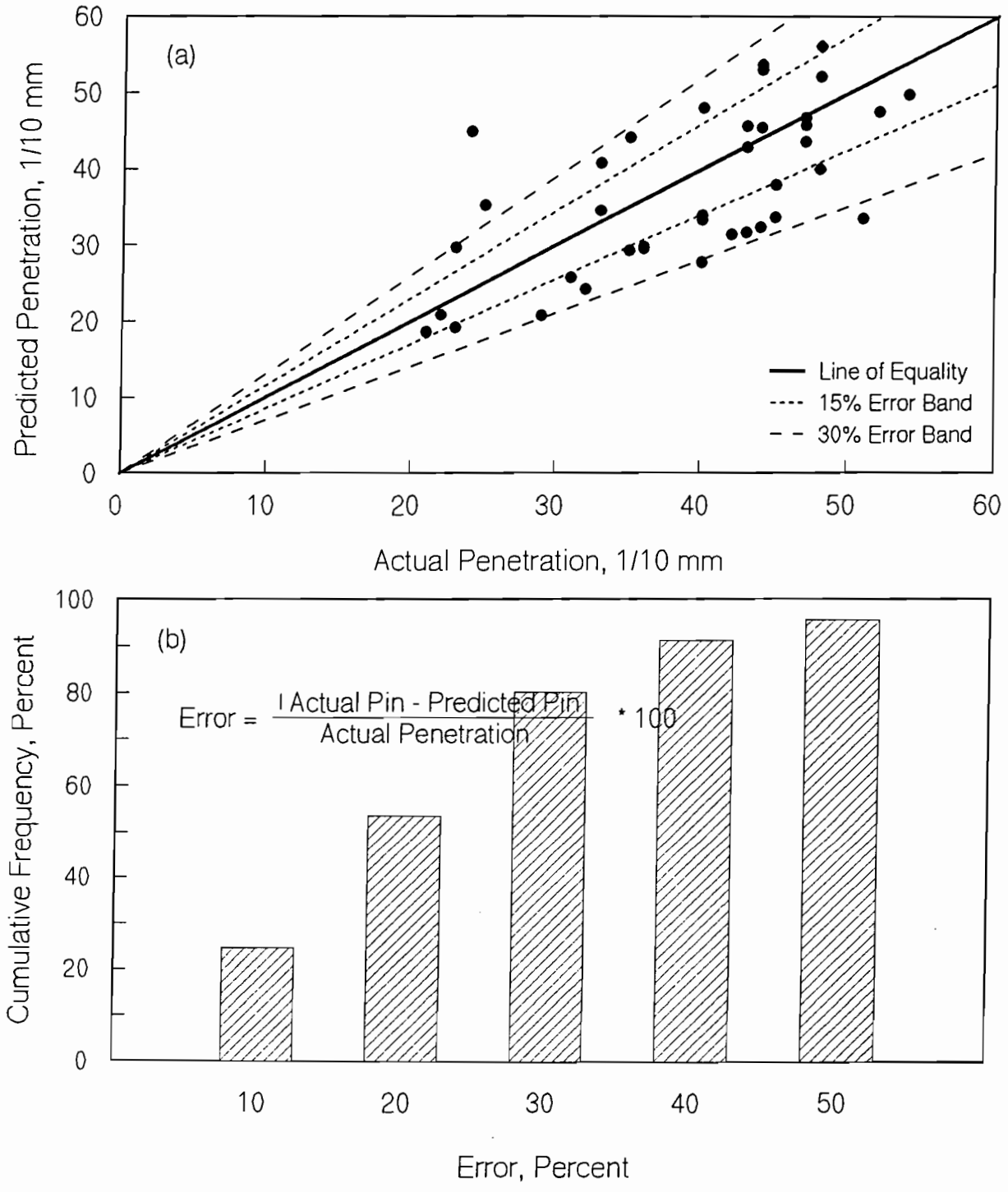

Figure F.8 Comparison of Actual and Predicted Penetration Values Using Equation 5.1 for El Paso Data a) Scatter Plot, b) Cumulative Percent Error.

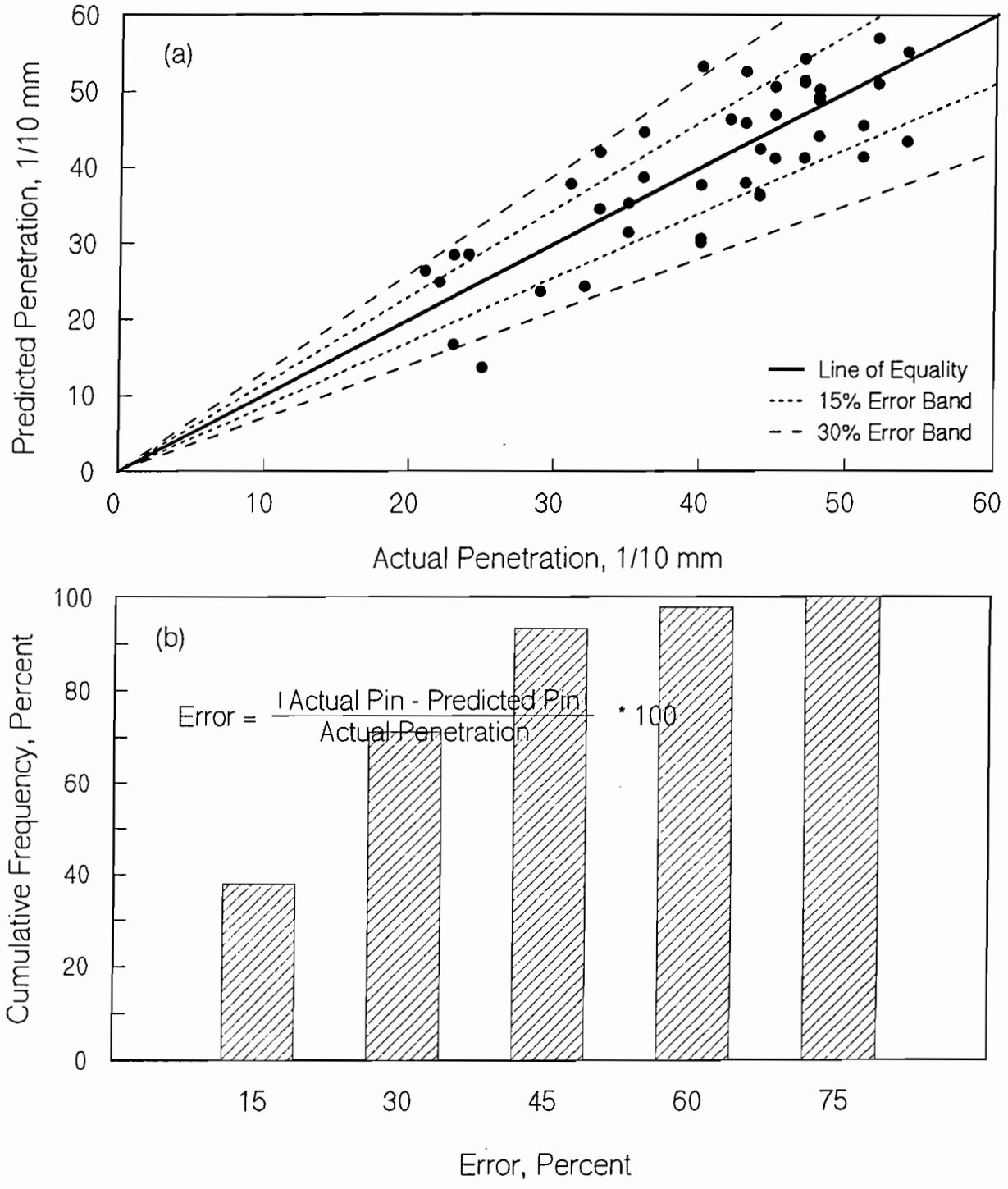

Figure F.9 Comparison of Actual and Predicted Penetration Values Using

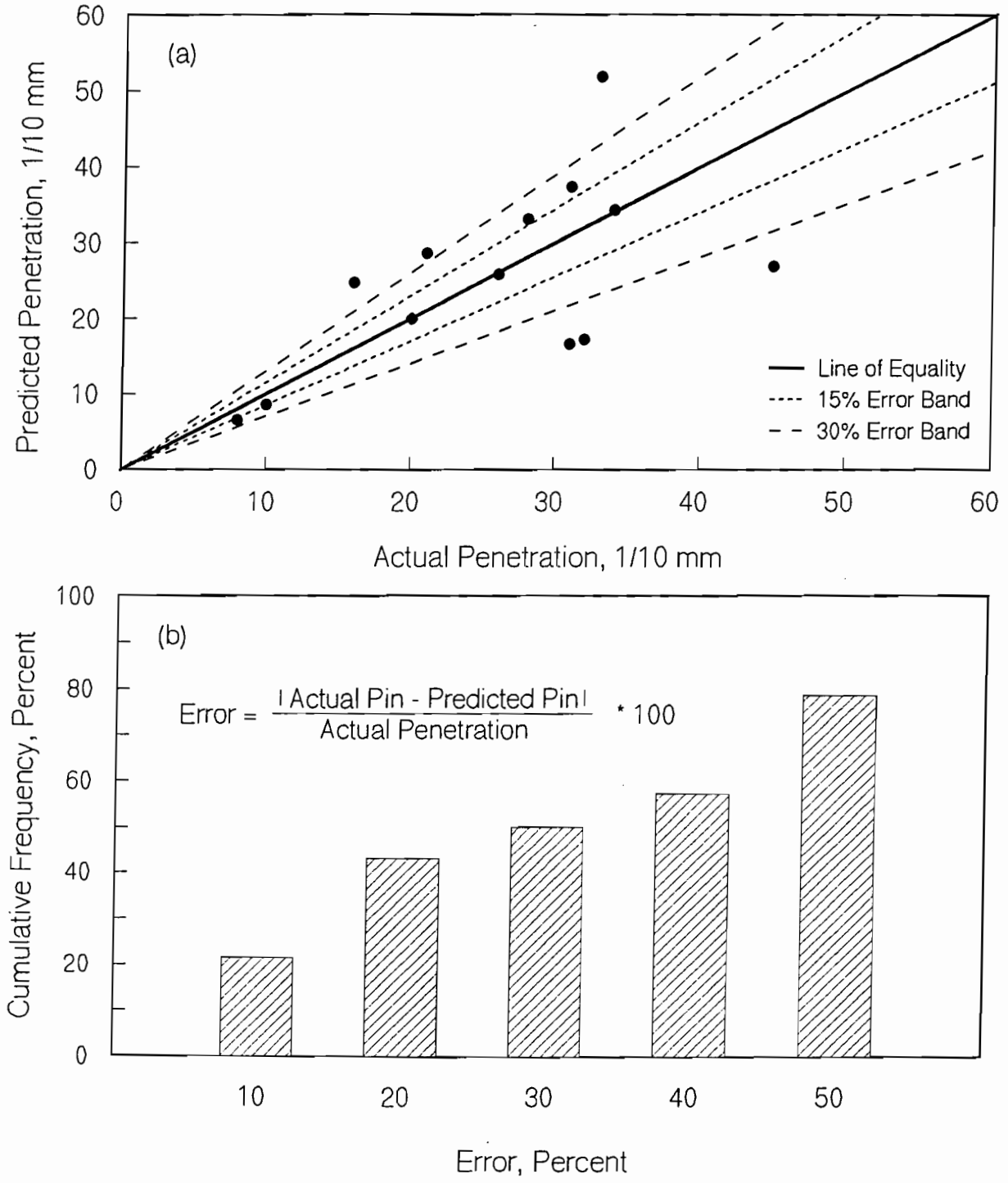

Figure F.10 Comparison of Actual and Predicted Penetration Values Using Equation 5.1 for Austin Data with 5 percent AC Content (without Outliers) a) Scatter Plot, b) Cumulative Percent Error.

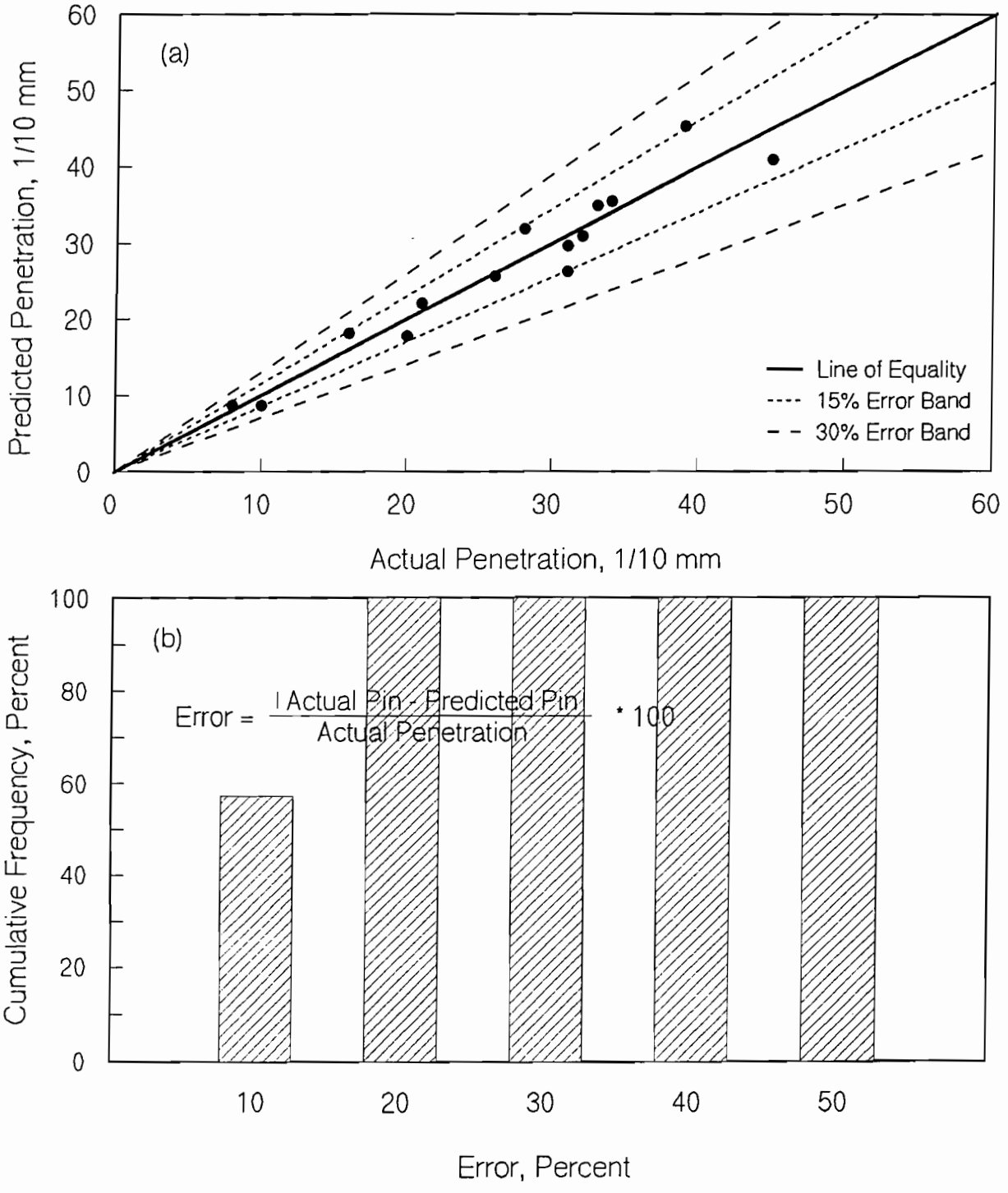

Figure F.11 Comparison of Actual and Predicted Penetration Values Using Equation 5.5 for Austin Data with 5 percent AC Content (without Outliers) a) Scatter Plot, b) Cumulative Percent Error.

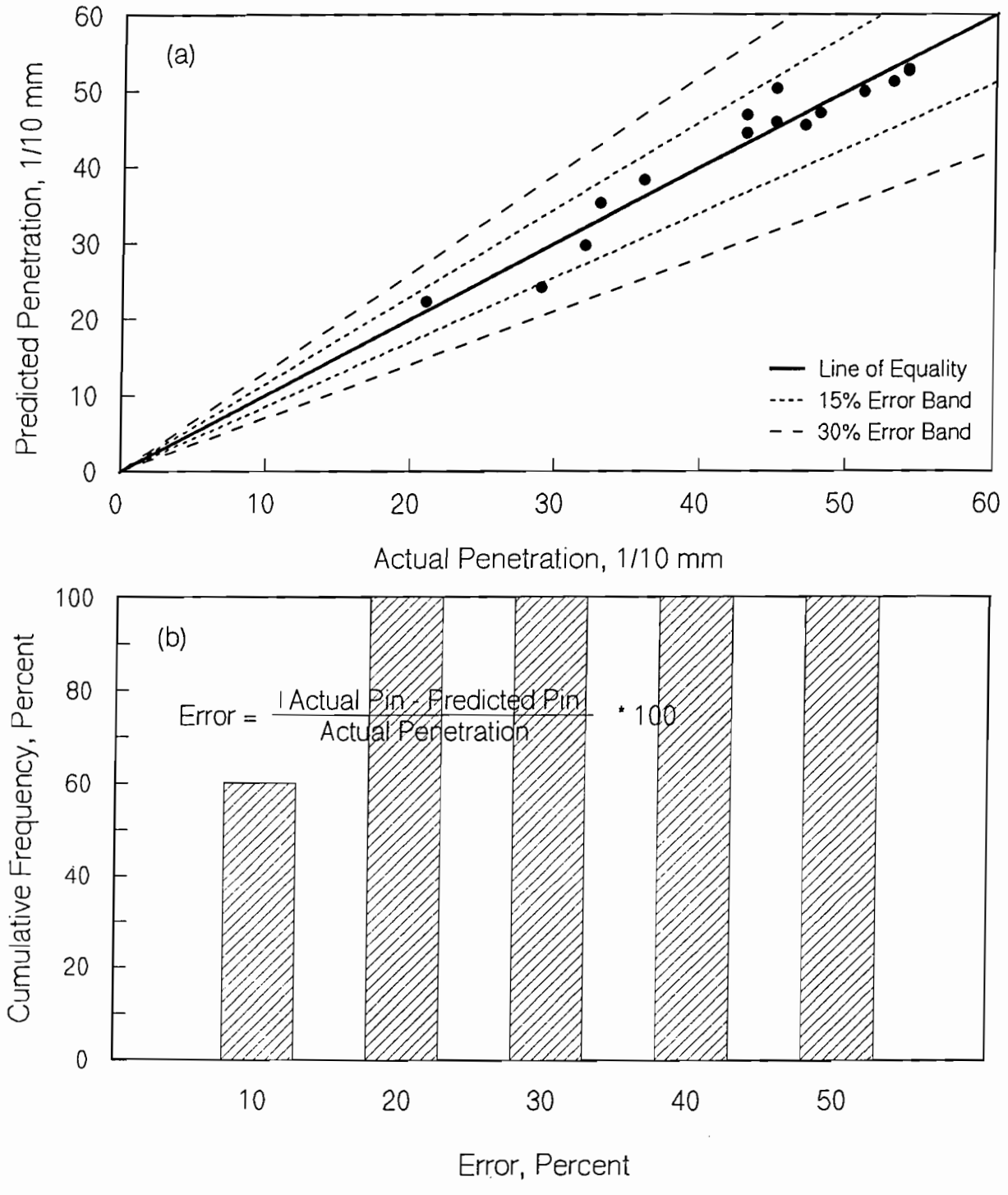

Figure F.12 Comparison of Actual and Predicted Penetration Values Using Equation 5.1 for El Paso Data with 5 percent AC Content (without Outliers) a) Scatter Plot, b) Cumulative Percent Error.

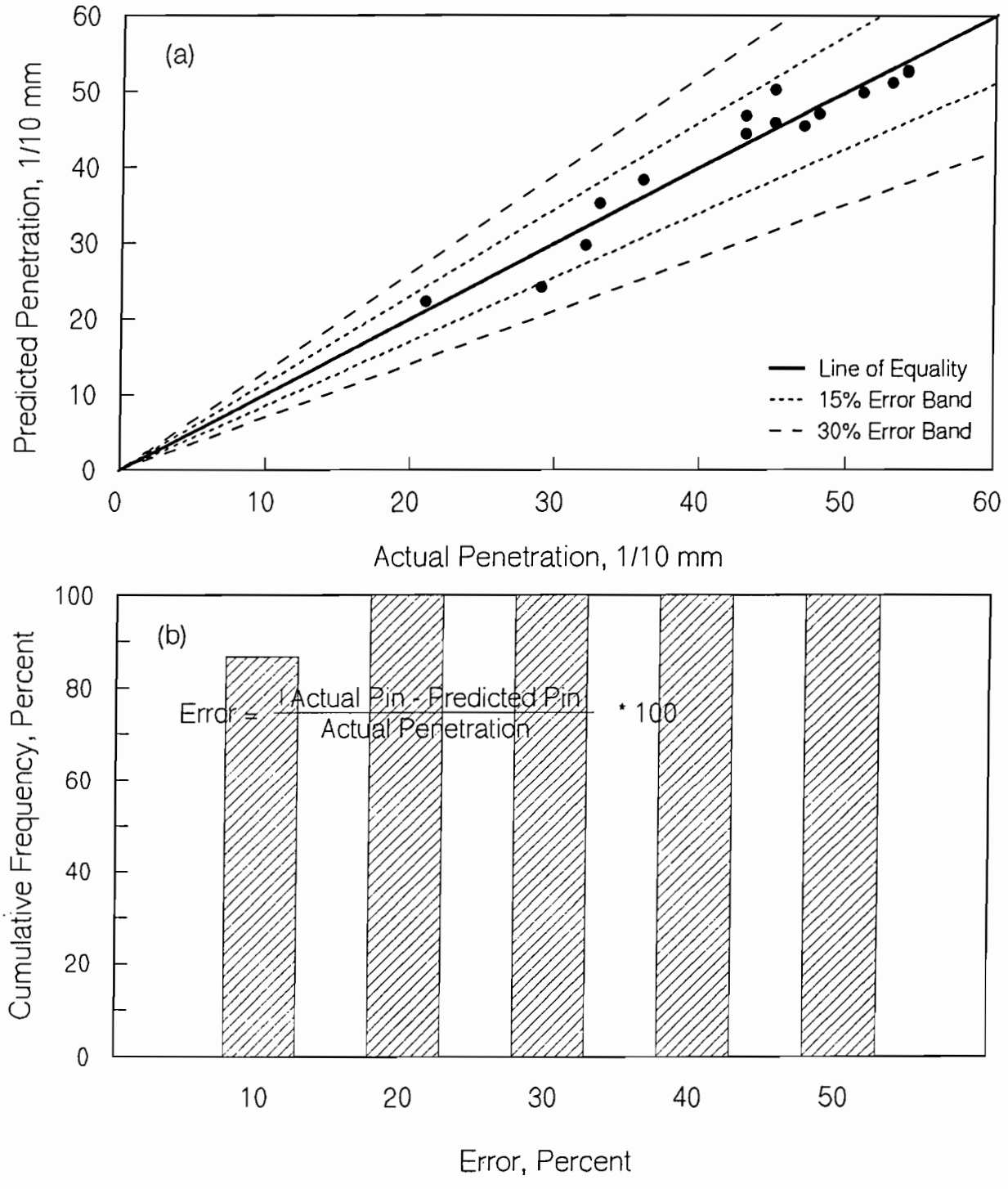

Figure F.13 Comparison of Actual and Predicted Penetration Values Using Equation 5.5 for El Paso Data with 5 percent AC Content (without Outliers) a) Scatter Plot, b) Cumulative Percent Error.

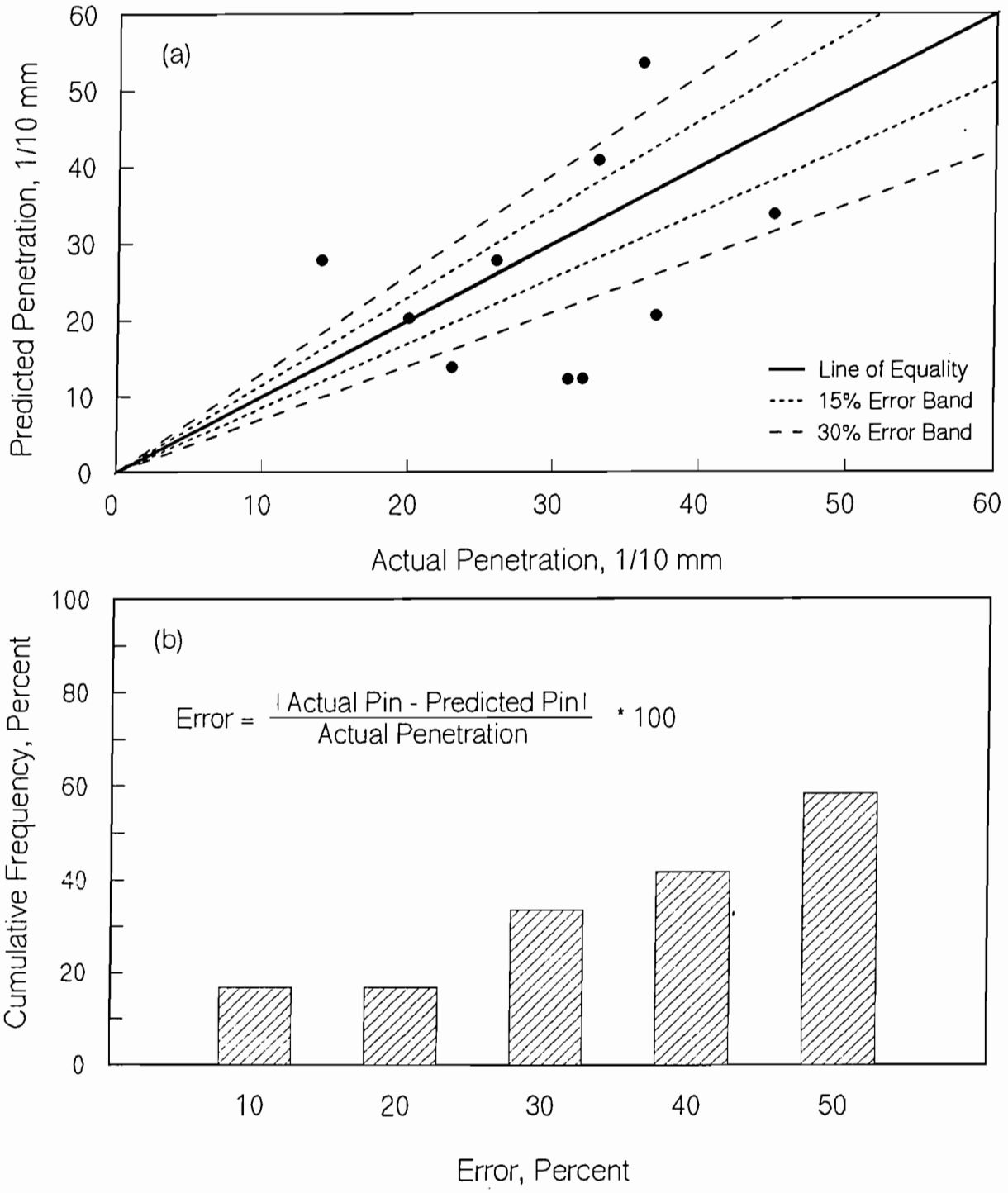

Figure F.14 Comparison of Actual and Predicted Penetration Values Using Equation 5.1 for Austin Data with 5 percent VTM (without Outliers) a) Scatter Plot, b) Cumulative Percent Error.

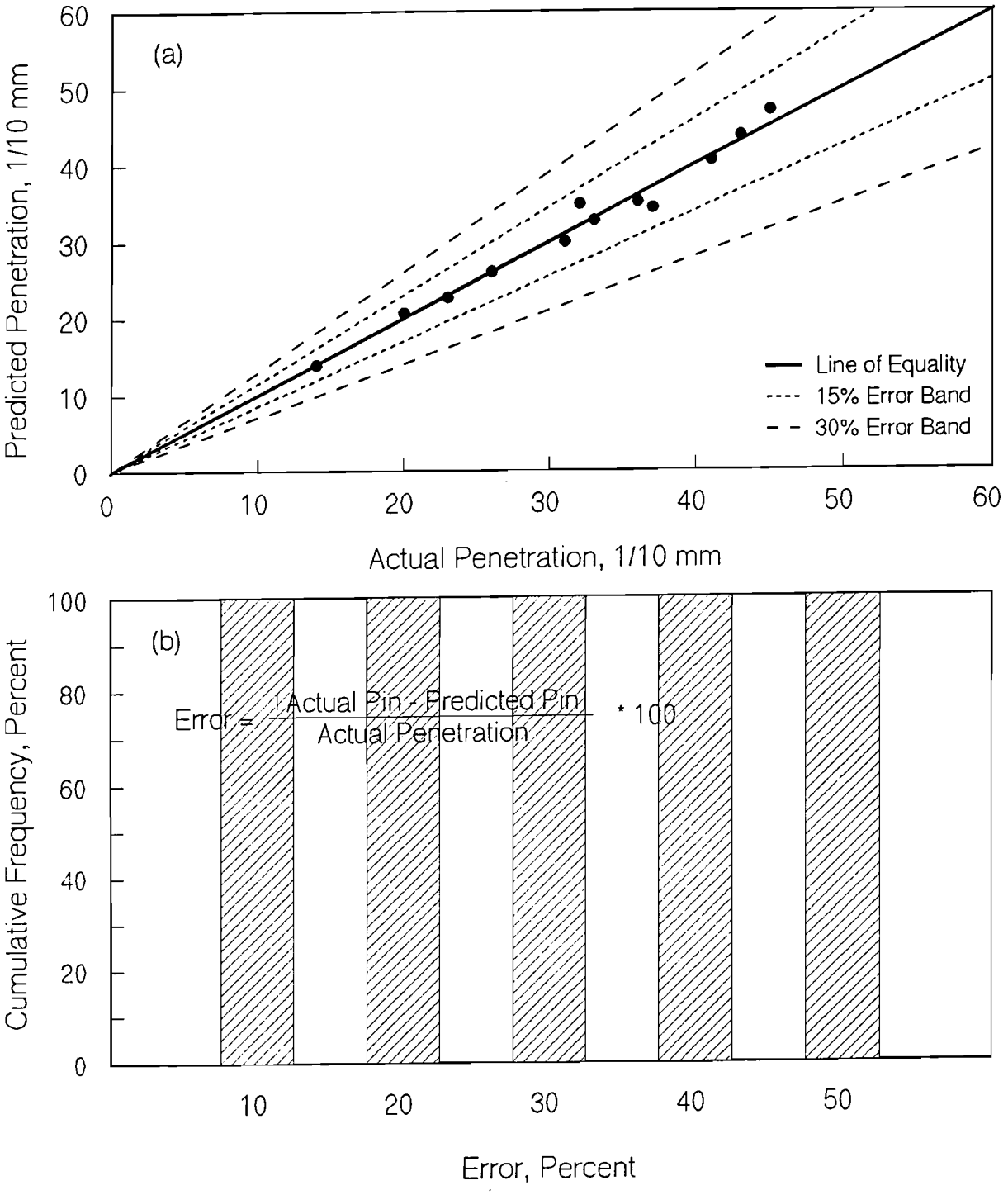

Figure F.15 Comparison of Actual and Predicted Penetration Values Using Equation 5.5 for Austin Data with 5 percent VTM (without Outliers) a) Scatter Plot, b) Cumulative Percent Error.

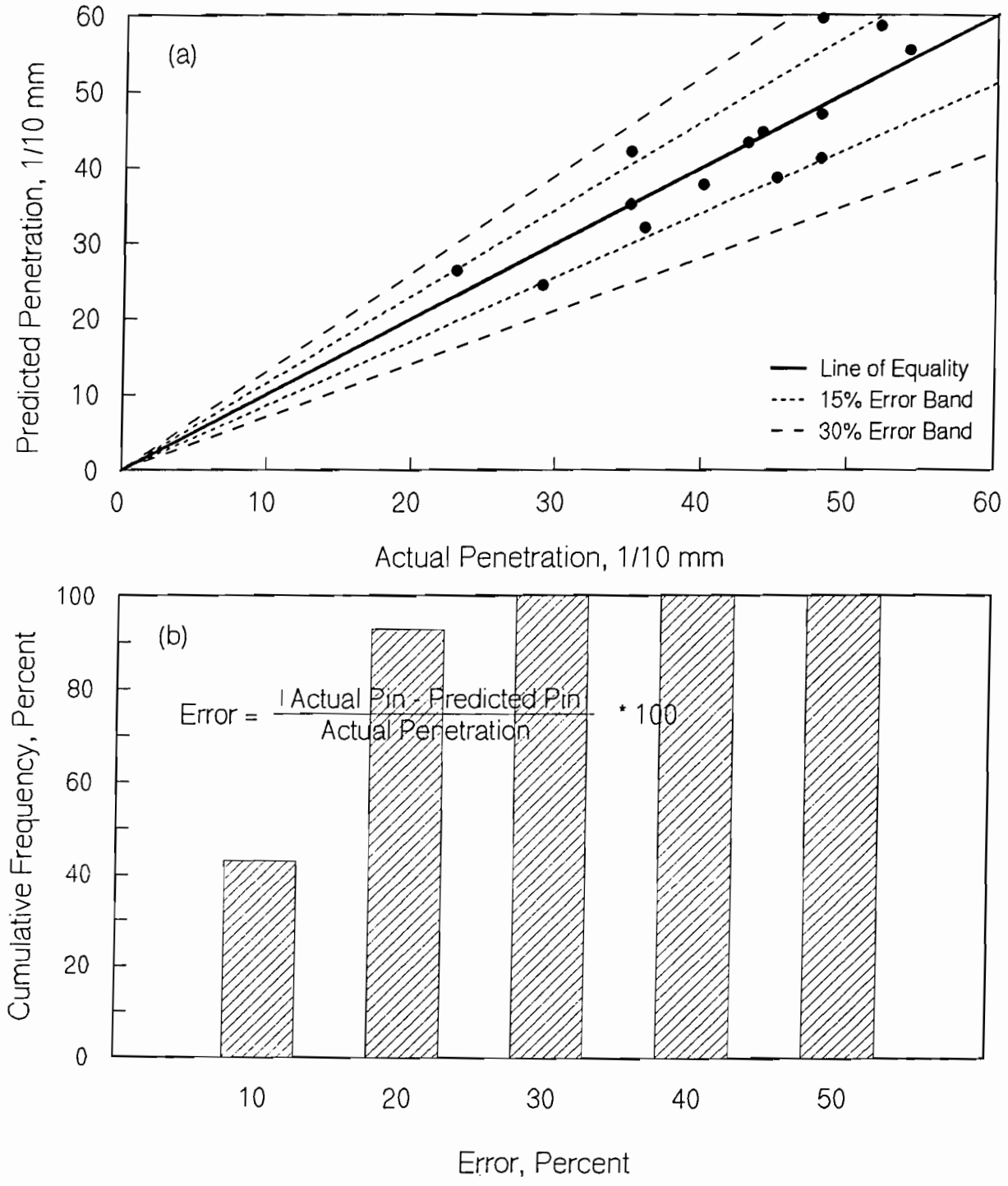

Figure F.16 Comparison of Actual and Predicted Penetration Values Using Equation 5.1 for El Paso Data with 5 percent VTM (without Outliers) a) Scatter Plot, b) Cumulative Percent Error.

APPENDIX G

Results from Optimization Tests

Asphalt AAK-1 Short Specimen 3% VTM

S1-R1

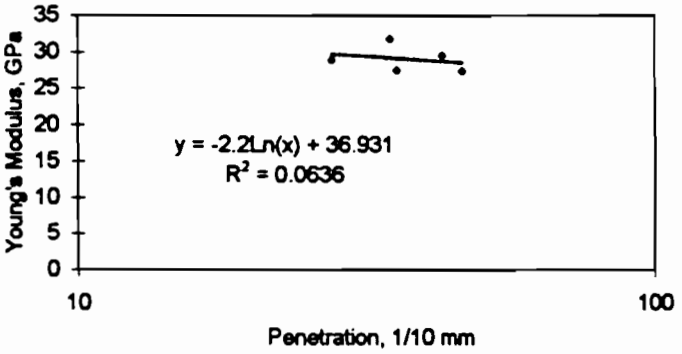

S1-R1

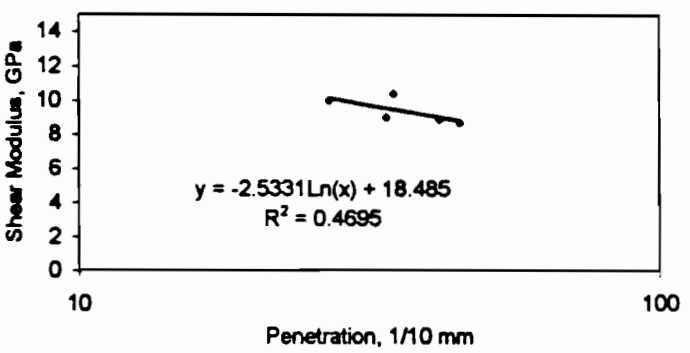

S2-R2

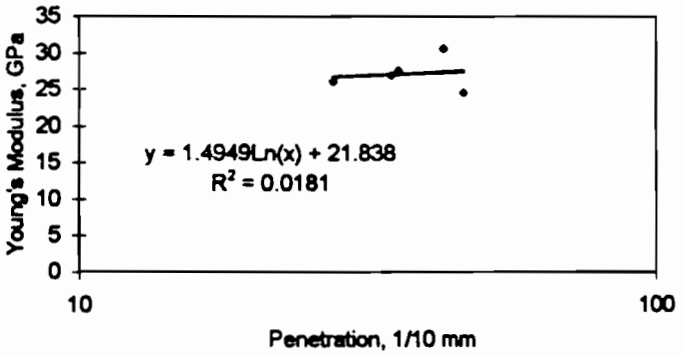

S2-R2

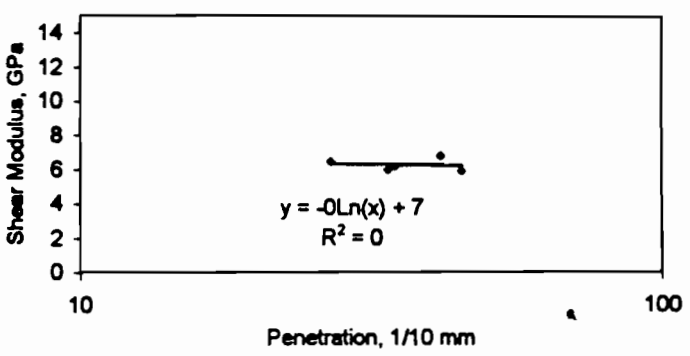

S3-R3

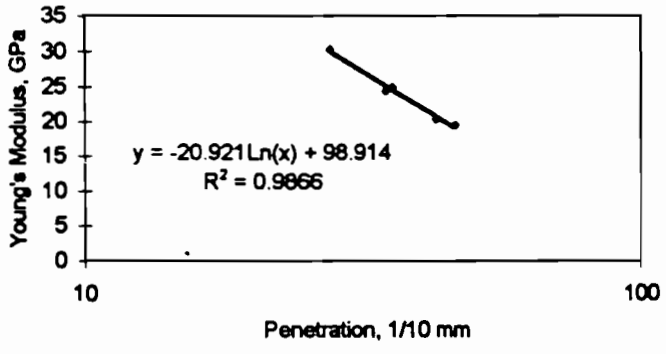

S3-R3

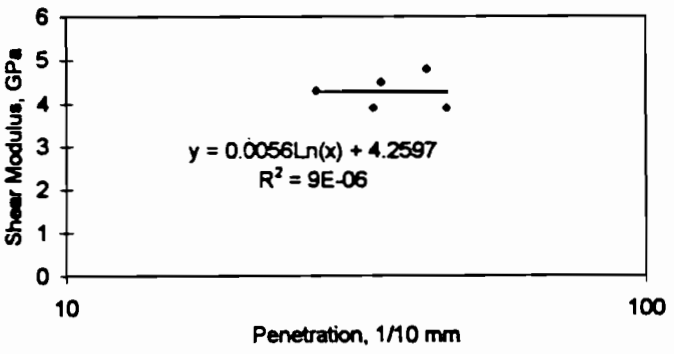

V-Meter

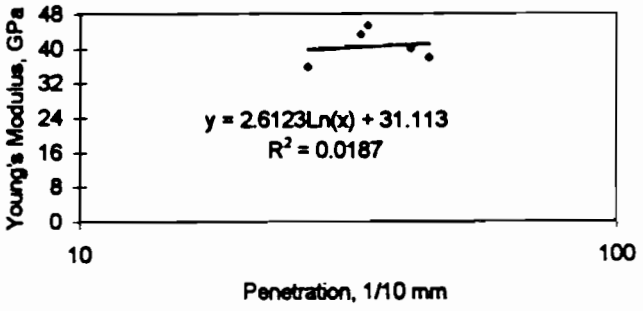

Asphalt AAK-1 Short Specimen 6% VTM

S1-R1

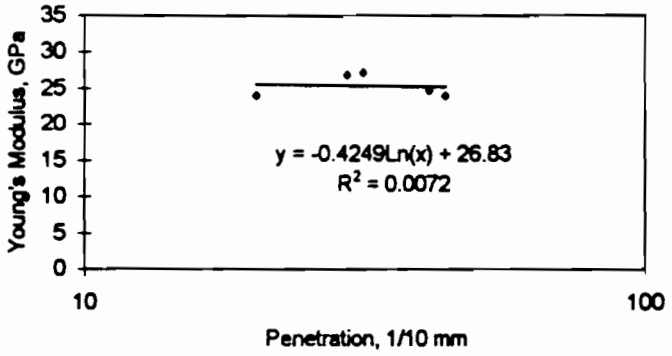

S1-R1

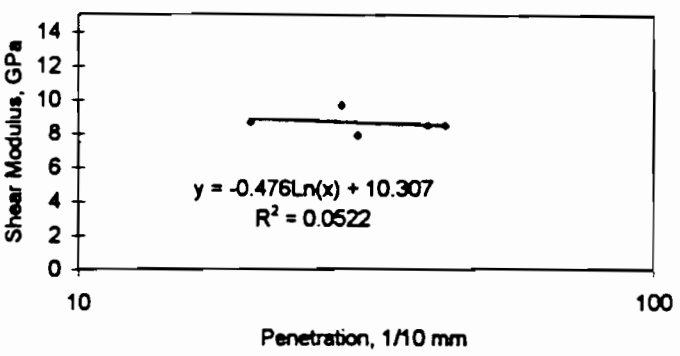

S2-R2

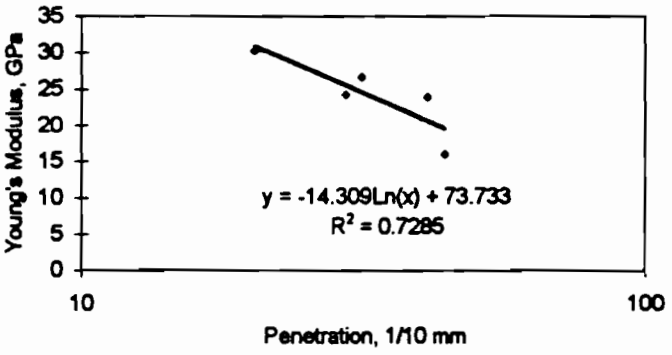

S2-R2

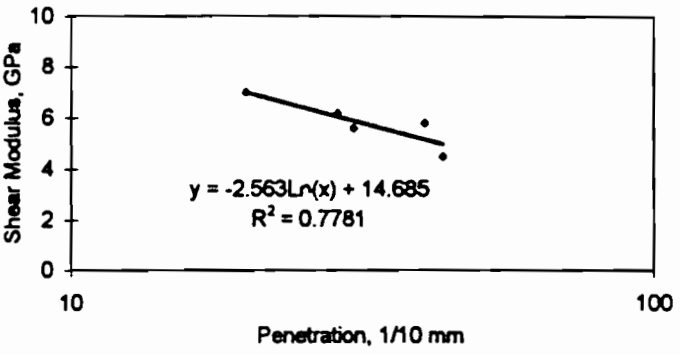

S3-R3

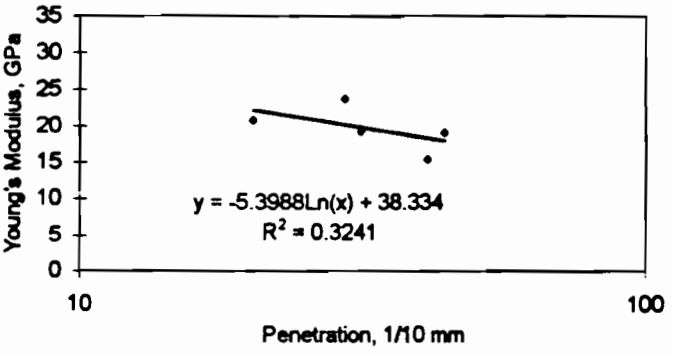

S3-R3

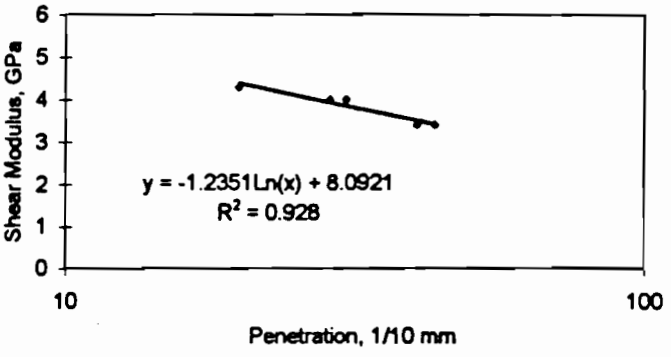

V-Meter

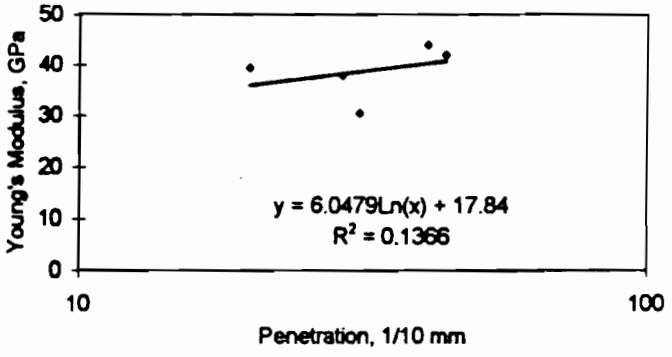

Asphalt AAK-1 Long Specimen 3% VTM

S1-R4

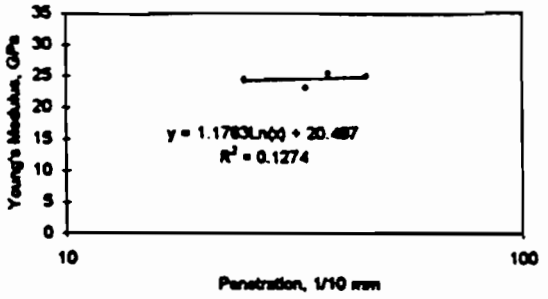

S1-R4

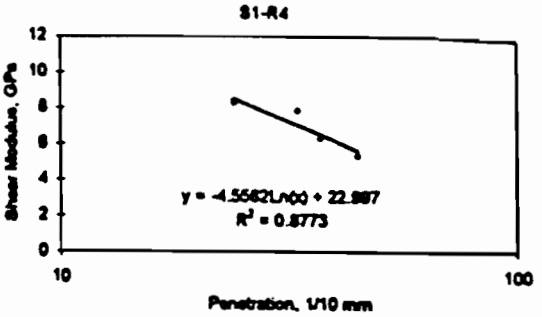

S1-R3

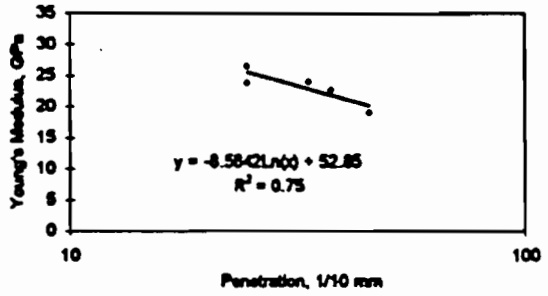

S1-R3

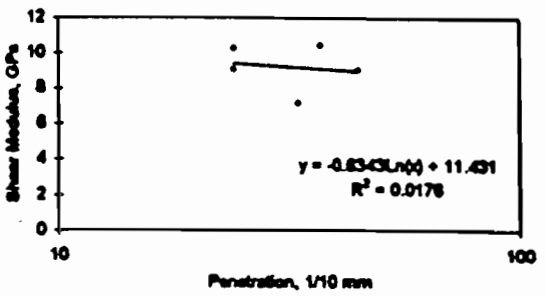

S2-R1

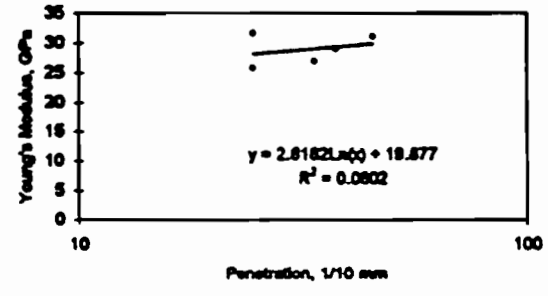

S2-R1

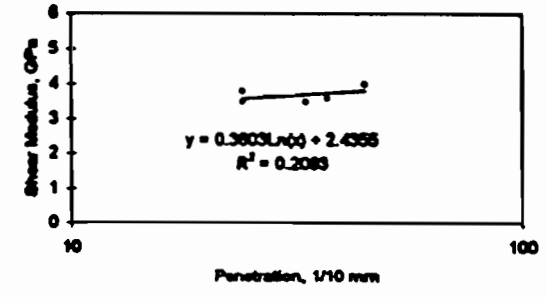

S2-R2

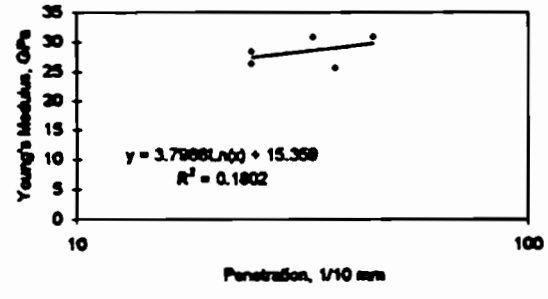

S2-R2

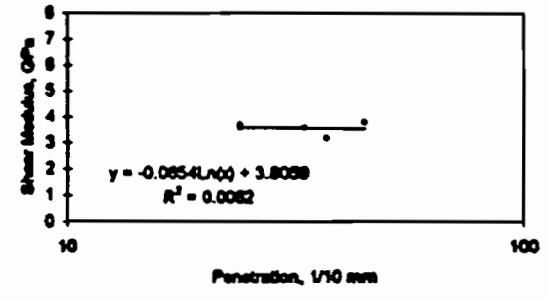

V-Meter

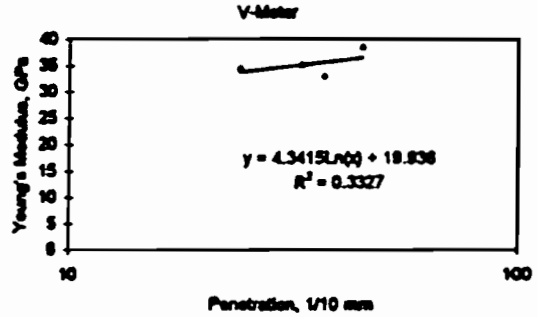

Asphalt AAK-1 Long Specimen 6% VTM

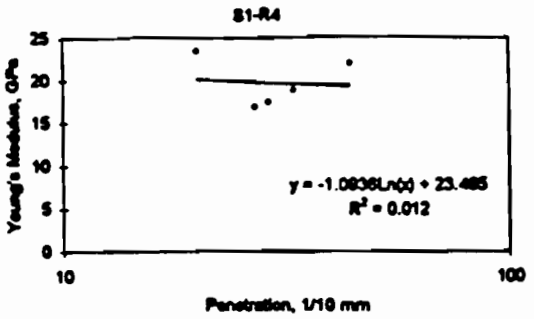

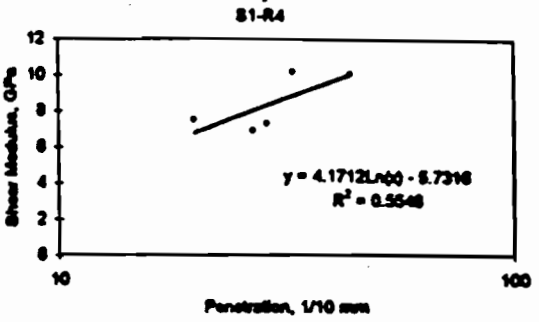

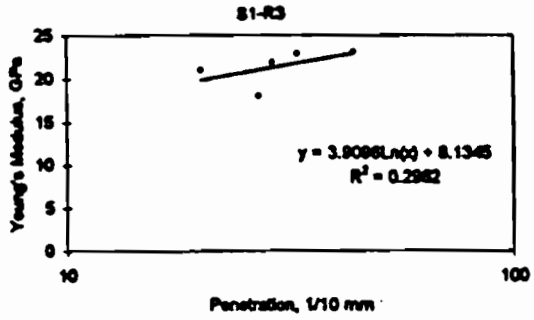

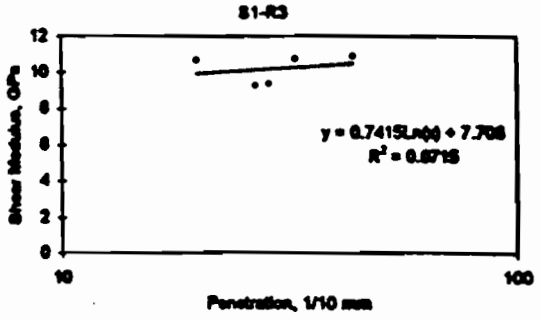

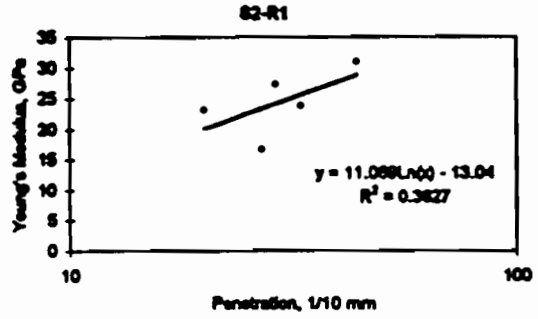

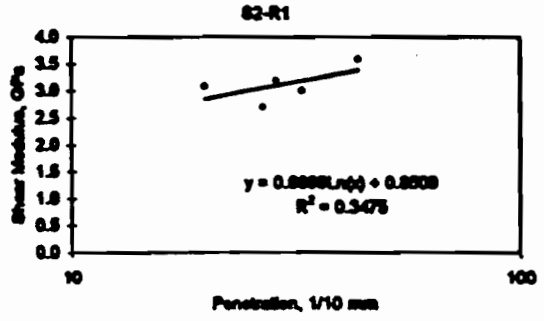

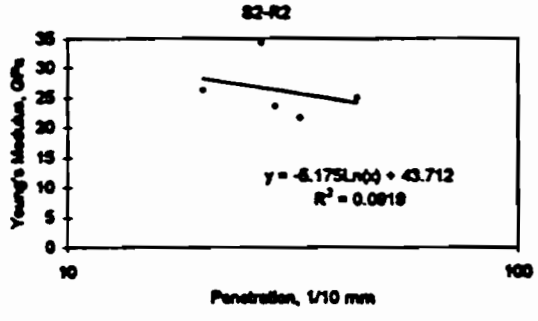

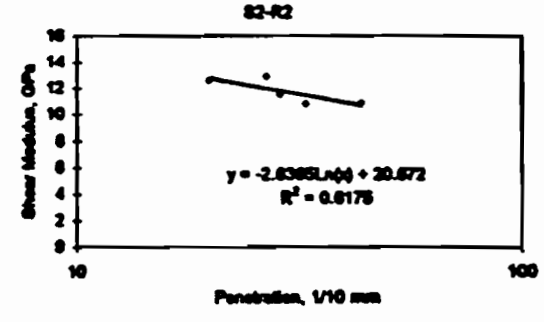

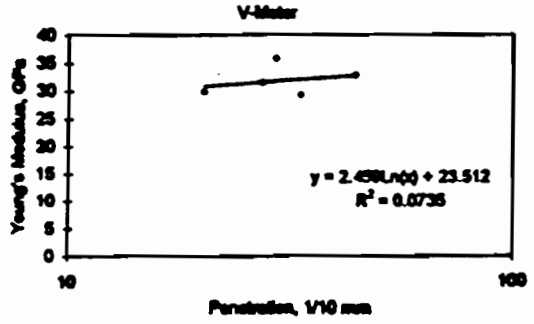

Asphalt AAOB-2 Short Specimen 3% VTM

S1-R1

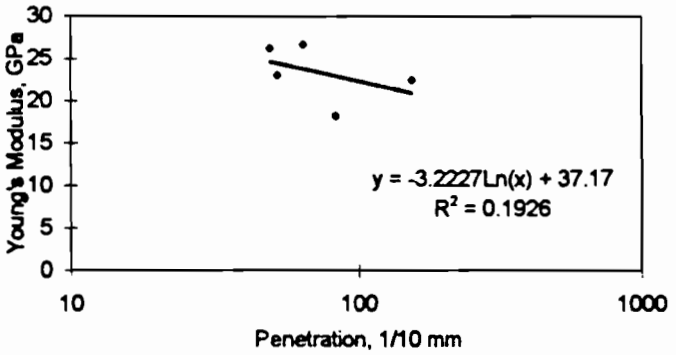

S1-R1

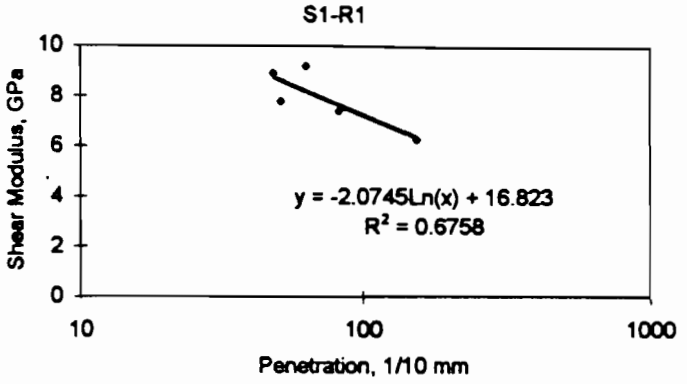

S2-R2

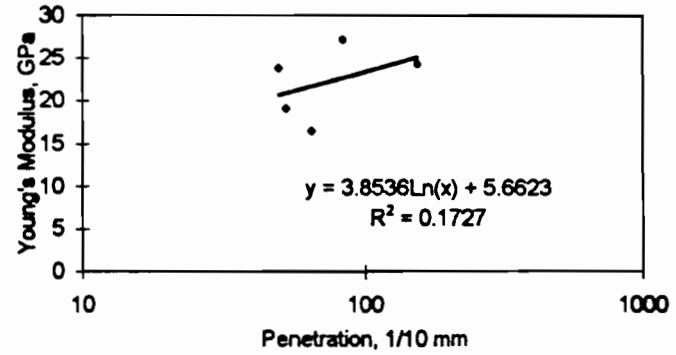

S2-R2

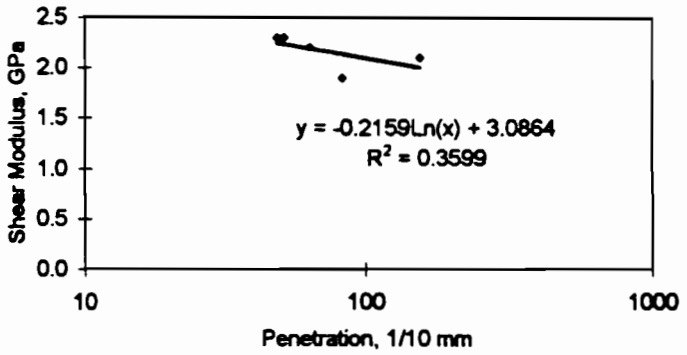

S3-R3

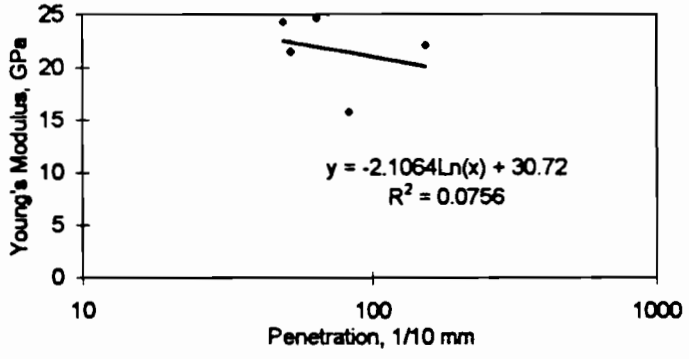

S3-R3

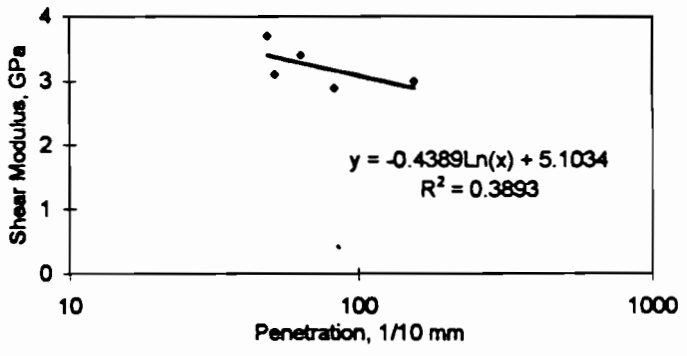

V-Meter, E

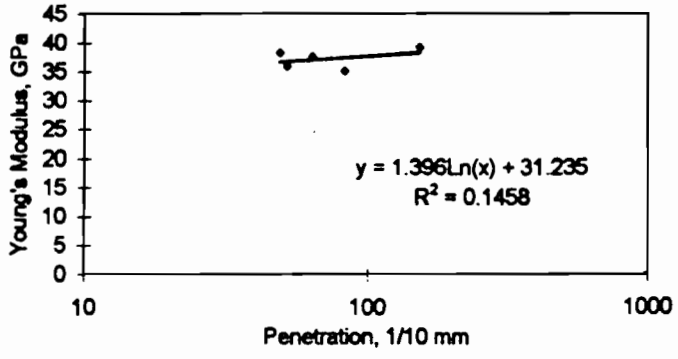

Asphalt AAOB-2 Short Specimen 6% VTM

S1-R1

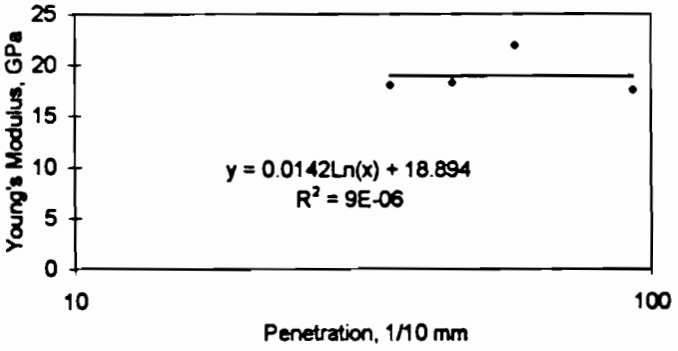

S1-R1

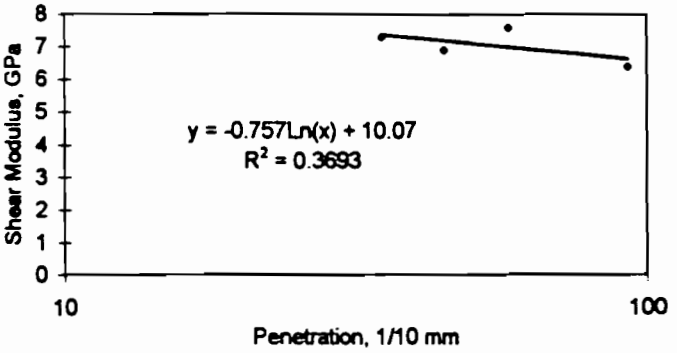

S2-R2

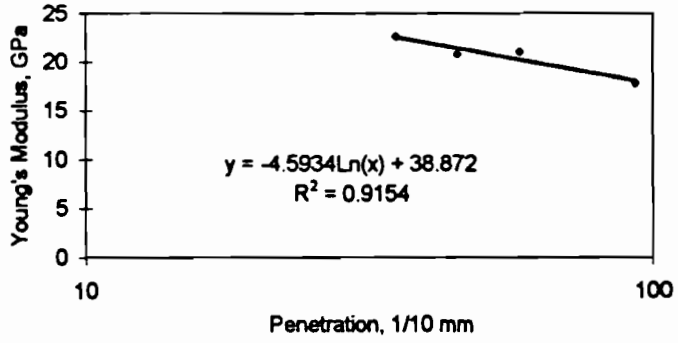

S2-R2

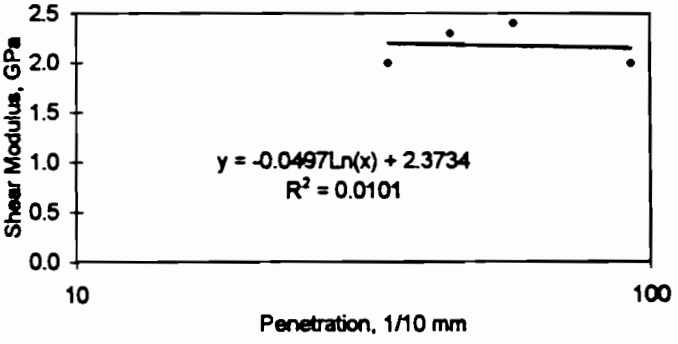

S3-R3

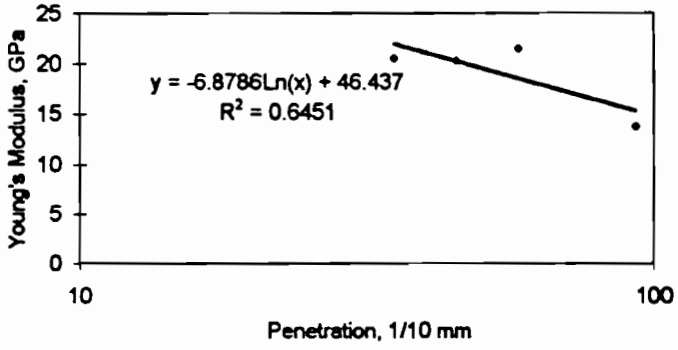

S3-R3

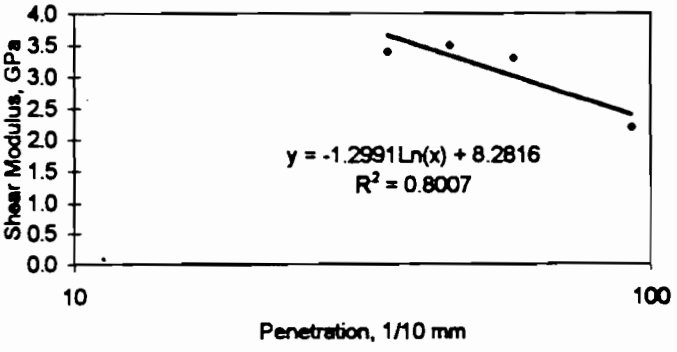

V-Meter

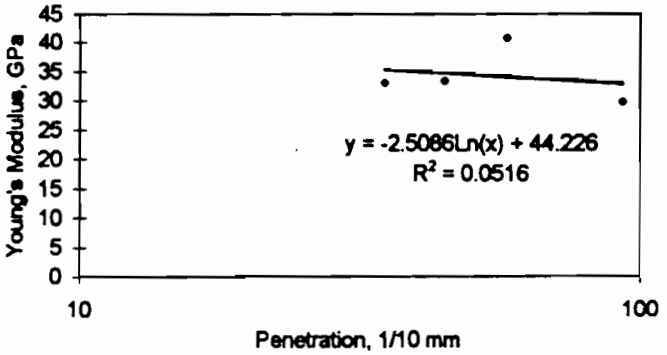

Asphalt AAOB-2 Long Specimen 3% VTM

S1-R4

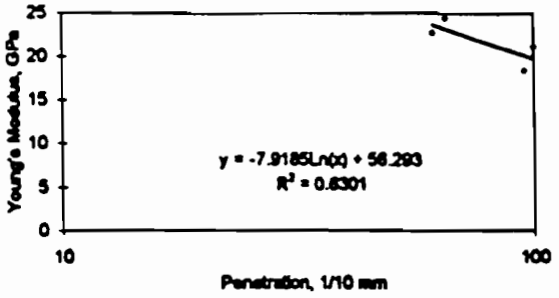

S1-R4

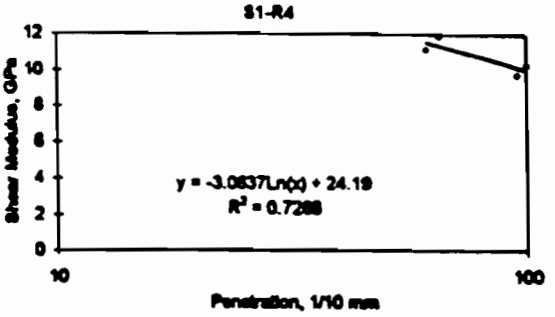

S1-R3

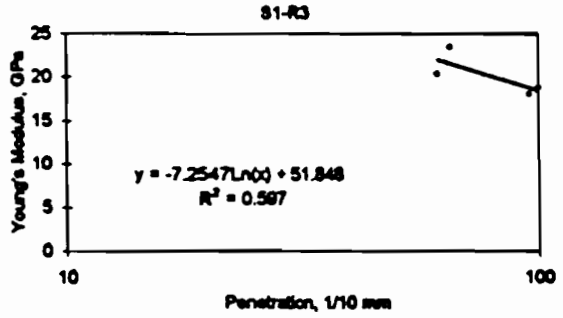

S1-R3

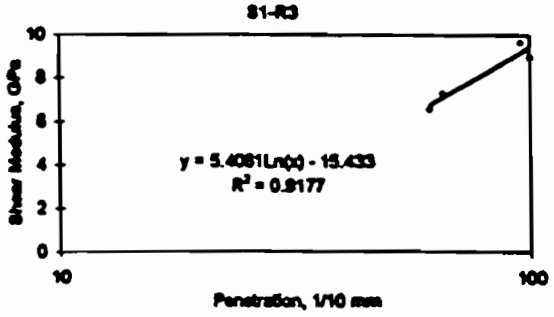

S2-R1

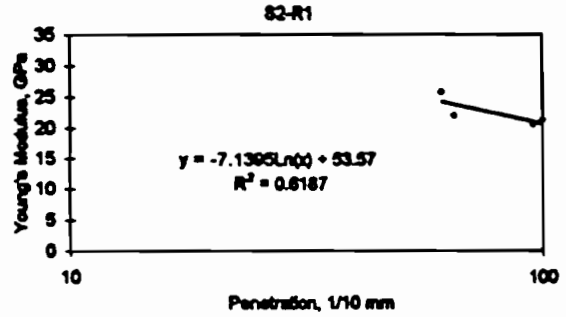

S2-R1

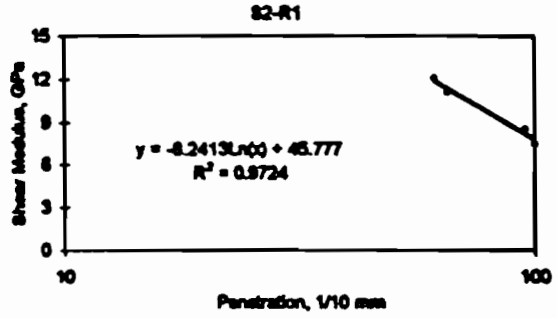

S2-R2

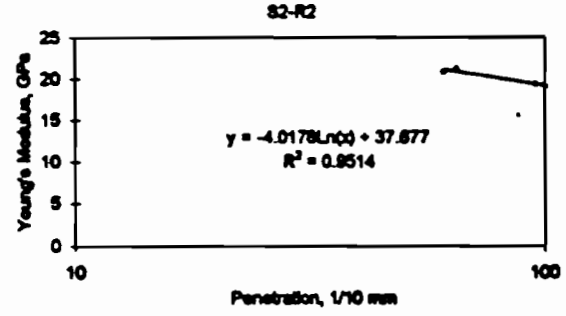

S2-R2

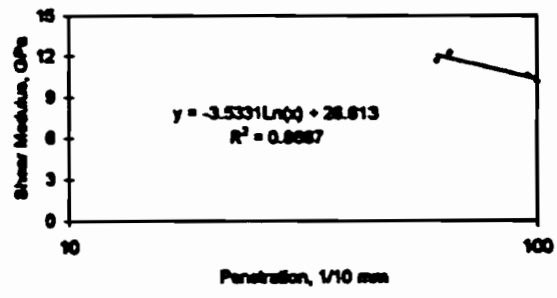

V-Meter

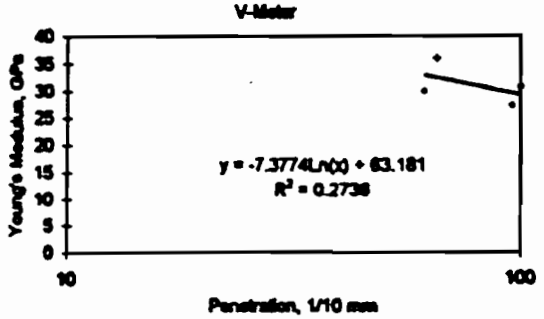

Asphalt AAOB-2 Long Specimen 6% VTM